UNIVERSITY OF YAOUNDE I
UNIVERSITÉ DE YAOUNDÉ I

POST-GRADUATE AND TRAINING
SCHOOL OF LIFE SCIENCE-HEALTH
AND ENVIRONMENT

CENTRE DE RECHERCHE ET DE
FORMATION DOCTORALE SCIENCE
DE LA VIE-SANTE ET
ENVIRONNEMENT

FACULTY OF SCIENCE
FACULTÉ DES SCIENCES

POST-GRADUATE AND TRAINING
UNIT OF LIFE SCIENCE-HEALTH

UNITE DE RECHERCHE ET DE
FORMATION DOCTORALE

DEPARTMENT OF BIOCHEMISTRY
DEPARTEMENT DE BIOCHIMIE

LABORATORY FOR PHYTOBIOCHEMISTRY AND MEDICINAL PLANTS STUDIES
LABORATOIRE DE PHYTOBIOCHIMIE ET D'ETUDE DES PLANTES MEDICINALES

ANTIMICROBIAL AND BIOCONTROL AGENTS UNIT
UNITE DES AGENTS ANTIMICROBIENS ET DE BIOCONTROLE

Validation of *Pf*LDH-based assay and Bioguided search of *P. falciparum* inhibitors from *Terminalia ivorensis* A. Chev and *Terminalia brownii* Frosen (Combretaceae).

Thesis presented in partial fulfilment of the requirements for the award of a Doctorate / PhD Degree in Biochemistry

By

TCHATAT TALI Mariscal Brice

Registration Nº 11R0837

M.sc in Biochemistry

Directed By:

Jean Claude TCHOUANKEU	**Fabrice FEKAM BOYOM**
Associate Professor	*Professor*
University of Yaounde I	**University of Yaounde I**

Academic Year 2023 - 2024

THE UNIVERSITY OF YAOUNDE I

Faculty of Science

Division of Programming and Follow-up

of Academic Affairs

UNIVERSITÉ DE YAOUNDÉ I

Faculté des Sciences

Division de la Programmation et du

Suivi des Activités Académiques

LIST OF PERMANENT TEACHING STAFF   LISTE DES ENSEIGNANTS PERMANENTS

ACADEMIC YEAR 2022/2023

(By Department and by Grade)

UPDATE: 31 May 2023

ADMINISTRATION

DEAN: TCHOUANKEU Jean- Claude, Associate Professor

VICE-DEAN / DPSAA: ATCHADE Alex de Théodore, Professor

VICE-DEAN/ DSSE: NYEGUE Maximilienne Ascension, Professor

VICE-DEAN / DRC : ABOSSOLO Monique, Associate Professor

Head of Administrative and Financial Division: NDOYE FOE Marie C. F., Associate

Professor

Head of Division of Academic affairs, Research and corporation: AJEAGAH Gideon

AGHAINDUM, *Professor*

1- DEPARTMENT OF BIOCHEMISTRY (BC) (43)
N°	**NAMES AND SURNAMES**	**GRADE**	**OBSERVATIONS**
1.	BIGOGA DAIGA Jude	Professor	On duty
2.	FEKAM BOYOM Fabrice	Professor	On duty
3.	KANSCI Germain	Professor	On duty
4.	MBACHAM FON Wilfred	Professor	On duty
5.	MOUNDIPA FEWOU Paul	Professor	**Head of Department**
6.	NGUEFACK Julienne	Professor	On duty
7.	NJAYOU Frédéric Nico	Professor	On duty
8.	OBEN Julius ENYONG	Professor	On duty
9.	ACHU Merci BIH	Associate Professor	On duty
10.	ATOGHO Barbara MMA	Associate Professor	On duty
11.	AZANTSA KINGUE GABIN BORIS	Associate Professor	On duty
12.	BELINGA née NDOYE FOE F. M. C.	Associate Professor	**Chief DAF / FS**
13.	DJUIDJE NGOUNOUE Marceline	Associate Professor	On duty

14.	DJUIKWO NKONGA Ruth Viviane	Associate Professor	On duty
15.	EFFA ONOMO Pierre	Associate Professor	**Vice Dean/FS/Univ Ebolowa**
16.	EWANE Cécile Annie	Associate Professor	On duty
17.	KOTUE TAPTUE Charles	Associate Professor	On duty
18.	LUNGA Paul KEILAH	Associate Professor	On duty
19.	MBONG ANGIE M. Mary Anne	Associate Professor	On duty
20.	MOFOR née TEUGWA Clotilde	Associate Professor	**Dean FS / UDs**
21.	NANA Louise épouse WAKAM	Associate Professor	On duty
22.	NGONDI Judith Laure	Associate Professor	On duty
23.	TCHANA KOUATCHOUA Angèle	Associate Professor	On duty
24.	AKINDEH MBUH NJI	Senior Lecturer	On duty
25.	BEBEE Fadimatou	Senior Lecturer	On duty
26.	BEBOY EDJENGUELE Sara Nathalie	Senior Lecturer	On duty
27.	DAKOLE DABOY Charles	Senior Lecturer	On duty
28.	DONGMO LEKAGNE Joseph Blaise	Senior Lecturer	On duty
29.	FONKOUA Martin	Senior Lecturer	On duty
30.	FOUPOUAPOUOGNIGNI Yacouba	Senior Lecturer	On duty
31.	KOUOH ELOMBO Ferdinand	Senior Lecturer	On duty
32.	MANANGA Marlyse Joséphine	Senior Lecturer	On duty
33.	OWONA AYISSI Vincent Brice	Senior Lecturer	On duty
34.	Palmer MASUMBE NETONGO	Senior Lecturer	On duty
35.	PECHANGOU NSANGOU Sylvain	Senior Lecturer	On duty
36.	WILFRED ANGIE ABIA	Senior Lecturer	On duty
37.	BAKWO BASSOGOG Christian Bernard	Assistant lecturer	On duty
38.	ELLA Fils Armand	Assistant lecturer	On duty
39.	EYENGA Eliane Flore	Assistant lecturer	On duty
40.	MADIESSE KEMGNE Eugenie Aimée	Assistant lecturer	On duty
41.	MANJIA NJIKAM Jacqueline	Assistant lecturer	On duty
42.	MBOUCHE FANMOE Marceline Joëlle	Assistant lecturer	On duty
43.	WOGUIA Alice Louise	Assistant lecturer	On duty

2- DEPARTMENT OF ANIMAL BIOLOGY AND PHYSIOLOGY(ABP) (52)			
1.	AJEAGAH Gideon AGHAINDUM	Professor	*DAARS/FS*

2.	BILONG BILONG Charles-Félix	Professor	**Head of Department**
3.	DIMO Théophile	Professor	On duty
4.	DJIETO LORDON Champlain	Professor	On duty
5.	DZEUFIET DJOMENI Paul Désiré	Professor	On duty
6.	ESSOMBA née NTSAMA MBALA	Professor	**DC and Vice dean/FMSB/UYI**
7.	FOMENA Abraham	Professor	On duty
8.	KEKEUNOU Sévilor	Professor	On duty
9.	NJAMEN Dieudonné	Professor	On duty
10.	NJIOKOU Flobert	Professor	On duty
11.	NOLA Moïse	Professor	On duty
12.	TAN Paul VERNYUY	Professor	On duty
13.	TCHUEM TCHUENTE Louis Albert	Professor	**Insp. Serv. Coord. Progr. in HEALTH**
14.	ZEBAZE TOGOUET Serge Hubert	Professor	On duty
15.	ALENE Désirée Chantal	Associate Professor	**Vice Dean /Univ Ebwa**
16.	BILANDA Danielle Claude	Associate Professor	On duty
17.	DJIOGUE Séfirin	Associate Professor	On duty
18.	GOUNOUE KAMKUMO Raceline épse FOTSING	Associate Professor	On duty
19.	JATSA BOUKENG Hermine épse MEGAPTCHE	Associate Professor	On duty
20.	LEKEUFACK FOLEFACK Guy B.	Associate Professor	On duty
21.	MAHOB Raymond Joseph	Associate Professor	On duty
22.	MBENOUN MASSE Paul Serge	Associate Professor	On duty
23.	MEGNEKOU Rosette	Associate Professor	On duty
24.	MOUNGANG LucianeMarlyse	Associate Professor	On duty
25.	NOAH EWOTI Olive Vivien	Associate Professor	On duty
26.	MONY Ruth épse NTONE	Associate Professor	On duty
27.	NGUEGUIM TSOFACK Florence	Associate Professor	On duty
28.	NGUEMBOCK	Associate Professor	On duty
29.	TAMSA ARFAO Antoine	Associate Professor	On duty
30.	TOMBI Jeannette	Associate Professor	On duty
31.	ATSAMO Albert Donatien	Senior Lecturer	On duty
32.	BASSOCK BAYIHA Etienne Didier	Senior Lecturer	On duty

33.	ETEME ENAMA Serge	Senior Lecturer	On duty
34.	FEUGANG YOUMSSI François	Senior Lecturer	On duty
35.	FOKAM Alvine Christelle Epse KENGNE	Senior Lecturer	On duty
36.	GONWOUO NONO Legrand	Senior Lecturer	On duty
37.	KANDEDA KAVAYE Antoine	Senior Lecturer	On duty
38.	KOGA MANG DOBARA	Senior Lecturer	On duty
39.	LEME BANOCK Lucie	Senior Lecturer	On duty
40.	MAPON NSANGOU Indou	Senior Lecturer	On duty
41.	METCHI DONFACK MIREILLE FLAURE EPSE GHOUMO	Senior Lecturer	On duty
42.	MVEYO NDANKEU Yves Patrick	Senior Lecturer	On duty
43.	NGOUATEU KENFACK Omer Bébé	Senior Lecturer	On duty
44.	NJUA Clarisse YAFI	Senior Lecturer	**Head Div. Univ. Bamenda**
45.	NWANE Philippe Bienvenu	Senior Lecturer	On duty
46.	TADU Zephyrin	Senior Lecturer	On duty
47.	YEDE	Senior Lecturer	On duty
48.	YOUNOUSSA LAME	Senior Lecturer	On duty
49.	AMBADA NDZENGUE GEORGIA ELNA	Assist. Lecturer	On duty
50.	KODJOM WANCHE Jacguy Joyce	Assist. Lecturer	On duty
51.	NDENGUE Jean De Matha	Assist. Lecturer	On duty
52.	ZEMO GAMO Franklin	Assist. Lecturer	On duty

3- DEPARTMENT OF PLANT PHYSIOLOGY AND BIOLOGY (PPB) (34)			
1.	AMBANG Zachée	Professor	**Head of Department**
2.	DJOCGOUE Pierre François	Professor	On duty
3.	MBOLO Marie	Professor	On duty
4.	MOSSEBO Dominique Claude	Professor	On duty
5.	YOUMBI Emmanuel	Professor	On duty
6.	ZAPFACK Louis	Professor	On duty
7.	ANGONI Hyacinthe	Associate Professor	On duty
8.	BIYE Elvire Hortense	Associate Professor	On duty
9.	MAHBOU SOMO TOUKAM. Gabriel	Associate Professor	On duty

10.	MALA Armand William	Associate Professor	On duty
11.	MBARGA BINDZI Marie Alain	Associate Professor	**DAAC /Univ , Douala**
12.	NDONGO BEKOLO	Associate Professor	On duty
13.	NGALLE Hermine BILLE	Associate Professor	On duty
14.	NGODO MELINGUI Jean Baptiste	Associate Professor	On duty
15.	NGONKEU MAGAPTCHE Eddy L.	Associate Professor	**CT / MINRESI**
16.	TONFACK Libert Brice	Associate Professor	On duty
17.	TSOATA Esaïe	Associate Professor	On duty
18.	ONANA JEAN MICHEL	Associate Professor	On duty
19.	DJEUANI Astride Carole	Senior Lecturer	On duty
20.	GONMADGE CHRISTELLE	Senior Lecturer	On duty
21.	MAFFO MAFFO Nicole Liliane	Senior Lecturer	On duty
22.	NNANGA MEBENGA Ruth Laure	Senior Lecturer	On duty
23.	NOUKEU KOUAKAM Armelle	Senior Lecturer	On duty
24.	NSOM ZAMBO EPSE PIAL ANNIE CLAUDE	Senior Lecturer	**In détachment/UNESCO MALI**
25.	GODSWILL NTSOMBOH NTSEFONG	Senior Lecturer	On duty
26.	KABELONG BANAHO Louis-Paul-Roger	Senior Lecturer	On duty
27.	KONO Léon Dieudonné	Senior Lecturer	On duty
28.	LIBALAH Moses BAKONCK	Senior Lecturer	On duty
29.	LIKENG-LI-NGUE Benoit C	Senior Lecturer	On duty
30.	TAEDOUNG Evariste Hermann	Senior Lecturer	On duty
31.	TEMEGNE NONO Carine	Senior Lecturer	On duty
32.	MANGA NDJAGA JUDE	Assistant lecturer	On duty
33.	DIDA LONTSI Sylvere Landry	Assistant lecturer	On duty
34.	METSEBING Blondo-Pascal	Assistant lecturer	On duty

4- DEPARTMENT OF INORGANIC CHEMISTRY (IC) (28)			
1.	GHOGOMU Paul MINGO	Professor	**Minister in charge of mission. P.R.**
2.	NANSEU NJIKI Charles Péguy	Professor	On duty
3.	NDIFON Peter TEKE	Professor	**TC MINRESI**

4.	NENWA Justin	Professor	On duty
5.	NGAMENI Emmanuel	Professor	**Dean FS Univ. Ngaoundere**
6.	NGOMO Horace MANGA	Professor	**Vice Chancelor/Univ. Buea**
7.	NJOYA Dayirou	Professor	On duty
8.	ACAYANKA Elie	Associate Professor	On duty
9.	EMADAK Alphonse	Associate Professor	On duty
10.	KAMGANG YOUBI Georges	Associate Professor	On duty
11.	KEMMEGNE MBOUGUEM Jean C.	Associate Professor	On duty
12.	KENNE DEDZO GUSTAVE	Associate Professor	On duty
13.	MBEY Jean Aime	Associate Professor	On duty
14.	NDI NSAMI Julius	Associate Professor	**Head of Department**
15.	NEBAH Née NDOSIRI Bridget NDOYE	Associate Professor	**Senator/SENAT**
16.	NJIOMOU C. épse DJANGANG	Associate Professor	On duty
17.	NYAMEN Linda Dyorisse	Associate Professor	On duty
18.	PABOUDAM GBAMBIE AWAWOU	Associate Professor	On duty
19.	TCHAKOUTE KOUAMO Hervé	Associate Professor	On duty
20.	BELIBI BELIBI Placide Désiré	Associate Professor	**Head of division/ ENS Bertoua**
21.	CHEUMANI YONA Arnaud M.	Associate Professor	On duty
22.	KOUOTOU DAOUDA	Associate Professor	On duty
23.	MAKON Thomas Beauregard	Senior Lecturer	On duty
24.	NCHIMI NONO KATIA	Senior Lecturer	On duty
25.	NJANKWA NJABONG N. Eric	Senior Lecturer	On duty
26.	PATOUOSSA ISSOFA	Senior Lecturer	On duty
27.	SIEWE Jean Mermoz	Senior Lecturer	On duty
28.	BOYOM TATCHEMO Franck W.	Assistant Lecturer	On duty

5- DEPARTMENT OF ORGANIC CHEMISTRY (OC) (37)			
1.	Alex de Théodore ATCHADE	Professor	**Vice-Dean/PSAA**
2.	DONGO Etienne	Professor	**Vice Dean/CSA/ F. SED**
3.	NGOUELA Silvère Augustin	Professor	**Head of Department UDs**

4.	PEGNYEMB Dieudonné Emmanuel	Professor	**Director MINESUP/ Head of Department**
5.	WANDJI Jean	Professor	On duty
6.	MBAZOA née DJAMA Céline	Professor	On duty
7.	AMBASSA Pantaléon	Associate Professor	On duty
8.	EYONG Kenneth OBEN	Associate Professor	On duty
9.	FOTSO WABO Ghislain	Associate Professor	On duty
10.	KAMTO Eutrophe Le Doux	Associate Professor	On duty
11.	KENMOGNE Marguerite	Associate Professor	On duty
12.	KEUMEDJIO Félix	Associate Professor	On duty
13.	KOUAM Jacques	Associate Professor	On duty
14.	MKOUNGA Pierre	Associate Professor	On duty
15.	MVOT AKAK CARINE	Associate Professor	On duty
16.	NGO MBING Joséphine	Associate Professor	**Head of cell MINRESI**
17.	NGONO BIKOBO Dominique Serge	Associate Professor	**Study charge Ass. n°3/MINESUP**
18.	NOTE LOUGBOT Olivier Placide	Associate Professor	**DAAC/Univ. Bertoua**
19.	NOUNGOUE TCHAMO Diderot	Associate Professor	On duty
20.	TABOPDA KUATE Turibio	Associate Professor	On duty
21.	TAGATSING FOTSING Maurice	Associate Professor	On duty
22.	TCHOUANKEU Jean-Claude	Associate Professor	**Dean /FS/ UYI**
23.	YANKEP Emmanuel	Associate Professor	On duty
24.	ZONDEGOUMBA Ernestine	Associate Professor	On duty
25.	MESSI Angélique Nicolas	Senior Lecturer	On duty
26.	NGNINTEDO Dominique	Senior Lecturer	On duty
27.	NGOMO Orléans	Senior Lecturer	On duty
28.	NONO NONO Éric Carly	Senior Lecturer	On duty
29.	OUAHOUO WACHE Blandine M.	Senior Lecturer	On duty
30.	OUETE NANTCHOUANG Judith Laure	Senior Lecturer	On duty
31.	SIELINOU TEDJON Valérie	Senior Lecturer	On duty
32.	TCHAMGOUE Joseph	Senior Lecturer	On duty
33.	TSAFFACK Maurice	Senior Lecturer	On duty
34.	TSAMO TONTSA Armelle	Senior Lecturer	On duty
35.	TSEMEUGNE Joseph	Senior Lecturer	On duty
36.	MUNVERA MFIFEN Aristide	Assistant lecturer	On duty

37.	NDOGO ETEME Olivier	Assistant lecturer	On duty

6- DEPARTMENT OF COMPUTER SCIENCE (CS) (22)			
1	ATSA ETOUNDI Roger	Professor	**Chief Div. MINESUP**
2	FOUDA NDJODO Marcel Laurent	Professor	**Head of department HTTC/Chief IGA. MINESUP**
3	NDOUNDAM Réné	Associate Professor	On duty
4	TSOPZE Norbert	Associate Professor	On duty
5	ABESSOLO ALO'O Gislain	Senior Lecturer	**Head of cell MINFOPRA**
6	AMINOU HALIDOU	Senior Lecturer	**Head of Department**
7	DJAM Xaviera YOUH - KIMBI	Senior Lecturer	On duty
8	DOMGA KOMGUEM Rodrigue	Senior Lecturer	On duty
9	EBELE Serge Alain	Senior Lecturer	On duty
10	HAMZA Adamou	Senior Lecturer	On duty
11	JIOMEKONG AZANZI Fidel	Senior Lecturer	On duty
12	KOUOKAM KOUOKAM E. A.	Senior Lecturer	On duty
13	MELATAGIA YONTA Paulin	Senior Lecturer	On duty
14	MESSI NGUELE Thomas	Senior Lecturer	On duty
15	MONTHE DJIADEU Valery M.	Senior Lecturer	On duty
16	NZEKON NZEKO'O ARMEL JACQUES	Senior Lecturer	On duty
17	OLLE OLLE Daniel Claude Georges Delort	Senior Lecturer	**C/D ENSET Ebolowa**
18	TAPAMO Hyppolite	Senior Lecturer	On duty
19	BAYEM Jacques Narcisse	Assistant lecturer	On duty
20	EKODECK Stéphane Gaël Raymond	Assistant lecturer	On duty
21	MAKEMBE. S . Oswald	Assistant lecturer	**Director CUTI**
22	NKONDOCK. MI. BAHANACK.N.	Assistant lecturer	On duty

7- DEPARTMENT OF MATHEMATICS (MA) (33)			
1.	AYISSI Raoult Domingo	Professor	**Head of Department**
2.	KIANPI Maurice	Associate Professor	On duty
3.	MBANG Joseph	Associate Professor	On duty
4.	MBEHOU Mohamed	Associate Professor	On duty
5.	MBELE BIDIMA Martin Ledoux	Associate Professor	On duty

6.	NOUNDJEU Pierre	Associate Professor	**Chief Service of Programs & Diploms/FS/UYI**
7.	TAKAM SOH Patrice	Associate Professor	**On duty**
8.	TCHAPNDA NJABO Sophonie B.	Associate Professor	**Director/AIMS Rwanda**
9.	TCHOUNDJA Edgar Landry	Associate Professor	On duty
10.	AGHOUKENG JIOFACK Jean Gérard	Senior Lecturer	**Chief Cell MINEPAT**
11.	BOGSO ANTOINE Marie	Senior Lecturer	On duty
12.	CHENDJOU Gilbert	Senior Lecturer	On duty
13.	DJIADEU NGAHA Michel	Senior Lecturer	On duty
14.	DOUANLA YONTA Herman	Senior Lecturer	On duty
15.	KIKI Maxime Armand	Senior Lecturer	On duty
16.	LOUMNGAM KAMGA Victor	Senior Lecturer	On duty
17.	MBAKOP Guy Merlin	Senior Lecturer	On duty
18.	MBATAKOU Salomon Joseph	Senior Lecturer	On duty
19.	MENGUE MENGUE David Joël	Senior Lecturer	**Head department / ENS Maroua**
20.	MBIAKOP Hilaire George	Senior Lecturer	On duty
21.	NGUEFACK Bernard	Senior Lecturer	On duty
22.	NIMPA PEFOUKEU Romain	Senior Lecturer	On duty
23.	OGADOA AMASSAYOGA	Senior Lecturer	On duty
24.	POLA DOUNDOU Emmanuel	Senior Lecturer	**In training course**
25.	TCHEUTIA Daniel Duviol	Senior Lecturer	On duty
26.	TETSADJIO TCHILEPECK M. Eric.	Senior Lecturer	On duty
27.	BITYE MVONDO Esther Claudine	Assistant lecturer	On duty
28.	FOKAM Jean Marcel	Assistant lecturer	On duty
29.	GUIDZAVAI KOUCHERE Albert	Assistant lecturer	On duty
30.	MANN MANYOMBE Martin Luther	Assistant lecturer	On duty
31.	MEFENZA NOUNTU Thiery	Assistant lecturer	On duty
32.	NYOUMBI DLEUNA Christelle	Assistant lecturer	On duty
33.	TENKEU JEUFACK Yannick Léa	Assistant lecturer	On duty

8- DEPARTMENT OF MICROBIOLOGY (MIB) (24)

1.	ESSIA NGANG Jean Justin	Professor	**Head of Department**
2.	NYEGUE Maximilienne Ascension	Professor	**Vice Dean/DSSE**
3.	ASSAM ASSAM Jean Paul	Associate Professor	On duty
4.	BOUGNOM Blaise Pascal	Associate Professor	On duty
5.	BOYOMO ONANA	Associate Professor	On duty
6.	KOUITCHEU MABEKU Epse KOUAM Laure Brigitte	Associate Professor	On duty
7.	RIWOM Sara Honorine	Associate Professor	On duty
8.	NJIKI BIKOÏ Jacky	Associate Professor	On duty
9.	SADO KAMDEM Sylvain Leroy	Associate Professor	On duty
10.	ESSONO Damien Marie	Senior Lecturer	On duty
11.	LAMYE Glory MOH	Senior Lecturer	On duty
12.	MEYIN A EBONG Solange	Senior Lecturer	On duty
13.	MONI NDEDI Esther Del Florence	Senior Lecturer	On duty
14.	NKOUDOU ZE Nardis	Senior Lecturer	On duty
15.	TAMATCHO KWEYANG Blandine Pulchérie	Senior Lecturer	On duty
16.	TCHIKOUA Roger	Senior Lecturer	**Head of school division**
17.	TOBOLBAÏ Richard	Senior Lecturer	On duty
18.	NKOUE TONG Abraham	Assistant lecturer	On duty
19.	SAKE NGANE Carole Stéphanie	Assistant lecturer	On duty
20.	EZO'O MENGO Fabrice Télésfor	Assistant lecturer	On duty
21.	EHETH Jean Samuel	Assistant lecturer	On duty
22.	MAYI Marie Paule Audrey	Assistant lecturer	On duty
23.	NGOUENAM Romial Joël	Assistant lecturer	On duty
24.	NJAPNDOUNKE Bilkissou	Assistant lecturer	On duty

9- DEPARTMENT OF PHYSICS (PY) (43)			
1	BEN- BOLIE Germain Hubert	Professor	On duty
2	DJUIDJE KENMOE spouse ALOYEM	Professor	On duty
3	EKOBENA FOUDA Henri Paul	Professor	**Vice-Rector Univ. Ngaoundéré**

x

4	ESSIMBI ZOBO Bernard	Professor	On duty
5	HONA Jacques	Professor	On duty
6	NANA ENGO Serge Guy	Professor	On duty
7	NANA NBENDJO Blaise	Professor	On duty
8	NDJAKA Jean Marie Bienvenu	Professor	**Head of Department**
9	NJANDJOCK NOUCK Philippe	Professor	On duty
10	NOUAYOU Robert	Professor	On duty
11	SAIDOU	Professor	**Chief of centre /IRGM/MINRESI**
12	TABOD Charles TABOD	Professor	**Dean FS Univ. Bamenda**
13	TCHAWOUA Clément	Professor	On duty
14	WOAFO Paul	Professor	On duty
15	ZEKENG Serge Sylvain	Professor	On duty
16	BIYA MOTTO Frédéric	Associate Professor	**General director /HYDRO Mekin**
17	BODO Bertrand	Associate Professor	On duty
18	ENYEGUE A NYAM épse BELINGA	Associate Professor	On duty
19	EYEBE FOUDA Jean sire	Associate Professor	On duty
20	FEWO Serge Ibraïd	Associate Professor	On duty
21	MBINACK Clément	Associate Professor	On duty
22	MBONO SAMBA Yves Christian U.	Associate Professor	On duty
23	MELI'I Joelle Larissa	Associate Professor	On duty
24	MVOGO ALAIN	Associate Professor	On duty
25	NDOP Joseph	Associate Professor	On duty
26	SIEWE SIEWE Martin	Associate Professor	On duty
27	SIMO Elie	Associate Professor	On duty
28	VONDOU DerbetiniAppolinaire	Associate Professor	On duty
29	WAKATA née BEYA Annie Sylvie	Associate Professor	**Director/ENS/UYI**
30	WOULACHE Rosalie Laure	Associate Professor	**In training course**
31	ABDOURAHIMI	Senior Lecturer	On duty
32	AYISSI EYEBE Guy François Valérie	Senior Lecturer	On duty
33	CHAMANI Roméo	Senior Lecturer	On duty
34	DJIOTANG TCHOTCHOU Lucie Angennes	Senior Lecturer	On duty
35	EDONGUE HERVAIS	Senior Lecturer	On duty

36	FOUEJIO David	Senior Lecturer	**Chief of Cell MINADER**
37	KAMENI NEMATCHOUA Modeste	Senior Lecturer	On duty
38	LAMARA Maurice	Senior Lecturer	On duty
39	OTTOU ABE Martin Thierry	Senior Lecturer	**Director of reagents production Unit IMPM**
40	TEYOU NGOUPO Ariel	Senior Lecturer	On duty
41	WANDJI NYAMSI William	Senior Lecturer	On duty
42	NGA ONGODO Dieudonné	Assistant lecturer	On duty
43	SOUFFO TAGUEU Merimé	Assistant lecturer	On duty

10- DEPARTMENT OF EARTH SCIENCES (ES) (43)			
1	BITOM Dieudonné-Lucien	Professor	**Dean / FASA /Univ. Dschang**
2	NDAM NGOUPAYOU Jules-Remy	Professor	On duty
3	NDJIGUI Paul-Désiré	Professor	**Head of Department**
4	NGOS III Simon	Professor	On duty
5	NKOUMBOU Charles	Professor	On duty
6	NZENTI Jean-Paul	Professor	On duty
7	ONANA Vincent Laurent	Professor	**Head of Department/ Univ. Ebolowa**
8	YENE ATANGANA Joseph Q.	Professor	**Head of Division /MINTP**
9	ABOSSOLO née ANGUE Monique	Associate Professor	**Vice-Dean / DRC**
10	BISSO Dieudonné	Associate Professor	On duty
11	EKOMANE Emile	Associate Professor	**Head of Division /Univ Ebolowa**
12	Elisé SABABA	Associate Professor	On duty
13	FUH Calistus Gentry	Associate Professor	**State secretary /MINMIDT**
14	GANNO Sylvestre	Associate Professor	En poste
15	GHOGOMU Richard TANWI	Associate Professor	**Head of division /Univ. Bertoua**
16	MBIDA YEM	Associate Professor	On duty

17	MOUNDI Amidou	Associate Professor	**TC /MINIMDT**
18	NGO BIDJECK Louise Marie	Associate Professor	On duty
19	NGUEUTCHOUA Gabriel	Associate Professor	**CEA/MINRESI**
20	NJILAH Isaac KONFOR	Associate Professor	On duty
21	NYECK Bruno	Associate Professor	On duty
22	TCHAKOUNTE Jacqueline épse NUMBEM	Associate Professor	**Chief of Cell /MINRESI**
23	TCHOUANKOUE Jean-Pierre	Associate Professor	On duty
24	TEMGA Jean Pierre	Associate Professor	On duty
25	ZO'O ZAME Philémon	Associate Professor	**General Director/ART**
26	ANABA ONANA Achille Basile	Senior Lecturer	On duty
27	BEKOA Etienne	Senior Lecturer	On duty
28	ESSONO Jean	Senior Lecturer	On duty
29	EYONG John TAKEM	Senior Lecturer	On duty
30	MAMDEM TAMTO Lionelle Estelle, épouse BITOM	Senior Lecturer	On duty
31	MBESSE Cécile Olive	Senior Lecturer	On duty
32	METANG Victor	Senior Lecturer	On duty
33	MINYEM Dieudonné	Senior Lecturer	**Head of division /Univ. Maroua**
34	NGO BELNOUN Rose Noël	Senior Lecturer	On duty
35	NOMO NEGUE Emmanuel	Senior Lecturer	On duty
36	NTSAMA ATANGANA Jacqueline	Senior Lecturer	On duty
37	TCHAPTCHET TCHATO De P.	Senior Lecturer	On duty
38	TEHNA Nathanaël	Senior Lecturer	On duty
39	FEUMBA Roger	Senior Lecturer	On duty
40	MBANGA NYOBE Jules	Senior Lecturer	On duty
41	KOAH NA LEBOGO Serge Parfait	Assistant lecturer	On duty
42	NGO'O ZE ARNAUD	Assistant lecturer	On duty
43	TENE DJOUKAM Joëlle Flore, spouse KOUANKAP NONO	Assistant lecturer	On duty

DISTRIBUTION OF PERMANENT LECTURERS IN THE FACULTY OF SCIENCE OF THE UNIVERSITY OF YAOUNDE I ACCORDING TO DEPARTMENTS

NUMBER OF LECTURERS

DEPARTMENT	Professor	Associate Professor	Senior lecturer	Assistant lecturer	Total
BCH	8 (01)	15 (11)	13 (03)	7 (05)	**43 (20)**
ABP	14 (01)	16 (09)	18 (04)	4 (02)	**52 (16)**
PBP	6 (01)	12 (02)	13 (07)	3 (00)	**34 (10)**
IC	7 (01)	15 (04)	5 (01)	1 (00)	**28 (06)**
OC	6 (01)	18 (04)	11 (04)	2 (00)	**37 (09)**
CS	2 (00)	2 (00)	14 (01)	4 (00)	**22 (01)**
MAT	1 (00)	8 (00)	17 (01)	7 (02)	**33 (03)**
MIB	2 (01)	7 (03)	8 (04)	7 (02)	**24 (10)**
PHY	15 (01)	15 (04)	11 (01)	2 (00)	**43 (06)**
ES	8 (00)	17 (03)	15 (04)	3 (01)	**43 (08)**
Total	**69 (07)**	**125 (40)**	**125 (30)**	**40 (12)**	**359 (89)**

A total of **359 (89)** including

-Professors	**69(07)**
-Associate professors	**125 (40)**
-Senior lecturers	**125 (30)**
-Assistant lecturer	**40 (12)**
( ) = Number of women	**89**

DEDICATION

I DEDICATE THIS WORK TO:

MY GRAND MOTHER

ACKNOWLEDGEMENTS

All senior researchers and students in the Laboratory of Phytobiochemistry and Medicinal Plants Studies, for their constructive ideas, advice, assistance and contribution to this work.

Special thanks to my closest friends **DOUANGUIM NGUEMO Joel** and **NGAMO TCHIAMENI Yvon** for all your support and advice You have always been my push-up, guys.

The **Tali** and **Mbakop** families for their constant encouragement, May God bless and guide them in all their activities.

All those whose names are not mentioned here; your contributions have been of great help for the success of this work.

TABLE OF CONTENTS

LIST OF ABBREVIATIONS AND ACRONYMS

Symbol and Acronyms	Full Names
COVID19	Coronavirus Disease 2019
WHO	World Health Organization
ACT	Artemisinin-based Combination Therapies
*Pf*LDH	*Plasmodium falciparum* lactate dehydrogenase
GTS	Global Technical Strategy
HIV	Human Immunodeficiency Virus
HRP II	Histidine-Rich Protein II
OECD	Organization for Economic Co-operation and Development
*Pf*Hda2	*Plasmodium falciparum* Histone deacetylase
*Pf*HP1	*Plasmodium falciparum* Hetero-Proteins 1
*Pf*AP2 G	*Plasmodium falciparum* Apelata 2G
ROS	Reactive Oxygen Species
TNF	Tumor Necrosis Factors
TLR4	Toll-Like Receptor-4
RDTs	Rapid Diagnostic Tests
AL	Artemether-Lumefantrine
AS-AQ	Artesunate-Amodiaquine
AS-MQ	Artesunate-Mefloquine
AS-SP	Artesunate-Sulphodoxine-Pyrimethamine (
DHA+PPQ	Dihydroartemisinin-Piperaquine
EPSPS	5-enolpyruvl shikimate 3-phosphate synthase
DOXP	1-deoxy-D-xylulose-5-5phosphate
HPLC	HighPressure Liquid Chromatography
UV	Ultra Violet
UHPLC	Ultra-Hight Performance Liquid Chromatography
TOF	Time Of Fly
MS	Mass Spectrometry
NMR	Nuclear Magnetic Resonance
APAD	acetylpyridine adenine dinucleotide
NBT	nitrotetrazolium blue chloride
PES	phenazine ethosulphate
MMV	Medicine for Malaria Venture
UPLC	Ultra-Performance Liquid Chromatography
QTOF	Quqdrupole Time of Fly
RPMI 1640	Roosevelt Park Memorial Institute 1640
S/N	Signal to Noise ratio
S/B	Signal to Background ratio
CQ	Chloroquine
Art	Artemisinin
NMR	Nuclear Magnetic Resonance
COSY	Correlated Spectroscopy
HMBC	Heteronuclear Multiple Bond Connectivity

LIST OF FIGURES

LIST OF PHOTOGRAPHS

LIST OF TABLES

LIST OF ANNEXES:

ABSTRACT

Antimalarial drug resistance is a pressing issue, necessitating the development of new therapeutic agents. Plants from Cameroon, *Terminalia ivorensis* and *Terminalia brownii*, have been used for malaria treatment. To address this, a simple and reproducible *Plasmodium falciparum* Lactate Dehydrogenase (*Pf*LDH) screening model was validated to identify novel antimalarial hits from these plants and their specificity of action. The study validated a *Pf*LDH-based assay to detect *Plasmodium falciparum* Dd2 and 3D7 strains. Extracts from *T. brownii* and *T. ivorensis* stem barks were tested for antiplasmodial activity and selectivity on normal Raw and Vero cells. The most active extracts were found to be aqueous extract of *T. ivorensis* (Ti^W) and methanolic extract of *T. brownii* (Tb^M) and further screened *in vivo* for their antimalarial efficacy in *Plasmodium berghei* (strain NK65) infected mice. The dual-step activity guided fractionation of Ti^W and Tb^M using column chromatography resulted in fractions and subfractions that were screened for antiplasmodial and selectivity. The phytochemical profile of most active fractions was determined using UPLC-QTOF-MS analysis. The isolated bioactive molecules were characterized using UPLC MS/MS and NMR data analysis. The activity of hits subfractions and isolated compounds was further investigated using tests such as gametocyte, haemozoin, and oxidative stress. The pharmacodynamics profile of potent hits was assessed through stage-specific analysis and time kill-kinetics using standard protocols. As results, the *Pf*LDH assay showed acceptable linearity profiles for *Pf*3D7 and *Pf*Dd2 at 2% parasitemia and 1% hematocrit. It was robust with an inter-assay reproducibility of 5.47. Nine (09) extracts were active against *P. falciparum* strains (IC$_{50}$ values ranging from 0.13 µg/mL to 10.59 µg/mL), with Ti^W and Tb^M showing higher activities and good selectivity. They were safe *in vivo* and significantly suppressed parasitemia levels in *P. berghei* infected mice. The bio-guided fractionation of Tb^M and Ti^W led to four fractions and eight (08) subfractions along with one compound, Eschweilenol C, with good antiplasmodial activity. The phytochemical analysis revealed ellagic acid, leucodelphidin, and papyriogenin D. All subfractions and Eschweilenol C showed transmission-blocking activity on late gametocyte stages. Hits subfractions significantly reduced haemozoin production and showed strong killing activity on ring and trophozoite stages. In conclusion, A *Pf*LDH-based assay was established and validated using standard antimalarial drugs. The bio-guided study of *T. ivorensis* and *T. brownii* extracts supports their traditional malaria treatment.

Keywords: Malaria, *Pf*LDH assay, Antimalarial efficacy, *Terminalia ivorensis*, *Terminalia brownii*, Stage-specific kill kinetics.

RESUME

La résistance aux médicaments antipaludiques est un problème urgent qui nécessite le développement de nouveaux agents thérapeutiques. Des plantes du Cameroun, *Terminalia ivorensis* et *Terminalia brownii*, sont traditionnellement utilisées pour le traitement du paludisme. Un modèle simple et reproductible basé sur le lactate déshydrogénase de *Plasmodium falciparum* (*Pf*LDH) a été validé pour identifier de nouveaux antipaludiques de ces plantes et leur spécificité d'action. Le test basé sur le *Pf*LDH a été validé pour détecter les souches de *Plasmodium falciparum* Dd2 et 3D7. Des extraits d'écorces de *T. brownii* et de *T. ivorensis* ont été testés pour leur activité antiplasmodiale et leur sélectivité sur des cellules normales. Les extraits les plus actifs se sont révélés être l'extrait aqueux de *T. ivorensis* (Ti^W) et l'extrait méthanolique de *T. brownii* (Tb^M) et ont ensuite été examinés *in vivo* pour leur efficacité antipaludique. Le fractionnement guidé par l'activité en deux étapes de Ti^W et de Tb^M à l'aide de la chromatographie sur colonne a abouti à des fractions et sous-fractions qui ont été criblées pour leur activité antiplasmodial et leur sélectivité. Le profil phytochimique de la plupart des fractions actives a été déterminé par analyse UPLC-QTOF-MS. Les molécules isolées ont été caractérisées par analyse de données UPLC MS/MS et RMN. L'activité des sous-fractions et des composés isolés a été étudiée plus en détail à l'aide de tests tels que les gamétocytes, l'hémozoïne et le stress oxydatif. Le profil pharmacodynamique a été évalué par une analyse spécifique des stades et une cinétique de destruction temporelle à l'aide de protocoles standard. En guise de résultats, le test *Pf*LDH a montré des profils de linéarité acceptables pour *Pf*3D7 et *Pf*Dd2 à 2 % de parasitémie et 1 % d'hématocrite. Il était robuste avec une reproductibilité inter-essai de 5,47. Neuf (09) extraits étaient actifs contre les souches de *P. falciparum* (IC$_{50}$: 0,13 à 10,59 µg/mL), Ti^W et Tb^M montrant des activités plus élevées et une bonne sélectivité. Ti^W et de Tb^M étaient non toxique *in vivo* et ont montré une bonne capacité à inhiber significativement la parasitemie des animaux. Le fractionnement bio-guidé du Tb^M et du Ti^W a conduit à quatre fractions et huit sous-fractions ainsi qu'un composé, l'Eschweilenol C, présentant une bonne activité antiplasmodiale. La phytochimie a révélé la présence de l'acide ellagique, la leucodelphidine et la papyriogénine D. Toutes les sous-fractions et l'eschweilenol C ont montré une activité de blocage de la transmission aux stades tardifs des gamétocytes. Les sous-fractions « hits » ont inhibé la formation de l'hémozoïne et avec une activité préférentielle sur les stades en anneaux et trophozoïte. En conclusion, un test basé sur la *Pf*LDH a été établi et validé à l'aide de médicaments antipaludiques standards. L'étude bio-guidée de *T. ivorensis* et de *T. brownii* soutient leur usage traditionnel contre le paludisme.

Mots clés : Paludisme, Lactate Déshydrogénase, Efficacité antipaludique, *Terminalia ivorensis*, *Terminalia brownii*, Cinétique d'inhibition.

INTRODUCTION

INTRODUCTION

Despite great control and management efforts, malaria is still one of the major causes of death and poverty in Africa. Vulnerable groups, including pregnant women and children, are disproportionately affected. Endemic countries are now facing the double challenge of protecting their citizens not only from malaria but also from emerging diseases such as COVID-19. The World Health Organization (WHO) estimated that in 2022, there were 249 million cases and 608000 deaths from malaria worldwide, and *P. falciparum,* the most virulent and drug-resistant human malaria parasite, accounted for 90% of malaria cases in the African Region (WHO., 2023). Most of the cases and deaths averted were in the WHO African Region (cases 82%, deaths 94%), with children under five bearing the highest burden (WHO., 2023). In the absence of an effective vaccine, the management of malaria relies mainly on vector control and chemotherapy. These efforts are frustrated by a lack of treatment compliance, and vector and parasite drug resistance. Existing malaria treatment in Africa includes artemisinin-based combination therapies (ACTs). However, parasites resistant to artemisinin and their partner drugs have emerged and are now undermining all malaria control efforts (Menard and Dondorp., 2017). One of the most serious threats to malaria control has been resistance to ACTs in the Greater Mekong Subregion. If artemisinin resistant strains of *P. falciparum* arise in or are imported to Africa, it would be catastrophic for malaria control on the African continent. Of note, a high frequency of unexplained slow parasite clearance times has been reported among Ugandan children treated with intravenous artesunate for severe malaria (Asua et al., 2021; Rosenthal, 2021).

Emphasis must therefore be placed on the search for new active agents with novel modes of action to fight against parasite resistance. These include innovative antimalarial drugs with a novel mode of action displaying not only efficacy against symptom-causing malaria but also transmission-blocking properties. Looking back in history, malaria chemotherapy has a strong historical link to natural products. The most successful antimalarial agents such as artemisinin and its predecessor quinine have their origins in plant metabolites (Tajuddeen and Heerden, 2019) and give the hope that other antimalarial drugs could be developed from medicinal plants in the future. In Africa and Cameroon in particular, plant extracts are still widely used to combat malaria (Tsabang *et al.,* 2012; Yamthe *et al.,* 2015). Therefore, the investigation of Cameroonian antimalarial medicinal plants could lead to the identification and isolation of potent molecules with the ability to inhibit *P. falciparum* with a novel mechanism of action. In this direction, widely distributed *Terminalia* spp. such as *T. ivorensis* A. Chev and *T. brownii*

Frosen are famous due to their usefulness in traditional medicines to treat malaria and yellow fever (Liu *et al.,* 2009)**.** However, little is known about the extent of their antiplasmodial activity across the *P. falciparum* life cycle. *T. ivorensis* and *T. brownii* are promising sources for the search for new multistage antiplasmodial hits with a novel mode of action. To discover such agents, standardized and validated screening assays are of great importance. The advancement in knowledge regarding parasite biology, materials science, and technology has led to several sensitive *in vitro* antiplasmodial assay methods (Fidock *et al.,* 2004) among which the *Plasmodium falciparum* lactate dehydrogenase-based assay (*Pf*LDH) remains one of the most reliable and cost-effective methods (Makler et al., 1993; Makler and Hinrichs, 1993).

Of note, the *Plasmodium falciparum* lactate dehydrogenase assay (*Pf*LDH) is among the *in vitro* methods used to assess antiplasmodial activity. Indeed, the design of the *Pf*LDH assay is based on the fact that L-lactate dehydrogenase from *P. falciparum* is essential for the anaerobic life-cycle of the *Plasmodium* parasite, and compounds that inhibit the enzyme also kill the parasite. Some methods have already been developed and validated based on *P. falciparum* lactate dehydrogenase (*Pf*LDH), a representative malaria biomarker, using a microfluidic microplate-based immunoassay (Lee *et al.,* 2020) and antimalarial drug screening (Penna-coutinho *et al.,* 2011). However, these methods are very expensive and not easily applicable for researchers in low- and middle-income countries. Therefore, a simple colorimetric assay based on plasmodial lactate dehydrogenase called the *Pf*LDH-based assay was validated. In fact, *Pf*LDH (LDH; L-lactate: NAD$^+$ -oxidoreductase, EC 1.1.1.27) is an important terminal enzyme of the glycolytic pathway in *Plasmodium* parasites, and thus it plays a critical role in anaerobic carbohydrate metabolism for ATP production. As a result, *Plasmodium* parasites consume 30–50 times more glucose than their host cells (Makler and Hinrichs. 1993; Makler *et al.,* 1993; Gomez *et al.*, 1997; Dunn *et al.,* 1996). Given that the architecture of *Pf*LDH differs from that of the host, with Ser163 replaced by Leu163 conferring activity with 3-acetylpyridine adenine dinucleotide (APAD$^+$), an analog of NAD$^+$, its production and accumulation are utilized as indicators to determine the viability of parasites ((Makler and Hinrichs. 1993 ; Makler *et al.,* 1993 ; Gomez *et al.*, 1997; Dunn *et al.,* 1996; Sherman. 1961; Brown *et al.*, 2004). Nevertheless, parasite lactate dehydrogenase exhibits high specificity for pyruvic acid, even more, restricted than the specificity of human lactate dehydrogenases M4 and H4. Parasite lactate dehydrogenase exhibits high catalytic efficiency in the reduction of pyruvate, kcat: Km=9.0×10^8 min^{-1}/M^{-1}. Additionally, parasite lactate dehydrogenase exhibits an enhanced kcat with the analog 3-acetylpyridine adenine dinucleotide (APAD$^+$) whereas the human isoforms exhibit a lower kcat. This differential response to

APAD$^+$ provides the kinetic basis for the enzyme-based detection of malarial parasites (Dunn *et al.,* 1996). Hence, the development of reduced APAD (APADH) is proportional to *Pf*LDH activity and parasitemia (Makler and Hinrichs. 1993). Furthermore, it has major advantages such as cost effectiveness, optimization potential, scalability and minimum demand in instrumentation. Moreover, this method is simple, fast, cheap, reproducible, requires minimal instrumentation, and can be automated with little data variability (Sinha *et al.,* 2017).

Research questions

- What is the effectiveness of *Plasmodium falciparum* lactate dehydrogenase-based assays in detecting malaria in culture?
- Can *Terminalia ivorensis* and *Terminalia brownii* extracts be used as potential inhibitors of *Plasmodium falciparum* growth *in vitro* and *in vivo*?
- How can the efficacy of *Terminalia ivorensis* and *Terminalia brownii* extracts as *Plasmodium falciparum* inhibitors be optimized through bio-guided search strategies?
- What is the mechanism by which *Terminalia ivorensis* and *Terminalia brownii* derivatives inhibit the growth of *Plasmodium falciparum*, and how can this knowledge be applied to developing new antimalarial drugs?

Hypothesis

- The validation of a simple and reproducible *Pf*LDH screening model could help to look for novel antimalarial hits from *T. ivorensis* and *T. brownii* and study their pharmacodynamics profiles.

General objective

- Examine assay conditions and validate a simple and reproducible *Pf*LDH screening model and applied it to the search for antimalarial hits from *T. ivorensis* and *T. brownii* coupled to the study of their pharmacodynamics profile.

Specific Objectives:

- Demonstrate reliability, robustness, and reproducibility of the *Pf*LDH-based method to be used for antiplasmodial drug screening.
- Determine active and selective plant extracts on resistant and sensitive strains of *P falciparum*; their class of toxicity and antimalarial efficacy in *P. berghei* NK65 infected mice.
- Identify selective *P. falciparum* inhibitors and their mode of action.

LITERATURE REVIEW

CHAPTER I

I-LITERATURE REVIEW

I.1-Generalities on the malaria

I.1.1- Malaria

Malaria is a parasitic disease caused by apicomplexan parasites of the genus *Plasmodium*. *Plasmodium falciparum, Plasmodium. vivax, Plasmodium ovale curtisi, Plasmodium ovale wallikeri, Plasmodium malariae* and *Plasmodium knowlesi* are the most common parasites causing diseases in humans (Ashley and Ashley, 2018). *Plasmodium falciparum* and *Plasmodium* vivax are the most prevalent (WHO. 2023). *P. vivax* and *P. ovale* are relapsing malaria with a dormant hypnozoite stage in the liver and *P. knowlesi* is a predominantly zoonotic infection with macaques acting as natural hosts. The World Malaria Report 2023, which was just published, presents a worrisome image of the malaria epidemic worldwide in 2022. Malaria is still a serious public health concern in spite of ongoing efforts; incidence and mortality are higher now than they were prior to the COVID-19 pandemic (WHO. 2023; Uwimana et al., 2020; 2021; Balikagala et al., 2021). The situation is made worse by the increasing effects of climate change, which, in addition to other difficulties, pose a threat to undo the advances made3 in the fight against the illness. According to the analysis, there was a 5 million rise in global malaria cases from 2021 to 2022, or around 249 million cases (WHO. 2023). The disease was estimated to have killed 608,000 people worldwide in 2019, an increase of over 6%. What is especially concerning is the persistently high illness burden in Africa. In 2022, the African continent borne a disproportionate share of the global malaria load, accounting for 94% of cases and 95% of deaths. Of these deaths, children under the age of five accounted for almost 78% (WHO. 2023; Uwimana et al., 2020; 2021; Balikagala et al., 2021).

The report for this year specifically highlights climate change as a major threat to the advancements made in the fight against malaria. Extreme weather events and other climate-related disruptions have made the disease's spread worse. For example, the floods in Pakistan in 2022 increased the number of malaria cases by over 2 million. The spread of malaria into the African highlands, which were formerly less affected because of their colder environment, is another noteworthy example (WHO. 2023). These changes highlight how the dynamics of malaria transmission might be affected by climate change, making efforts to manage and eradicate the illness even more difficult. Malaria prevention initiatives are under threat from many issues in

addition to climate change. Growing concern is the growing resistance to current management measures, including as pesticides and antimalarial medications. The world malaria report in 2023 also highlights the threat posed by the emergence and spread of the invasive *Anopheles stephensi* mosquito in Africa. This mosquito is particularly adept at breeding and sustaining malaria transmission in urban settings and highly resistant to current insecticides. These factors, coupled with health system challenges and a significant funding gap (which reached US$3.7 billion in 2022) paint a picture of a battle against malaria that is becoming increasingly complex (WHO. 2023).
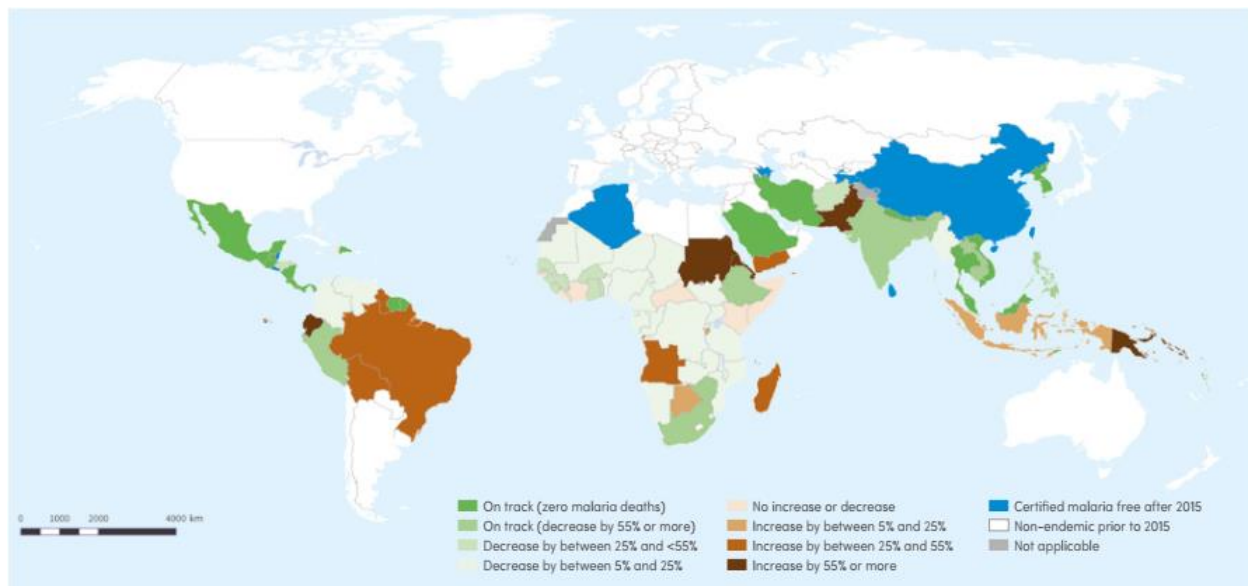
Figure 1: Map of malaria endemic countries (including the territory of French Guiana) showing progress towards the GTS 2025 malaria mortality rate milestone of at least 75% reduction from a 2015 baseline (World Malaria Report. 2023)**.**

In Cameroon, malaria is the primary cause of morbidity and mortality (WHO, 2013). Despite efforts to curb the disease's incidence, malaria accounts for 48% of all hospital admissions, 30% of morbidity and 67% of childhood mortality per year in the country (WHO. 2020; Ngum et al., 2023). The occurrence and transmission of malaria parasite in the tropics is influenced by climatic conditions such as temperature and humidity. In countries with endemic malaria, the annual economic growth rates over 25 years were 1.5% lower than in other countries (Gallup and Sachs, 2001). Malaria is commonly associated with poverty and may also be a major hindrance to economic development (Teklehaimanot and Mejia, 2008). Overall, malaria is a complicated disease and its spread may be attributed to a variety of factors such as ecological and

socioeconomic conditions, displacement of large populations, agricultural malpractice that causes an increase in vector breeding sites, parasite resistance to antimalarial drugs and vector resistance to insecticides.

I.1.2-*Plasmodium* species suitable for human disease research and vectors

Malaria parasites infect a variety of vertebrate hosts from mammals to birds and reptiles. The six human infective *Plasmodium* species of public health importance are *P. falciparum*, *P. vivax*, *P. malariae*, *P. ovale curtisi*, *P. ovale wallikeri* and *P. knowlesi*. (Ashley and Ashley, 2018; Ngotho *et al.,* 2019). *Plasmodium falciparum* malaria is the most lethal, and *P. vivax* malaria is the most prevalent outside of Africa. *P. knowlesi* has also emerged in the past decade as a significant source of zoonotic infections in Southeast Asia (Singh and Daneshvar, 2013). In preclinical research, *Plasmodium* cyno*molgi* has been used as an *in vivo* model for *P. vivax* in nonhuman primates. Similarly, *P. knowlesi* has been established as an *in vitro* model for *P. vivax* (Ngotho *et al.,* 2019). Rodent malaria parasites are the most popular *in vivo* malaria models used for different aspects of disease and immunological studies. Among these, *P. berghei* is the most studied of these parasites, as it can also be used to induce experimental cerebral malaria, thus modelling an important clinical complication of *P. falciparum* infection. The *P. berghei*-infected mouse model is also characterized by the ability to efficiently produce all parasite life cycle stages under laboratory conditions and its ease of genetic modification.

I.1.3- *Plasmodium parasite*

The *Plasmodium* is an intracellular Apicomplexan parasite characterized by the presence of a special apical complex that is involved in host-cell invasion and the apical complex is made up of the microneme, dense granules and rhoptries (Cowman and Crabb, 2006).
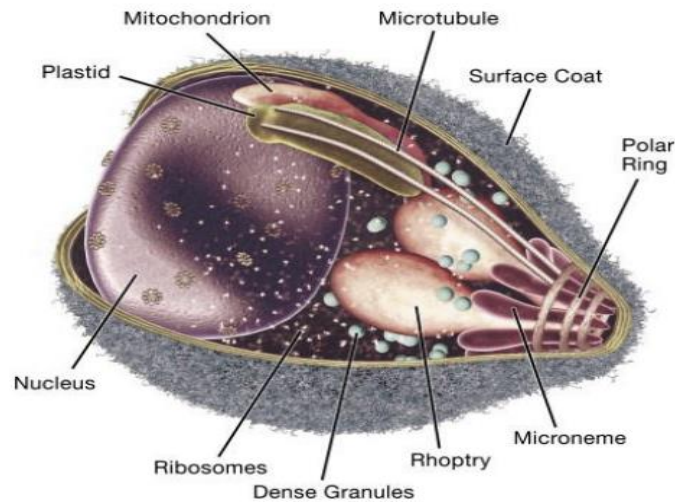
Figure 2: *Plasmodium falciparum* merozoite showing apical complex and other cellular organelles. (Cowman and Crabb, 2006).

I.1.3.1-Life cycle of *Plasmodium falciparum*

The malaria parasite is transmitted to the human host when an infected female Anopheles mosquito takes a blood meal and simultaneously injects a small number of sporozoites into the blood stream. After reaching the liver, the sporozoites invade hepatocytes, which develop into a liver schizont and replicate asexually (**Figure 3**). After approximately seven days of liver stage development, each infected hepatocyte releases up to 40,000 merozoites that enter the peripheral bloodstream. Once in the bloodstream, merozoites quickly invade circulating red blood cells (RBCs), thereby initiating the repeated asexual replication cycle. Over 48 hours, the parasite progresses through the ring and trophozoite stages before finally replicating into 8–32 daughter merozoites at the schizont stage (schizogony) (**Figure 3**). At this point, the parasitized RBC (pRBC) ruptures and releases merozoites into circulation, commencing another round of asexual replication. Mature asexual stages that display increased stiffness, trophozoites and schizonts, adhere to the vasculature in various organs, which allows them to avoid splenic clearance. During each cycle, a small subset of parasites diverts from asexual replication and instead produces sexual progeny that differentiates the following cycle into male and female sexual forms, known as gametocytes.

A subset of parasites leaves the peripheral circulation and enters the extravascular space of the bone marrow, where gametocytes mature and progress through stages I–V over eight to ten

days (gametocytogenesis) (**Figure 3**). Although evidence suggests that the bone marrow is the primary location of gametocyte maturation, some immature gametocytes have been observed elsewhere in the human body, such as in the spleen. By stage V, male and female gametocytes re-enter peripheral circulation, in which they become competent for infection with mosquitoes. Once ingested by a mosquito, male and female gametocytes rapidly mature into gametes (gametogenesis). Within the midgut, the male gametocyte divides into up to eight flagellated microgametes (exflagellation), whereas the female gametocyte develops into a single macrogamete. Fertilization of a macrogamete by a microgamete result in the formation of a zygote, which undergoes meiosis and develops into an invasive ookinete that penetrates the mosquito gut wall. The ookinete forms an oocyst within which the parasite asexually replicates, forming several thousand sporozoites (sporogony). Upon oocyst rupture, these sporozoites migrate to the salivary glands, where they can be transmitted back to the human host during a blood meal. Asexual parasites (in RBCs) are represented in pale yellow and sexual parasites are represented in green**.** (Nilsson *et al.,* 2015)**.**
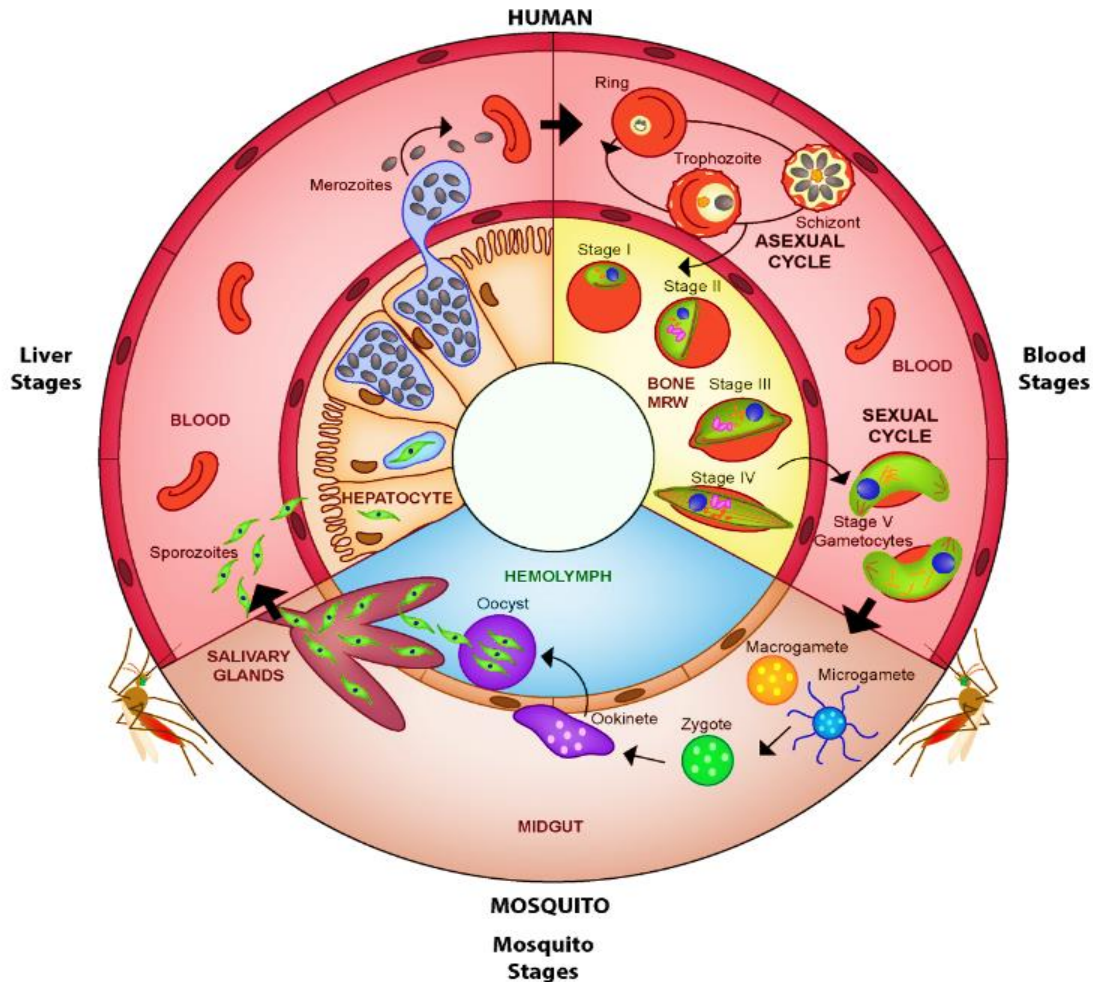
Figure 3: *Plasmodium* life cycle (Nilsson *et al.,* 2015)

During the trophozoite stage of the erythrocytic life cycle, *P. falciparum* ingests up to 80% of the host haemoglobin through a protozoan, phagocytic organelle known as the cytostome **(Figure 4)** (Goldberg *et al.,* 1990). The cytostome then transports haemoglobin into an acidic digestive vacuole. Here, it is broken down by proteolytic enzymes in an ordered catabolic process into small peptides to be used as nutrients by the parasite (Egan, 2008). Consequently, for every molecule of haemoglobin that is consumed, four molecules of haem (ferriprotoporphyrin IX, [Fe (III)PPIX]) are released. Due to the high toxicity of free heme, organisms must rapidly convert this molecule into an inert form, many through the enzyme heme oxygenase (Sigala *et al.,* 2012). Haematophagous organisms, such as the *Plasmodium*, *Schistosoma* and *Boophilus* species, do not contain any functional haem oxygenase activity (Sigala *et al.,* 2012). Instead, they must utilize a unique pathway to crystallize heme into a nontoxic biomineral, known as hemozoin (Sigala *et al.,* 2012). Similar to the tight regulation of intracellular heme levels in vertebrates, these parasites do not tolerate high levels of free heme without

harmful effects. Hemozoin is a biologically unique dimer of five-coordinate Fe (III)PPIX linked by reciprocating monodentate carboxylate linkages from one of the protoporphyrin IX's propionate moieties. The biomineral is composed of an extended network of these dimeric units hydrogen-bonded together via the second propionic acid group of protoporphyrin IX **(Figure 4)**. Hence, the formation of such an insoluble biomineral sequesters the bulk of the reactive iron, preventing any deleterious reactions. Disruption of this process has been demonstrated to be a prime target for antimalarial drugs, primarily since hemozoin is unique to the parasite (Egan, 2008).
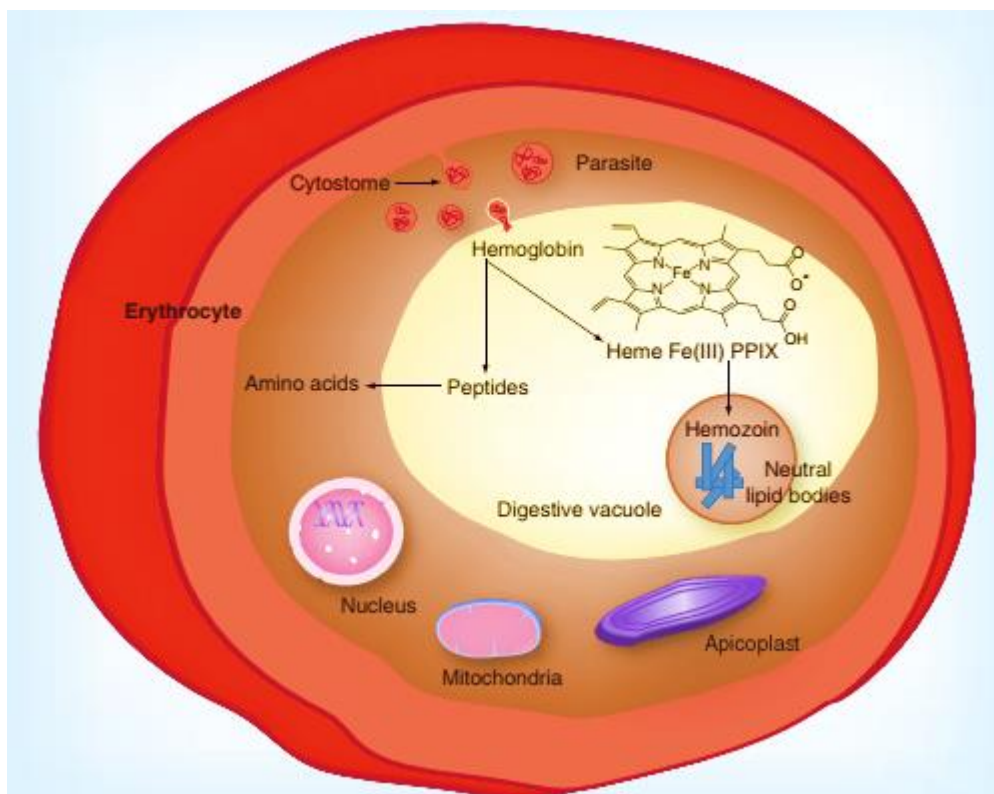
Figure 4: Representation of hemozoin formation within the intraerythrocytic life cycle of *Plasmodium falciparum*. Host haemoglobin is taken up by the parasite and transported to the digestive vacuole through the cytostome. In this acidic organelle, haemoglobin is digested into small peptides and four toxic heme units (ferriprotoporphyrin IX). Neutral lipid bodies mediate the detoxification of the haem byproduct through the formation of hemozoin (Sigala et al., 2012).

I.1.3.2-Biology of *Plasmodium falciparum* transmissible gametocyte stages

     Plasmodium gametocytes are the only parasite stage that can be transmitted to the mosquito vector. Gametocytes are sexual precursor cells of the malaria parasite that go between the

transmission of the parasite from its human host to the Anopheles mosquito vector. Gametocytes cause no clinical manifestations (Nilsson *et al.,* 2015). Once these gametocytes have matured, they are picked up by an Anopheles mosquito during a blood meal (**Figure 5, D**). In the mosquito midgut, they become activated and differentiate into male and female gametes. The male gamete then fertilizes the female gamete resulting in the formation of a zygote. The zygote further develops into a motile ookinete, which penetrates the gut epithelium and subsequently develops into an oocyst. The oocyst then matures releasing sporozoites, which migrate to the salivary gland of the mosquito. The parasite is transmitted to another mammalian host through an infected mosquito bite (**Figure 5, D**) (Kuehn and Pradel, 2010). Gametocytes, therefore, provide a link in malaria transmission from the human host to the mosquito, thereby making them prime targets for transmission-blocking intervention strategies. These strategies rely on either vaccines or drugs, that target the gametocyte or mosquito midgut stages to block parasite transmission from the human to the mosquito, thereby preventing the spread of the disease.
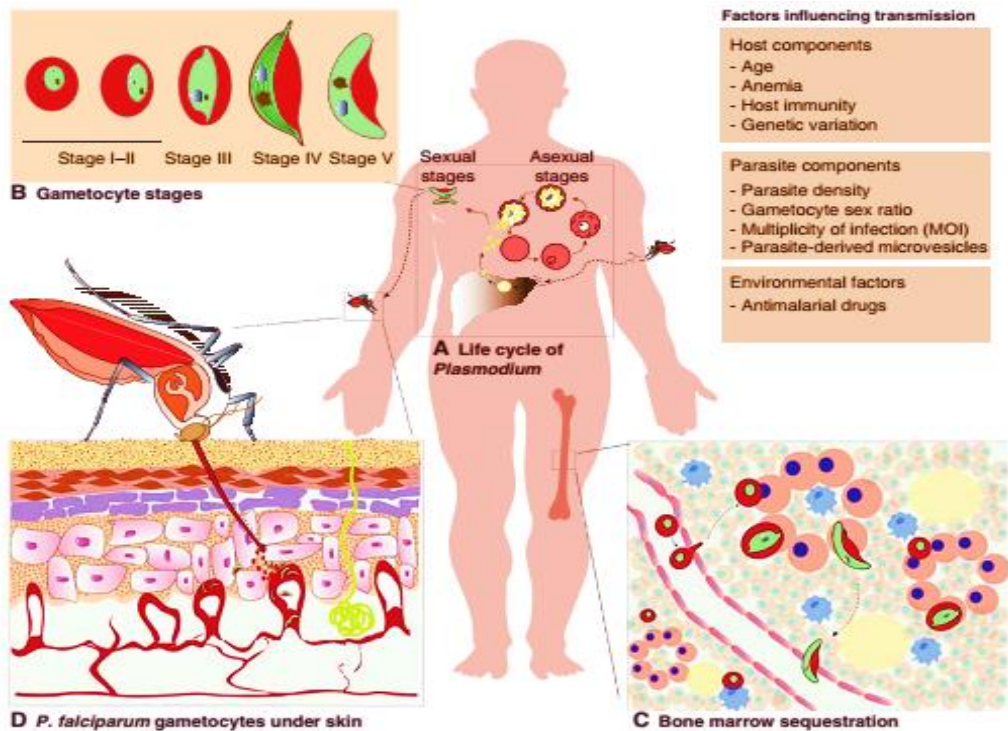
Figure 5: The *P. falciparum* transmissible stages in the human host (Meibalan and Marti, 2016).

Commitment to the sexual pathway occurs at a low "baseline" rate during each asexual replication cycle (Kafsack *et al.,* 2014; Sinha *et al.,* 2014), and the decision to switch is thought to be made before schizogony during the previous asexual replication cycle. In addition, merozoites

released from a single sexually committed schizont can either become male or female gametocytes and the characteristic female-biased sex ratio observed in the malaria parasite is due to the production of a higher percentage of committed female schizonts than their male counterparts (Bertuccini *et al.,* 2012). The switch to gametocytogenesis is governed by the essential master regulator of gametocytogenesis, the transcription factor *Pf*AP2 G, which is epigenetically controlled by *Pf*Hda2 and *Pf*HP1 (Coleman et al., 2014)**.**

The ambitious goal of malaria eradication needs to successfully target this area of study (Sinden, 2017; Wells *et al.,* 2009)**.** Nevertheless, strategies targeting the transmissible gametocyte stages would require a drug to be at pharmacologically relevant concentrations for as long as mature gametocytes circulate (up to 30 days), the most appropriate point of intervention is to target the host gametocytes and eliminate the parasite population thus interrupting transmission.

The pathophysiology of malaria involves oxidative stress arising from two main sources: first, as a result of the high metabolic rate of the rapidly growing and multiplying parasite within the erythrocyte and second as the result of the host immune response to the infection (Postma *et al.,* 1996).

I.1.3.3- *Plasmodium falciparum* **vs human Lactate Dehydrogenase**

Lactate dehydrogenase (LDH; L-lactate: NAD^+-oxidoreductase, EC 1.1.1.27), the last enzyme in the glycolytic pathway, is one of the most active enzymes expressed by *P. falciparum* (Vander and Hunsaker. 1990; Vander *et al.,* 1981). Parasite LDH (*Pf*LDH) is a 316 amino acid protein coded by a single gene on chromosome 13 and expressed as a 1.6-kb mRNA (Bzik *et al.,* 1993). The amino acid sequence predicted from genomic and complementary DNA sequencing indicates that essential catalytic residues are conserved, such as His195, Asp168, Arg109, and Arg171 (using standard numbering for LDH, (Eventoff *et al.,* 1977)). However, there are a number of interesting sequence differences between *Pf*LDH and human LDH, including an extra segment of five amino acids that are in a loop that helps to define the active site of LDH. Ile250 and Thr246, which from crystallographic analysis appear to be critical active site residues (Grau *et al.,* 1981; Dun *et al.,* 1991) that help to define substrate and cofactor binding sites and are conserved in other LDH, are replaced by proline in *Pf*LDH. Likewise, the conserved active site Asp197 is replaced by Asn197 in *Pf*LDH. These sequence differences suggest that the kinetic properties of *Pf*LDH may be distinct from those of human LDH. Indeed, previous kinetic studies of *Pf*LDH have demonstrated some unique properties of the parasite enzyme compared to human LDH, including

insensitivity to inhibition by pyruvate or by the pyruvate–NAD$^+$ complex (Vander *et al.,* 1981). Recently, the crystal structure of the ternary complex of *Pf*LDH, NADH, and oxamate was reported (Vander *et al.,* 1996).
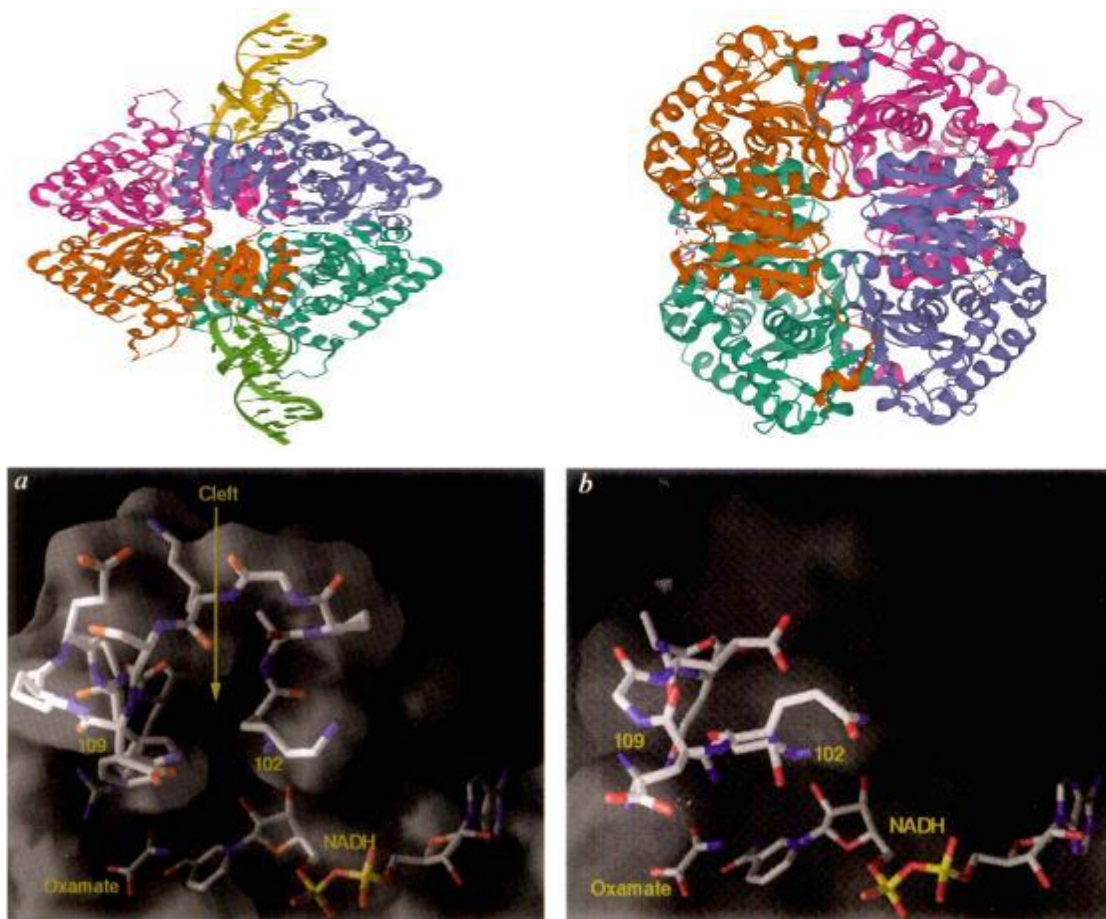
Figure 6: Human and *Plasmodium falciparum* lactate dehydrogenase. **a**: Surface representation showing the cavity (arrowed) in *Pf*LDH formed by the extended specificity loop adjacent to the substrate binding site. **b**: the equivalent surface region in mammalian LDH shows no cavity adjacent to the substrate specificity loop and substrate binding site (Dunn *et al.,* 1996).

In addition to a marker of parasite viability, *Pf*LDH is an appealing diagnostic biomarker for malaria for several reasons. First, *Pf*LDH is conserved across all four *Plasmodium* species known to infect humans, whereas histidine-rich protein II (HRPII), a common malarial biomarker, is specific only for *Plasmodium falciparum* (Brown et al., 2004). Second, pLDH activity in host circulation clears within 24 h after successful treatment, leading to fewer false-positive diagnoses due to biomarker persistence after elimination of infection, a common occurrence with HRPII (Iqbal et al., 2004). Hence, a drug-sensitivity assay, which displays inhibitory profiles of parasite

metabolic activity through estimation of enzyme *Pf*LDH was developed by Makler and Hinrichs (1993). The assay is rooted on monitoring the ability of LDH enzyme to quickly use a coenzyme, APAD which is a NAD analog, in reaction, that converts lactate into pyruvate. However, LDH of the host erythrocytes carries out the same reaction at a very slow pace in the presence of APAD. In the assay, development of reduced APAD (APADH) is measured, which interprets a direct correlation between parasitemia level and *Pf*LDH activity (Makler and Hinrichs, 1993; Makler et al., 1993). During validation of the enzymatic assay based on *Pf*LDH for antiplasmodial drug screening, different parameters for assay quality and performance are calculated. Out of these, we have standard deviation (SD), standard error of the mean (SEM), percent coefficient of variation (%CV), signal to background ratio (S/B), signal to noise ratio (S/N) and the Z-factor Zhang *et al.*, (1999). Among these parameters or statistical tests, the Z'-factor is a measure of statistical effect size where the results are given as a numerical value (ranging from 0 to 1), being more favourable as it approaches 1(Zhang *et al.*, 1999; Peatey *et al.*, 2012). % CV is acceptable at < 20% (Hawking *et al.*, 1971).

I.1.3.2- Oxidative stress in malaria

During the malaria life cycle, *Plasmodium* digests haemoglobin within its acidic food vacuole and releases toxic ferriprotoporphyrin IX (FP) and reactive oxygen species (ROS) (Postma *et al.,* 1996). Normally most of the released FP is polymerized into crystalline hemozoin or malaria pigment (Egan *et al.,* 2002), but a significant amount escapes polymerization and must be detoxified in the cytoplasm (Zhang *et al.,* 1999). Free FP can interact with phospholipid membranes causing structural defects due to the reactivity of its attached Fe^{3+} with unsaturated membrane lipids. This can lead to increased membrane permeability for ions, cell swelling and lysis (Famin *et al.,* 1999; Foster 1981). This fraction of FP is detoxified by glutathione-dependent pathways and FP-binding proteins of both the parasite and the host (Famin *et al.,* 1999). The host immune system, either in response to antigen presentation or in response to sequestered parasites, secretes several cytokines including tumor necrosis factor-alpha (TNF-α) which trigger inflammatory reactions leading to an increase in ROS through mechanisms such as respiratory burst by macrophages. The binding of FP to CD14 and toll-like receptor-4 (TLR4) triggers the production of TNF-α by macrophages (Figueiredo *et al.,* 2007). In addition, reoxygenation of hypoxic tissues that are primarily blocked by sequestering parasites can contribute to ROS production (Becker *et al.,* 2004). Therefore, finding antimalarial drugs that can scavenge ROS or

stimulate the production of ROS to contribute to *P. falciparum* death will be very important in the malaria drug discovery pipeline. In that way, oxidative stress induced by antimalarial agents is important in malaria parasite clearance as the most potent, both recent and current potent quinoline antimalarial drugs, and ACTs are thought to act by increasing cellular oxidative stress. In contrast, excessive production of ROS can exacerbate malaria pathology such as anemia (due to massive hemolysis) with eventual metabolic acidosis (due to reduced oxygenation of tissues as a result of anemia) and respiratory distress (Kavishe *et al.,* 2017). Therefore, combining the antimalarial properties and antioxidant potential of a given antimalarial drug will be very important for future malaria chemotherapy.

Measurement of antioxidant properties in plant-derived compounds require appropriate methods that address the mechanism of antioxidant activity and focus on the kinetics of the reactions involving the antioxidants. Methods based on inhibited autoxidations are the most suited for chain-breaking antioxidants and for termination-enhancing antioxidants, while different specific studies are needed for preventive antioxidants. A selection of chemical testing methods is critical to investigate both pure molecules and plant extracts (Amorati and Valgimigli. 2018).

Inhibited autoxidation methods are based on the measurement of the rate of autoxidation of a reference substrate, both in the presence and in the absence of antioxidants. These methods are the golden standard because they test antioxidants in close-to-real settings, i.e. they challenge their ability to protect a substrate from oxidation (Amorati and Valgimigli. 2015). The autoxidation can occur spontaneously at room or at high temperature, or it can be induced by the addition of specific initiators, such as an azo-compound or the Fenton reagent (H_2O_2 and Fe^{2+}). Compared to other methods of initiation, azo-initiators, such as the lipid-soluble AIBN (2,2′-azobis-isobutyronitrile), or water-soluble AAPH ((2,2′-azobis(2-amidinopropane) dihydrochloride), are better suited to perform kinetic studies because their decomposition occurs at a constant rate at a given temperature, thus providing a constant rate of initiation (Ri) throughout the reaction course.

Interestingly, many popular methods to assess antioxidant activity are based on the competitive reaction of radicals with the antioxidant or with a probe, whose transformation can be monitored by fluorimetry (e.g. the ORAC assay) by spectrophotometry (e.g. the crocin bleaching assay), by EPR (e.g. spin-trapping methods) or other techniques (Amorati and Valgimigli. 2015). All these methods, despite their popularity, do not involve any substrate autoxidation and offer limited information on the actual antioxidant activity (Amorati and Valgimigli. 2015; Amorati et

al., 2013). Another very popular family of methods is that of indirect methods, which are based on the reaction of the potential antioxidant with some unnatural colored persistent radical (e.g. the DPPH test, the TEAC test, the Galvinoxyl test), or with other oxidizing agents like Fe3+ ions (e.g. the FRAP test), or Cu2+ ions (e.g. the CUPRAC test) or others (e.g. the Folin-Ciocalteu test) (Amorati and Valgimigli. 2015; Niki. 2010). In general, these tests do not provide any measurement of the antioxidant activity, rather they tell, respectively, of the radical-trapping activity or of the reducing ability of a compound or extract, which should never be overlooked when interpreting or presenting their results (Amorati and Valgimigli. 2015).

I.1.4-Diagnosis of malaria

Prompt and accurate diagnosis of malaria is essential for successful malaria treatment and eradication (Berkley *et al.,* 1999)**.** The diagnosis of malaria is based on recognizing clinical symptoms and confirmation with the detection of parasites in the blood. In sub-Saharan Africa, many primary health care facilities lack diagnostic equipment, such as microscopes, and well-trained staff for high-quality laboratory diagnosis (Ngasala *et al.,* 2008)**.** Malaria diagnosis is therefore still based on clinical features such as fever and the presence of anaemia **(**WHO, 2009**)**. However, symptoms and signs of malaria are nonspecific. Symptoms of malaria commonly overlap with many other acute febrile illnesses and co-infections (Berkley *et al.,* 1999; Dempsey and Infirmary, 1993; Källander *et al.,* 2004; Tahita *et al.,* 2013)**,** as a result, malaria misdiagnosis and overdiagnosis are very common in sub-Saharan Africa (Amexo *et al.,* 2004; Gwer *et al.,* 2007; Reyburn *et al.,* 2004)**.** The laboratory methods of malaria diagnosis include light microscopy and parasite antigen detection also known as the rapid diagnostic tests (RDTs).

I.1.4.1-Light microscopy

Laboratory diagnosis by microscopy examination of stained blood smears remains the gold standard for case management, epidemiological studies, clinical trials of antimalarial drugs and vaccines, and quality assurance of other malaria diagnostics tests. The microscopy of Giemsa stained blood films has high sensitivity and specificity when used by well-trained staff, which can detect as few as 50 parasites/µl blood under field conditions such as COVID19 and dengue (Moody, 2002; Payne, 1988)**.** Other advantages of microscopy include low cost, determination of parasite densities, distinction between parasite species, differentiation between parasite stages and possible diagnosis of other diseases. However, the accuracy and usefulness of microscopy depend

on factors such as the quality of the microscope, reagents and experience of the technician (Makler *et al.,* 1998)**.**

I.1.4.2-Rapid diagnostic tests

Rapid diagnostic tests use immunechromatographic technology to detect antigens derived from malaria parasites (Wongsrichanalai *et al.,* 2002)**.** Malaria antigens currently used as diagnostic targets include histidine-rich protein II (HRP-II) specific for *P. falciparum* (Murray and Bennett, 2009)**.** Another antigen is parasite lactate dehydrogenase (pLDH) for the detection of *Plasmodium* species. Monoclonal antibodies against pLDH can differentiate between *P. falciparum* and *P. vivax* (Murray and Bennett, 2009)**.** There is limited data on the use of RDTs to identify *P. knowlesi*, however, findings from a study show that the pLDH antibodies that detect *P. falciparum* and *P. vivax* can also be used to detect and distinguish *P. knowlesi* (Mccutchan *et al.,* 2008)**.** *Plasmodium* aldose enzyme can also be used as a universal antigen target for all malaria parasites (Murray *et al.,* 2008)**.** Unlike HRP-II, pLDH is cleared from the blood at approximately the same time as the parasites following successful treatment (Moody *et al.,* 2000; Wongsrichanalai *et al.,* 2007)**.** However, both pLDH and aldolase are expressed in gametocytes, limiting their use in monitoring the response to therapy (Mueller *et al.,* 2007)**.** Rapid diagnostic tests offer a good alternative to microscopy, they are simple to perform and do not require skilled personnel (Murray *et al.,* 2003)**.** However, limitations to RDTs include high cost, lack of density determination, persistent positivity and low sensitivity (Murray *et al.,* 2003)**.**

I.1.5-Malaria treatment and therapeutics targets

Due to the development and spread of *P. falciparum* resistance to conventional monotherapies such as chloroquine and sulfadoxine-pyrimethamine (Myint *et al.,* 2004)**,** the WHO has recommended treatment of malaria with combination therapy such as ACTs (Wells et al., 2009)**.** Artemisinin derivatives are extremely potent antimalarials also active on gametocytes (Barnes *et al.,* 2005; Sutherland *et al.,* 2005). The WHO currently recommends the following ACTs: artemether-lumefantrine (AL), artesunate-amodiaquine (AS+AQ), artesunate-mefloquine (AS+MQ), artesunate-sulfadoxine-pyrimethamine (AS+SP) and dihydroartemisinin-piperaquine (DHA+PPQ) (**Figure 6; Table 1**) (**WHO 2010).** Many countries in Africa, including Cameroon, have adopted ACTs in the past decade to treat uncomplicated malaria. Severe malaria is treated

with cinchona alkaloids (quinine and quinidine) and artemisinin derivatives (artesunate, artemether and artemotil) **(WHO 2012)**.
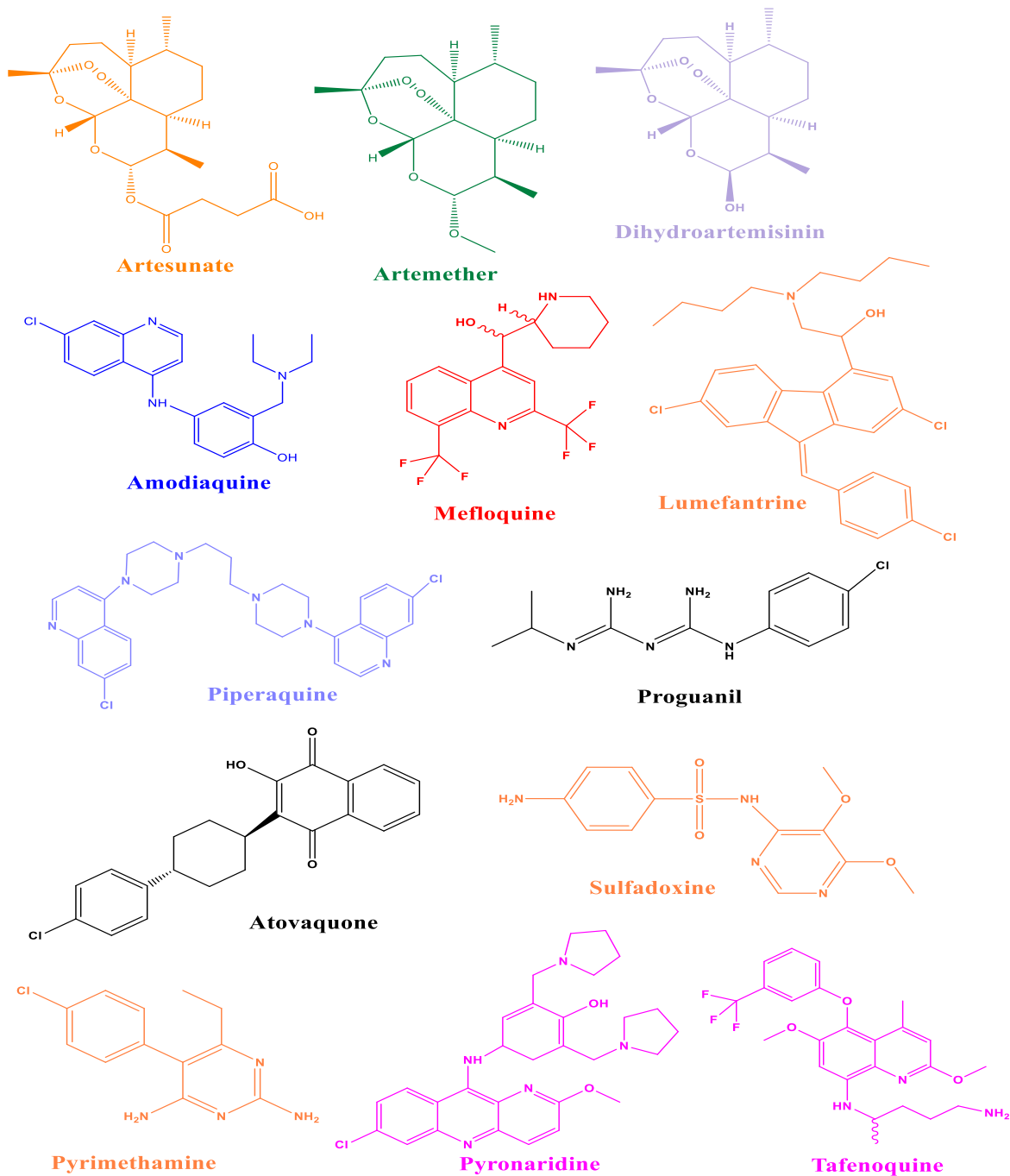

Figure 7: Structure of drug approved for use against malaria. (Tse *et al.,* 2019)**.**

Table 1: The existing and novel drug targets for *P. falciparum* asexual-blood stages.

Target Location	Pathway/mechanism of action	Target molecule	Examples of therapies for *P. falciparum* asexual-blood stages		Drawbacks and adverse effects
			Existing therapy	**New therapy**	
Cytosol	Folate Metabolism	Dihydrofolate reductase	Pyrimethamine, Proguanil	Chlorproguanil	Gastrointestinal disturbances, headache, dizziness, redness, Photosensitivity leukopenia, haemolytic anaemia
		Dihydropteroate synthase	Sulfadoxine, dapsone		
	Pyrimidine metabolism	Thymidylate synthase		5-Fluoroorotate	
	Purine metabolism	HGPRT		Immucillin-H	
	Glycolysis	Lactate dehydrogenase		Gossypol derivatives	
		Peptidedeformylase		Actinonin	
	Protein Synthesis	Heat shock protein 90		Geldanamycin	
	Glutathione metabolism	Glutathione reductase		Enzyme inhibitors	
	Redox system	Thioredoxin reductase		5,8-Dihydrooxy-1,4-napthoquinone	
		Gamma-GCS		Buthionine sulfoximine	
	Signal transduction	Protein kinases		Oxindole derivatives	
	Shikimate	EPSPS		Glyphosate	
	CDK	Pfmrk		Oxindole derivatives, thiophene sulfonamide	
	Generation of free-radical which in turn damage proteins required for parasite survival	Haem and *Pf*ATP6 (Ca2+ transporter); *Pf*PI3K.	Artemisinins		Drug resistances
Parasite membrane	Phospholipid synthesis	Choline transporter		G25	
	Membrane transport	Unique channels	Quinolines	Dinucleoside dimers	Hypoglycemia, hematologic disorders, neurotoxic.
		Hexose transporter		Hexose derivatives	
Food vacuole	Haem polymerization	Haemozoin	Chloroquine	New quinolines	Pruritus, hepatitis, skin eruptions, headache and drug resistances.
	Haemoglobin hydrolysis	Plasmepsins		Protease inhibitors, pepstatin	
		Falcipains		Protease inhibitors, leupeptin	
x	Free radical generation	Unknown	Artemisinin	New peroxides	Drug resistances

Table 2: (Continued) The existing and novel drug targets for *P. falciparum* asexual-blood

Mitochondrion	Electron transport	Cytochrome c oxidoreductase	Atovaquone		High – grade resistance
Apicoplast	Protein synthesis	Apicoplast ribosome	Tetracyclines, Clindamycin		
	DNA synthesis	DNA gyrase	Quinolines		Hypoglycemia, hematologic disorders, neurotoxic.
	Transcription	RNA polymerase	Rifampin		
	Type II fatty acid biosynthesis	FabH		Thiolactomycin	
		FabI/PfENR		Triclosan	
	Isoprenoid synthesis	DOXP reductoisomerase		Fosmidomycin	
	Protein farnesylation	Farnesyl transferase		Peptidomimetics	
Extracellular	Erythrocyte invasion	Subtilisin serine proteases		Protease inhibitors	

Abbreviations: EPSPS, 5-enolpyruvl shikimate 3-phospate synthase; CDK, cyclin dependent protein kinase; DOXP, 1-deoxy-D-xylulose-5phosphate; GSC, glutamylcysteine synthetase; HGRT, hypoxanthine-quanine-zanthine phosphoribosyltransferase; PfENR, *Plasmodium falciparum* enoyl-ACP reductase; *Pf*PI3K, *P. falciparum* phosphatidylinositol-3-kinase (Baruah *et al.,* 2017; Fidock *et al.,* 2004; Jana and Paliwal, 2007; Pan *et al.,* 2018; Rosenthal, 2003; Tse *et al.,* 2019).

Table 3: Current transmission blocking Therapies and those under Development for *Plasmodium falciparum* sexual stages

Target Location	Pathway/mechanism of action	Target molecule	Transmission blocking Therapies		Drawbacks or adverse effects
			Gametocytocidal Therapies	**Sporontocidal Therapies**	
Current transmission-blocking Therapies					
	Metabolism	electron transport functions of ubiquinone	Primaquine		Toxicity in patient with Glucose-6-phosphate deficiency.
Red blood cells	Heme polymerization and the haemoglobin catabolic pathway	Haemoglobin	Artemisinin and ACTs		Parasite resistance
Transmission blocking Therapies under Development					
	All sexual stages and sporogonic development		Tafenoquine	Tafenoquine	Toxicity in patient with Glucose-6-phosphate deficiency.
			Trioxaquines		Low Toxicity in patient with Glucose-6-phosphate deficiency.
Cytosol	Protein's synthesis	Cysteine proteases and Proteasomes	*Epoxomicin*		
		Disulfide reductases and Heme detoxification	Methylene Blue (Methylthioninium Chloride)		
			Sodium beta-Artelinate		
			Alpha/beta arteether		
	Sporogonic development			Dyhydroacridine-dione	
Cytosol	Gametocytogenesis	Protease	Tipranavir (Aptivus)		
Red blood cell	Gametocytogenesis	Haemoglobin	*Riboflavin*		

Abbreviations: ACTs: Artemisinin Based Combination Therapy

(Brueckner *et al.,* 1998; Coleman *et al.,* 2001; Crockett and Kain, 2007; Czesny *et al.,* 2009; Pandey *et al.,* 1999; Peatey *et al.,* 2010)

Referring to chemoprevention, intermittent preventive treatment (IPT) in infants (IPTi), pregnant women (IPTp) and seasonal malaria chemoprevention (SMC) in children aged 3-59 months are control measures aimed at preventing clinical episodes of malaria in highly susceptible populations. For the widely adopted IPTp strategy, two doses of Sulphadoxine-pyrimethamine (SP) were recommended for all pregnant women in their second trimester and were associated with a reduction in placental malaria, anaemia, neonatal mortality and low birth weight (Eisele et al., 2012; Kuile et al., 2015). IPTi using SP has been recommended for use in areas of high transmission intensity provided SP resistance has not compromised its efficacy. Its use has been associated with over 30% protective efficacy against clinical episodes of malaria and hospital admissions associated with malaria parasitaemia (Aponte et al., 2007). In areas with highly seasonal malaria, SMC treatment with amodiaquine and SP has been associated with up to 80% reduction in clinical malaria and anaemia (Cairns et al., 2012; Wilson and Taskforce, 2011). Despite the clear potential gains and their recommendation by WHO, chemoprevention, particularly IPTi and SMC have not been fully adopted in endemic regions. While IPTp is in use in over 20 countries in sub-Saharan Africa, only 31% of eligible pregnant women received the full dose in 2015 (WH0, 2017). One concern over the widespread implementation of either of the above prophylaxis measures in endemic regions is the emergence and spread of drug-resistant parasites that might make the control measure obsolete (Tilley et al., 2016).

One of the most serious threats to malaria control has been resistance to ACTs in the Greater Mekong Subregion and Africa. Emphasis must therefore be placed on the search for alternative active agents that can replace ACTs in the event of widespread resistance. One potential vast source that remains relatively unscrutinized in this effort remains medicinal plant species (Moyo *et al.,* 2016).

I.2- Medicinal plants: A promising alternative to malaria treatment

Medicinal plants play a vital role in medicines in many developing countries. They are the main ingredients of plant-derived phytodrugs used for the treatment of malaria and other diseases (Tlhapi *et al.,* 2018)**.** In addition**,** medicinal plants remain credible reservoirs of bioactive molecules (Ghasemzadeh and Ghasemzadeh, 2011). Historically, the clear majority of existing drugs for all indications are based on natural compounds or derivatives thereof (Atanasov *et al.,* 2015). Additionally, plants constitute a huge reservoir for antimalarial, as evidenced by the Cinchona tree and *Artemisia annua* which contain quinine and artemisinin, respectively.

Africa, in general, is known for its very rich traditional knowledge on the use of medicinal plants to control, prevent and cure malaria. In Cameroon, most of the people in the endemic region rely widely on medicinal plants for malaria prevention and treatment. The importance of traditional medicines, derived from plants, is of great importance in most parts of both Africa and Asia (Geach, 2005; Moshi and Mbwambo, 2005; Steenkamp *et al.,* 2004).

In the light of the enormous role and the importance of medicinal plants together with the necessity to discover novel bioactive agents to combat malaria, we find it opportune to contribute in the same line with the investigation of two *Terminalia* genera (*Combretaceae family*) from Cameroonian flora for their antimalarial properties.

I.2.1- Generalities on *Combretaceae* Family

The family *Combretaceae* comprises of 20 genera and approximately 475 species (Thiombiano *et al.,* 2006)**.** Of these, about 200 belong to the genus *Terminalia*, making it the second-largest genus of the family after *Combretum* (Masevhe and Mabogo, 2007)**.** The family is distributed throughout the tropical and subtropical regions of the world (Lamb and Ntima, 1971)**.** Approximately 54 species of *Terminalia* are naturally distributed throughout western, eastern and southern Africa (Lebrun and Stork, 1991; Smith *et al.,* 2004).

I.2.1.1-The genus *Terminalia*

The genus *Terminalia* derives its Latin name (*terminalis* = end) from the position of the leaves, which are crowded at the ends of the shoots (Lamb and Ntima, 1971; Rogers and Verotta, 1996). *Terminalia spp*. range from small and medium-sized shrubs or trees to large deciduous forest trees, ranging in height from 1.5 to 75 m tall (Lebrun and Stork 1991; Schmidt *et al.,* 2002). *Terminalia trees* are bisexual or hermaphroditic with male and female flowers carried on the same plants. These flowers are apetalous, small, and cream to pale, bright yellow or greenish-white, in spicate in florescence. The stalked male flowers tend to be grouped towards the apex and the bisexual flowers tend to be grouped towards the base of the inflorescences (Coates-Palgrave 1977). Many *Terminalia spp*. have been identified as sources of medicines, for their use in pharmaceuticals and cosmetic production (Dalziel, 1937; Irvine, 1961).

I.2.2- *Terminalia ivorensis* A. Chev
I.2.2.1-Botanic Description.

Terminalia ivorensis (local name: Black Afara) is a large deciduous forest tree ranging in height from 15 to 46 m, branchless for up to 30 m. Bole clean, very straight with small

buttresses and sometimes fluted. Mature trees are very flat-topped with a wide horizontal canopy of evenly distributed foliage arising from the apex of the straight bole. In young trees, the branches are whorled; deciduous, young shoots and foliage fall a few years after initial growth, leaving sockets to mark their original position on the bole. Bark smooth and light gray to dark brown when young and on branchlets; in mature trees often blackish, with deep longitudinal fissures. The bark flakes off in long thin strips. Slash yellow. *T. ivorensis* forms a good taproot supported by 6-8 powerful lateral roots. There is also evidence of a widespread and rather superficial root system (Foli, 2009). Leaves 6.4-12.7 x 2.5-6 cm, whorled, simple, oval, blunt-tipped with orange - brown hairs below and on veins above, also on the short stalks; 6-7 pairs widely spaced veins, prominent below. Flowers in axillary spikes 7.6-10.2 cm long with bisexual flowers nearly to the apex. The lower receptacle is densely tomentose, and the upper receptacle is less tomentose (Foli, 2009)**.**

I.2.2.2- Ecology and Distribution.

T. ivorensis is sometimes found in rainforest conditions but is predominantly a tree of seasonal forest zones. It emerges in the upper Torey of the seasonal forest but sometimes loses its vertical-growing leader, resulting in considerable variation in the height of mature trees. As a strong light demander and a good colonizer of abandoned farmlands, *T. ivorensis* can withstand short periods of inundation, although it is usually sensitive to waterlogging. For optimum development, *T. ivorensis* requires high, well-distributed rainfall. It is very vulnerable to fire. The plant is distributed in West and Central Africa (Foli, 2009).

Photography 1: Photograph of Stem bark of *Terminalia ivorensis*. (Tchatat, 2020).

I.2.2.3- Ethnobotanical uses

Terminalia ivorensis is widely used in traditional medicine on several continents in the world for the treatment of numerous diseases including, abdominal disorders, bacterial infections, colds, sore throats, conjunctivitis, diarrhoea, dysentery, fever, gastric ulcers,

headaches, heart diseases, hookworm, hypertension, jaundice, leprosy, nosebleed, oedema, pneumonia and skin diseases (Eloff *et al.,* 2008).

I.2.2.4- Previous studies

Bongo et al. (2018) reported the potential of petroleum ether, Ethyl acetate and methanol extract of *T. ivorensis* against Mycobacterium tuberculosis H37Rv and Mycobacterium tuberculosis spp. on Middlebrook 7H10 agar using a qual approach where the activity was determined by the presence or the absence of growth on the plate. From this investigation, the methanolic extract displayed a good activity on both strains than the petroleum ether and Ethyl acetate (Bongo *et al.,* 2018).

Wande and Babatunde (2017) screened methanolic and acetone extract of leaves of *T. ivorensis* (Combretaceae) by applying the inhibition of β-hematin synthesis, a simple and robust colourimetric assay. As result, the best inhibitory concentration. ($IC_{50} = 2.58 \pm 0.447$ mg/mL) was observed with *T. ivorensis* methanol extract. (TIM) which was comparable with chloroquine standard drug ($IC_{50} = 0.55 \pm 0.1$ 79 mg/mL). Moreover, the *T. ivorensis* methanol extract showed statistically significant activity (P<0.05) at the different concentrations used, comparable to chloroquine (Wande and Babatunde, 2017)**.**

Annan *et al.,* (2012) evaluated the antiplasmodial activity of ethanolic extract of *T. ivorensis* stem bark against chloroquine-resistant strains of *P. falciparum* by using thin blood films to assess the level of parasitemia and parasite growth inhibition. Results from these studies showed that ethanolic extract *T. ivorensis* inhibit *P. falciparum* growth *in vitro* with an IC_{50} of 6.94µg/ml (Annan *et al.,* 2012).

I.2.3-*Terminalia Brownii* Fresen

I.2.3.1- Botanic Description

Terminalia brownii (local name: kuuku, muvuku (Kamba, Kenya), koloswa (northern region, Kenya), weba (Ethiopia), lbukoi (Samburu, Kenya), orbukoi (Maasai, Tanzania), and mbarao or mwalambe, in Kiswahili) is a leafy deciduous tree with an attractive somewhat layered appearance, usually, 4-15(25) m high with a rounded, flat-topped, spreading crown, and a straight bole; branches reaching close to the ground. Slash dull red-brown, the bark of branchlets gray fibrous. Young bark smooth, whitish, old bark gray, longitudinally fissured, and dense hairy (Foli, 2009).

Leaves spirally arranged, crowded at the ends of branches, the underside with white hairs, turning bright red before falling. Broadly elliptic to obovate, wider towards the apex, 6-

16 x 2.5-8 cm, glabrous on the underside, lateral veins prominent, approximately 7 pairs arising from the mid-rib; apex pointed, sometimes notched; margin wavy; petiole 1.5-4 cm long, acuminate, with white hairs (Foli, 2009). Flowers long, white to cream, 0.5 mm wide, glabrous, calyx lobes acuminate, unpleasantly scented, in axillary spikes 9.5-12 cm in length (inflorescence), peduncle 1.5-2 cm long, tomentose. Each inflorescence contains bisexual and male flowers, the male ones towards the apex and the bisexual ones towards the base. Fruit winged, smooth, greenish when young, purplish-red to brown when mature, broadly elliptic to ovate, apex obtuse to rounded, emarginated, base acute to obtuse, 3.5 x 4.2(5) x 2.5 sometimes up to 7.5 cm long; pedicel 0.5-0.7 cm long; endocarp woody, containing long and delicate seeds. Seeds 2-winged, 3 cm long, 2 cm wide, red to purple (Foli, 2009).

I.2.3.2- Ecology and Distribution

Drought-resistant species occur in the high rainfall woodlands, bushlands, and wooded savannah of the arid and semiarid regions but can also be found in the subhumid areas. It is often found near rivers in very dry areas (Foli, 2009) and occurs in parts of Eastern and Central Africa (Mbwambo *et al.,* 2007).

Photography 2: Photograph of *Terminalia brownii* (Tchatat., 2020).

I.2.3.3- Ethnobotanical uses

T. brownii Fresen. is traditionally used as a remedy for malaria, yellow fever, diarrhoea, ulcers, cough, hepatitis, stomach ache and sexually transmitted diseases (Mbwambo *et al.,* 2007).

I.2.3.4- Previous studies

Biruk et al. (2020) evaluated the *in vivo* antimalarial activity of 80% methanol and aqueous extracts of *T. brownii* barks against *P. berghei* in Swiss albino mice using a 4-day suppressive test. The *in vivo* acute toxicity test indicated that both extracts of *T. brownii* did not cause mortality. The 4-day early infection test revealed that the 80% methanol and aqueous extracts exhibited significant inhibition of parasitemia ($p < 0.001$) compared to the negative control. The maximum level of chemosuppression (60.2%) was exhibited at a 400 mg/kg dose of 80% methanol extract. Moreover, the 80% methanol extract showed a significant ($p < 0.001$) attenuation of anaemia associated with infection in a dose-dependent manner. The aqueous extract, on the other hand, exhibited a per cent inhibition of 51.1% at the highest dose (400 mg/kg/day) (Biruk *et al.,* 2020).

Salih et al. (2018) screened eighty extracts and fractions of the stem bark, stem wood, roots, leaves and fruits of *T. brownii* and nine pure compounds present in the active extracts against Mycobacterium smegmatis ATCC 14468 using agar diffusion and microplate dilution methods. On the other hand, phytochemical analysis was employed to identify the compounds in the growth inhibitory extracts using HPLC UV/DAD, GC/MS and UHPLC/Q-TOF MS. As result, the roots of *T. brownii* gave the best antimycobacterial effects (Inhibition Zone 22 –27 mm) against Mycobacterium smegmatis. Sephadex LH- 20 column chromatography purification of *T. brownii* roots resulted in low MIC values of 62.5 µg/ml and 125 µg/ ml for acetone and ethanol fractions, respectively, compared to 5000 µg/ml for the crude methanol extract. Methyl (S)-flavogallonate was suggested to be the main active compound in the Sephadex LH- 20 acetone fraction, while ellagic acid xyloside and methyl ellagic acid xyloside were suggested to give good antimycobacterial activity in the Sephadex LH-20 ethanol fraction. 1,18-octadec-9-ene-dioate, stigmast-4-en-3-one, 5 α -stigmastan-3,6-dione, triacontanol, sitostenone and β -sitosterol were found in antimycobacterial hexane extracts of the stem bark of studied plant. Of these compounds, 1,18-octadec-9-ene-dioate, stigmast-4-en-3-one, 5 α -stigmastan-3,6-dione, triacontanol, sitostenone have not been previously identified in *T. brownii*. Moreover, *T. brownii* contained friedelin, betulinic acid, β-amyrine and two unknown oleanane-type triterpenoids. Of the listed compounds, friedelin, triacontanol and sitostenone

gave a MIC of 250 µg/ml against *M. smegmatis*, whereas stigmasterol and β-sitosterol gave MIC values of 500 µg/ml (Salih *et al.,* 2018).

Machumi et al. (2013) reported that the ethyl acetate-soluble fraction of stem bark extract of an African medicinal plant *Terminalia brownii* led to the isolation of a new oleanane-type triterpenoid, along with seven known triterpenoids, seven ellagic acid derivatives, and 3-*O*-β-D-glucopyranosyl-β-sitosterol. The isolated new compound was identified using spectroscopic methods, notably 1D- and 2D NMR, as 3β,24-*O*-ethylidenyl-2α,19α-dihydroxyolean-12-en-28-oic acid. The isolated compounds were evaluated for their antimicrobial and antiplasmodial activities. Two compounds with a galloyl group (**4** and **6**) were found to be active against chloroquine sensitive (D6) and chloroquine-resistant (W2) strains of *Plasmodium falciparum*, whereas three ellagic acid derivatives (**5**-**7**) were found active against three species of fungi and one species of bacteria (Machumi *et al.,* 2013).

MATERIALS AND METHODS

CHAPTER II
II-MATERIALS AND METHODS

II.1-Materials

II.1.1- Plant collection and authentication

The stem barks of *T. ivorensis* (also known as idigbo, black afara, shingle wood, brimstone and black bark) and *T. brownii* (also known as Embu; Koloswo) were harvested in August 2017 at Carrefour MEEC-Nkolbisson, Yaounde-Cameroon, 3°52′00.0" N 11°3100.1″ E. The plant names were checked with http://www.theplantlist.org and botanical identification was confirmed at the National Herbarium of Cameroon, Yaoundé where voucher specimens are deposited under the reference numbers 48878/HNC and 36394/HNC for *T. ivorensis* (*Ti*) and *T. brownii* (*Tb*) respectively.

II.1.2-*Plasmodium falciparum* strains

The chloroquine-sensitive *Plasmodium falciparum* 3D7 (*Pf*3D7- MRA-102), multidrug resistant *P. falciparum* Dd2 (*Pf*Dd2-MRA-150) and mutant resistant *P. falciparum* GNF-156 strains were obtained from Malaria Research and Reference Reagent Resource (MR4) centre, BEI Resources, 10801 University Blvd. Fax: 703-365-2898 Manassas, VA 20110-2209 USA (www.beiresources.org), and used for this work.

II.1.3- Cell lines

Vero ATCC CRL 1586 (African green monkey kidney) cells and RAW264.7 (macrophage cell) cells were obtained from Centre Pasteur du Cameroun (CPC) and Noguchi Memorial Institute (Ghana) respectively.

II.1.4- Antimalarial standards and reagents

Artemisinin, mefloquine and chloroquine diphosphate were purchased from Sigma-Aldrich, Germany, and compounds. Dihydroartemisinin (MMV000004); Artemisinin (MMV000006); Chloroquine (MMV000008); Lumefantrine (MMV000014); Mefloquine (MMV000015); Piperaquine (MMV000022); Primaquine (MMV000023); Pyrimethamine (MMV000024); Artemisone (MMV000039); Tafenoquine (MMV000043); Atovaquone (MMV000046); 2-Aminopyridine (MMV390048); Quinine sulfate dihydrate (MMV000054); Methylene blue (MMV000061); MMV000052; MMV000147; MMV018912; MMV642943; and MMV000130 were generously provided by Medicines for Malaria Venture, Switzerland and H3D, South Africa. Reagents including acetylpyridine adenine dinucleotide, DMSO, D-

sorbitol, L-lactic acid, acetylpyridine adenine dinucleotide (APAD), phenazine ethosulfate, Triton X-100, nitrotetrazolium blue chloride (NBT), phenazine ethosulfate (PES), RPMI 1640, and gentamicin were all purchased from Sigma-Aldrich, Germany. Albumax I, HEPES, and hypoxanthine were purchased from Gibco, Waltham, MA, USA. Stock solutions of drugs were prepared at 10 mM using absolute DMSO distilled water for chloroquine diphosphate.

II.1.5. Ethical consideration

This study was performed in accordance with the recommendations of the guide for care and use of human samples and laboratory animals in research validated by the Antimicrobial and Biocontrol Agents Unit (AmBcAU), University of Yaoundé I, Cameroon. The protocol was approved by the Institutional Review Board (IRB No. 001/UY11 BTC/IRBI 2022), Biotechnology Centre, University of Yaoundé 1, Cameroon.

II-2- Methods

II.2.1- Implementation and continued validation of malaria *Pf*LDH-based colorimetric assay for its use in malaria drug screening

II.2.1.1-Maintenance of *Plasmodium falciparum* asexual blood stages

II.2.1.1.1- Preparation of host erythrocytes for *Plasmodium falciparum* culture and assays

In vitro culturing of intra-erythrocytic *P. falciparum* parasites and volunteer blood donation for human erythrocytes holds ethics approval from the Biotechnology Centre, University of Yaoundé 1, Cameroon (IRB No. 001/UY11 BTC/IRBI 2022). Human O$^+$ red blood cells for malaria parasite culture were prepared by drawing blood into EDTA vacuum tubes and washing three (03) times in incomplete RPMI 1640 medium to separate the erythrocytes from the plasma. Separation was achieved by centrifuging the blood at 3500 rpm for 5 minutes (Tº: 4ºC) in a Beckman Coulter, Allegra® X-15R centrifuge. The cleaning process was repeated three times. Clean leukocyte-free erythrocytes were stored at 50% hematocrit for further usage.

II.2.1.1.2-Thawing of cryopreserved *Plasmodium falciparum* strains

Plasmodium falciparum strains were thawed by hand and the dissolved parasite-infected RBC suspensions were transferred to a 50 mL tube. One hundred microliters of thawing solution A (12% [w/v] NaCl in distilled water) was added dropwise under constant agitation to the thawed culture. After being allowed to stand for 5 min, 5mL of thawing solution B (1.6%

NaCl in distilled water) was added drop-wise under agitation. The obtained suspension was centrifuged (T°: 4°C) at 2500 rpm for 3 min and the supernatant was removed. Fresh, uninfected RBCs were added to the infected RBC pellet at a ratio of 1:1 and the cells were resuspended in 5 mL of complete RPMI 1640 medium and incubated at 37°C in an atmosphere of 5% O_2, 5% CO_2, and 90% N_2.

II.2.1.1.3- Maintenance of *Plasmodium falciparum* asexual-blood stages

P. falciparum strains 3D7 and Dd2 were maintained in culture as described by (Trager and Jensen 1976). Briefly, parasites were cultured in fresh O positive human red blood cells suspended at 4% (v/v) hematocrit in complete RPMI 1640 medium (500 mL RPMI 1640 (Sigma, Munich, Germany) supplemented with 25 mM HEPES, 10% Albumax I (Gibco, Waltham, MA, USA), 1X hypoxanthine (Gibco, Waltham, MA, USA) and 50 mg/mL gentamicin (Sigma–Aldrich, Munich, Germany). Cultures were incubated at 37°C in a humidified atmosphere of 5% CO_2 and the medium was renewed daily to propagate the culture. Parasite growth was monitored by microscopic examination of Giemsa-stained thin blood smears under immersion oil.

II.2.1.2- Implementation of malaria *Pf*LDH-based colorimetric assay

II.2.1.2.1-Synchronization of asexual-blood stage culture

In a continuous cycle of development, malaria parasites consist of merozoites, ring stages, trophozoites and schizonts stages. Therefore, to obtain the ring stage parasites, the cultures were synchronized using D-sorbitol (Lambros and Vanderberg 1979). Briefly, mixed stage parasite cultures were treated with an equal volume of 5% D-sorbitol solution for 10 min, centrifuged and washed three times with incomplete RPMI 1640. Synchronized *P. falciparum* strains were suspended in a complete medium and the parasitemia was adjusted at 2% parasitemia and 1% hematocrit for the assay.

II.2.1.2.2- Assessment of *Pf*LDH absorbance linearity in drug susceptibility assays

✦ Principle

Plasmodium falciparum LDH in an infected lysed blood sample oxidizes lactate to pyruvate while reducing cofactor $APAD^+$ to APADH. The APADH then reduces a yellow tetrazolium dye, nitroblue tetrazolium (NBT), to a blue diformazan compound with the assistance of phenazine ethosulfate (PES) which is followed at 650 nm.
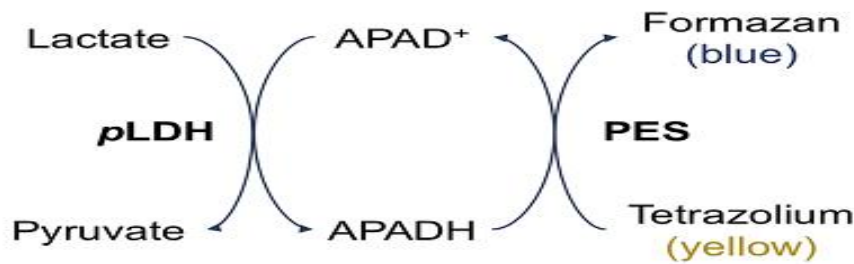
Figure 8: Biochemical reaction of *Plasmodium* lactate dehydrogenase for the detection of malaria parasite in culture.

✚ Procedure

Experimental assay conditions and Tecan M200 microplate reader settings were verified and/or adjusted by examining the *Pf*LDH absorbance linearity of parasitemia values between 0 and 6% (v/v), as determined by microscopic examination of Giemsa-stained malaria parasites. Practically, quadruplets of wells of asynchronous *Pf*Dd2-and *Pf*3D7-parasitized red blood cell cultures containing healthy trophozoites were serially diluted with noninfected erythrocytes at a final hematocrit of 1% in the culture medium. After that, 20 μL (2% parasitemia and 1% hematocrit) of each infected red blood cell culture was transferred to a separate 96-well plate containing 100 μL per well of Malstat solution **[55 mM Tris, 0.22 M L-lactic acid, 0.17 mM acetylpyridine adenine dinucleotide [APAD], 0.2% (v/v) Triton X-100, pH 9.0],** after which 25 μL NBT/PES solution (1.96 mM nitrotetrazolium blue chloride, 0.24 mM phenazine ethosulfate) was added to each well, and the plate was left to develop in the dark for 30 min before recording the absorbance at 650 nm in a Tecan M200 microplate reader. The percent parasitemia (*x* values) was generated using MS Excel, further plotted against the absorbance (*y* values, after background subtraction of noninfected erythrocytes) and analysed by linear regression to determine the goodness of fit (*r*2 value) using GraphPad Prism 5.0.

II.2.1.2.3- Preparation of predosed microplates for *Pf*LDH-assay validation

Predosed microtiter plates were prepared in sterile 96-well tissue culture plates by dissolving the standard antimalarial drugs using a fivefold serial dilution starting from 10 μM to 0.00064 μM in incomplete RPMI 1640 culture medium and frozen at -80°C until use or freshly made the day of the assay. Practically, 2µl of stock solution at 10mM were introduced in the first well (A1, B1, C1 and D1) of 96 well-plates containing 198µl of incomplete RPMI1640. 160 µl were introduced in the remaining wells follow by a fivefold serial to obtain a concentration ranging from 10 µM to 0.00064

II.2.1.2.4- *P. falciparum* growth inhibition assay and assay confirmation.

Antimalarial drugs were evaluated for their inhibitory potential against multi-resistant (PfDd2) strains of *P. falciparum* using the *Pf*LDH assay as described above. In 96-well microtiter plates, 10 µl of inhibitors and 90 µL of synchronized parasites (ring stages) at 2% parasitemia and 1% hematocrit were dispensed in each well. The test concentrations ranged from 0.0064 µM to 1 µM with a final DMSO concentration of less than 0.5% in all wells. The plates were then incubated at 37°C, under a 5% CO_2 atmosphere for 72 h after which the growth inhibition was assessed using a *Pf*LDH-based assay as described by Makler and Hinrichs (1993). In addition, the SYBR green I-based fluorescence method (Smilkstein et al., 2004) and microscopy were also used. For the SYBR green I-based assay, 100 µL (2% parasitemia and 1% hematocrit) of the culture in each well was gently mixed with 100 µl of the SYBR green I lysis buffer solution [0.2 µL of 10,000×SYBR Green I (Invitrogen) per mL of lysis buffer {Tris (20 mM; pH 7.5), EDTA (5 mM), saponin (0.008%; wt/vol), and Triton X-100 (0.08%; vol/vol)}]. The plates were incubated for 1 hour in the dark at room temperature and fluorescence was measured using a Tecan Infinite M200 plate reader (Tecan) at excitation and emission wavelengths of 485 and 538 nm respectively. For microscopy, the parasitemia was determined from thin blood smears stained with 10% Giemsa solution and used to calculate the percentage of growth inhibition. The data analysis was performed with Graphpad Prism 5.0 fitting nonlinear regression and dose - response curves were drawn to determine the inhibitory concentration that reduces 50% of parasite viability (IC_{50}).

II.2.1.3- Assessment of assay quality.

To determine the assay quality or assay performance, the standard deviation (SD), standard error of the mean (SEM), percent coefficient of variation (%CV), signal to background ratio (S/B), signal to noise ratio (S/N) and the Z-factor were calculated according to the formula by Zhang *et al.,* (1999). At least three independent experiments in triplicate for each assay were used to calculate all the parameters. The results are expressed as the percentage of inhibition compared to untreated controls.

The parameters were calculated using the following formulas**:**

$$\mathbf{Z}' = 1 - \frac{3 \times (\text{SD}_{\text{positive}} + \text{SD}_{\text{background}})}{|\text{Mean}_{\text{positive}} + \text{Mean}_{\text{background}}|}$$

$$\%\boldsymbol{CV} = \frac{\text{Mean}}{SD} \times 100$$

$$\frac{S}{B} = \frac{Mean_{positive}}{Mean_{background}}$$

$$\frac{S}{N} = \frac{Mean_{positive} - Mean_{background}}{SD_{background}}$$

II.2.2- *In vitro* **antiplasmodial activity and** *in vivo* **antimalarial efficacy of crude extract from** *T. ivorensis* **and** *T. brownii***.**

II.2.2.1-*In vitro* **antiplasmodial activity and selectivity against erythrocytes and normal cells**

II.2.2.1.1-Processing of plants

The collected samples were dried under shade at room temperature (25°C) for 2 weeks and ground to fine powders. Each powder (1.5 kg) was separately macerated in 4.5 L of ethanol, methanol, ethyl-acetate, hydroethanol (70%) and distilled water for three consecutive days. The macerates were then filtered using Whatman No 1 filter. The process was repeated thrice and the filtrates were pooled and evaporated using a rotary evaporator (Rotavapor, BUCHI 071, Switzerland) at 65°C for alcoholic and hydroethanolic extracts and 75°C ethyl acetate extracts. The aqueous extracts and the remaining aqueous extract from the hydroethanolic extract were lyophilized using a Virtis Wizard 2.0 Freeze Dryer Lyophilizer:Model: XLS-70. The extraction yields were determined and the dried crude extracts were stored at 4 °C for further experiments.

II.2.2.1.2- Predilution of extracts (master plate) for antiplasmodial assay.

The stock of each sample was dissolved at 100 mg/ml in DMSO (Sigma-Aldrich, Germany) and sterilized by using 0.22 µm syringe-adapted filters. Master plates were then prepared by mixing 2 µL of the extract with 198 µl L of fresh incomplete RPMI 1640 to yield a concentration of 1 mg/ml (1% DMSO and 2.5%). Chloroquine and artemisinin (Sigma-Aldrich, Germany), used as standard drugs were prepared at 1 mM in sterile distilled water and 100% DMSO respectively. In all assay plates, except for chloroquine (diluted in distilled water), the final concentration of DMSO was ≤ 0.5%, which was found to be nontoxic to the parasite. Extracts were tested at concentrations ranging from 0.16 to 100 μg/mL and chloroquine and artemisinin were included at the highest concentration of 1 µM (tested concentration: 1; 0.2; 0.04; 0.008; 0.0016).

II.2.2.1.3- Assessment of the hemolytic potential of crude extracts.

✦ Principle

The method is based on release of hemoglobin in response to erythrocyte lysis by tested substance, which can be measured spectrophotometrically at 540 nm.

✦ Experimental procedure

Prior to the evaluation of the antiplasmodial activity, the potential hemolytic effect of the crude extracts was assessed against red blood cells as described by Kazi *et al.,* (1994). Briefly, 250 µl of positive human red blood cells at 2% hematocrit were mixed with 250 µl of different extracts at a concentration range from 250 to 15.625 µg/mL in an Eppendorf tube followed by incubation for 2 h at 37°C. Controls were Triton X-100 0.1% (v/v) and phosphate buffer saline (PBS- negative control), corresponding to 100% and 0% hemolysis respectively. After 2 h of incubation at 37°C, the assay mixture composed of lysed red blood cells and free hemoglobin was centrifuged (1500 rpm, 5 min) and the amount of haemoglobin released was quantified spectrophotometrically in the supernatant at 540 nm using a Magellan Infinite M200 plate reader (Tecan) and compared to the negative control. The hemolysis percentage was calculated as follows:

$$\textbf{\% Haemolysis} = \frac{\text{Absorbance of sample}_{540\,nm} - \text{Absorbance of blank sample}_{540nm}}{\text{Absorbance of positive}_{control540\,nm}} \times 100$$

II.2.2.1.4- *In vitro PfLDH-based antiplasmodial assay of crude extract*

Crude extracts from *T. ivorensis* and *T. brownii* were evaluated for their inhibitory potential against chloroquine-sensitive (*Pf*3D7) and multiresistant (*Pf*Dd2) strains of *P. falciparum* using the *Pf*LDH assay as described in the validation assay. In 96-well flat-bottomed microtiter plates, 10 µL of each inhibitor was added to triplicate wells, followed by 90 µL of synchronized parasites (ring stage) at 2% parasitemia and 1% hematocrit. The test concentrations of the extracts ranged from 0.16 to 100 µg/mL. The negative control consisted of 0.5% DMSO, while the standard drugs (CQ and Art) were tested as positive controls with the highest concentration of 1 µM (tested concentration: 1; 0.2; 0.04; 0.008; 0.0016). The plates were then incubated at 37°C, under a 5% CO_2 atmosphere for 72 h and the inhibitory activity of the extracts was revealed as previously described in the assay validation. The Percent of inhibition was calculated and the dose - response curves generated were used to determine the median inhibitory concentration (IC_{50}) for each inhibitor using GraphPad Prism 5.0 software. The resistance index (RI) was determined as the ratio of the IC_{50} resistant strain to the IC_{50}

sensitive strain**.** RI values below 1 indicated inhibitors preferentially acting against the resistant strains and *vice versa.*

$$\textbf{Percentage of Inhibition } (\%) = \frac{\text{ODcontrol} - \text{ODsample}}{\text{ODcontrol}} \times 100$$

II.2.2.1.5- Resazurin-based *in vitro* cytotoxicity assay.

Defining the potential cytotoxic status of an inhibitor early in the drug development process is an opportunity for ranking and prioritizing selective inhibitors for further investigations (Miret *et al.,* 2006)**.** Cells were grown in T-25 cm^2 flask containing DMEM (Sigma - Aldrich, Munich, Germany) supplemented with 2 mM L-glutamine (Sigma-Aldrich, Munich, Germany) and 10% fetal bovine serum (ATCC) and maintained at 37°C in a humidified incubator containing 5% CO$_2$.

➕ Principle

The biochemical principle of this test relies on the reduction of weakly blue fluorescent resazurin initially blue in colour and very weakly fluorescent into pink and highly fluorescent resorufin (**figure xx**) by mitochondrial dehydrogenases of viable cells. The amount of resorufin produced is therefore proportional to the number of viable cells that can be quantified by fluorometry using a microplate reader at excitation and emission wavelengths of 530 nm and 590 nm respectively.
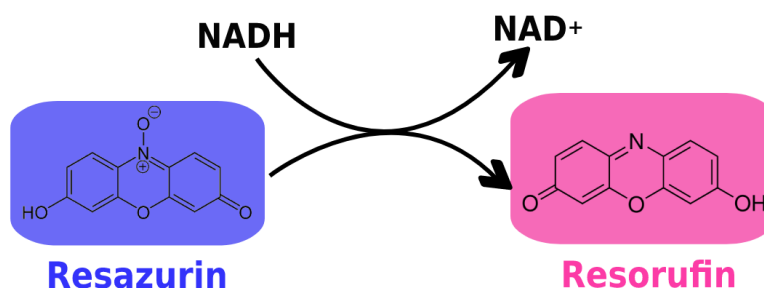

Figure 9: Biochemical reaction of the reduction of Resazurin into resorufin

➕ Procedure

For the experiments, 80–90% confluent cell culture was trypsinized and counted using a Neubeaur cell counter and seeded onto 96-well clear flat-bottomed plates treated for cell culture (Costar, USA) at a cell density of 10^4 cells/well and allowed to adhere overnight. Cells were then treated with serially diluted concentrations (200; 40; 8; 1.6 and 0.32µg/mL) of active crude extracts for 48 h. Afterwards, 10 µl of resazurin solution (0. 15 mg/mL prepared in PBS) was added to each well and plates were reincubated for 4 h (Delves *et al.,* 2019). Of note,

resazurin is a nontoxic, cell-permeable compound that utilizes the reducing power of living cells to detect cell viability by converting from a nonfluorescent blue dye to the highly fluorescent red dye resorufin in response to changes in the reducing environment within the cytosol of the cell. The level of fluorescence that positively correlates with cell viability was measured using a Magellan Infinite M200 plate reader (Tecan, Germany) at an excitation wavelength of 530 nm and an emission wavelength of 590 nm. The inhibitory percentage of cell proliferation was calculated with regard to the negative control. The dose-response curves were plotted using inhibitory percentages versus the logarithm of the drug concentration to determine the concentration of drug that reduces cell viability by 50% (CC_{50}) using GraphPad Prism 5.0. The selectivity index (formula below) was determined for each inhibitor based on their antiplasmodial activity (IC_{50}) and cell cytotoxicity (CC_{50} on Vero and Raw cells).

$$\textbf{Selectivity indices (SI)} = \frac{CC50}{IC50}$$

Cell count method using Neubauer: N= (field 1 + field 2 + field 3 + + field 4)/4

Calibration of cell load = $N*factor\ of\ dilution*10^4$

Active and selective crude extracts from both *Terminalia* species displaying good antiplasmodial activity against sensitive (*Pf*3D7) and mutiresistant (*Pf*Dd2) strains were subjected to an *in vivo* study in order to validate their antimalarial efficacy in an animal model.

II.2.2.2- *In vivo* antimalarial studies of promising crude extracts

In vivo studies were performed using female healthy BALB/C mice between 6–8 weeks old and weighing between 20 – 25g maintained in standard and constant laboratory conditions (23 – 25°C and light/dark cycles i.e., 12/12 h) with free access to food and tap water. Experiments with animals were performed according to the ethical standards formulated in the Declaration of Helsinki, and adequate measures were taken to protect animals from pain or discomfort.

II.2.2.2.1- Acute toxicity test

To assess the safety of *T. ivorensis* and *T. brownii* in animal models, mice were randomly divided into three groups and treated by the oral route with a single dose of aqueous extract of *T. ivorensis* (Ti^W) and methanolic extract of *T. brownii* (Tb^M) stem bark or distilled water for the control group. For Ti^W and Tb^M, the dose administered was 2000 mg/kg, while 20 mL/kg of distilled water was used for the control group. Oral gavage was chosen as a mode of

administration to mimic the traditional route of administration as described previously (Thu *et al.,* 2011). Oral gavage was achieved as per the guidelines of the Organization for Economic Cooperation and Development (OECD) (OECD, 2002). Following extract administration, animals were observed for 30 min and the first 4 h after treatment to record immediate deaths and once daily for 14 days to record any manifestation of toxicity.

II.2.2.2.2- Animals and *Plasmodium berghei* parasites

The chloroquine-sensitive *Plasmodium berghei* (NK65 strain) was used to assess the *in vivo* antimalarial efficacy of the test crude extract. Parasites were maintained in a BALB/C mouse by inoculation with 200 µl of a 1:1 (v/v) suspension of *P. berghei*-infected erythrocytes in phosphate-buffered saline (PBS). When parasitaemia reached 20%, the mice were sacrificed after sedated with a mixture of ketamine (120 mg/kg) and xylazine (16 mg/kg). After that, *P. berghei* infected erythrocytes were collected in EDTA tubes diluted with PBS and transferred to another group of mice for parasite multiplication.

II.2.2.2.3- *In vivo* antimalarial efficacy determination

The i*n vivo* antimalarial activity of aqueous and methanolic stem bark extracts of *T. ivorensis* (Ti^W) and *T. brownii* (Tb^M) was evaluated according to the 4-day suppressive standard test described by Knight and Peters (1980). Treatment was administered by oral gavage to mimic the traditional route of administration. For the model of infection used, twenty-four mice were randomly divided into four treatment groups of six mice each: Ti^W; Tb^M, chloroquine (positive control) and distilled water (negative control). On the 1st day (D0), whole blood from the donor mouse was drawn by jugular puncture into an EDTA tube, a suspension of *P. berghei* parasitized erythrocytes (1×10^6 parasitized RBCs/mL) in PBS was prepared and the test mice were infected intraperitoneally with 200 µl of this suspension. Two hours after infestation, the test groups were treated orally with 100 mg/kg of Ti^W or Tb^M. Positive and negative control mice received 10 mg/kg of chloroquine and 25 mL/kg distilled water, respectively. All mouse groups were treated similarly for 4 consecutive days (D0–D3) between 8 a.m. and 10 a.m. Weight, parasitemia and survival were rec daily. To evaluate the ability of Ti^W and Tb^M to prevent weight loss due to infection, weight differences between days post infestation and D0 were calculated. To measure parasitemia, thin blood smears were made every 48 h from tail blood from the 5th to the 15th day (D4 – D14). Blood smears were fixed with methanol and stained with a fast-acting variation of May-Grünwald Giemsa staining (RAL 555 kit, RAL diagnostics). Parasitemia was determined by light microscopy using a 100× objective lens as follows:

$$\%\textbf{Parasitemia} = \frac{\text{Number of parasitized RBC}}{\text{Total number of RBC counted}} \times 100$$

The average percentage of chemo-suppression was calculated at D7 for the treated groups as

$$\%\textbf{Chemo} - \textbf{suppression} = \frac{A - B}{B} \times 100$$

where A is the average percentage of parasitemia in the negative control group and B is the average percentage of parasitemia in the test group. Survival was monitored twice daily. The percent survival was determined over 14 days (D0–D13) and compared between groups.

Following *in vivo* validation of antimalarial efficacy, both aqueous and methanolic extracts of *T. ivorensis* and *T. brownii* were submitted to antiplasmodial-guided fractionation. The promising subfractions and active compounds were selected for a mode of action study.

II.2.3- Activity guided fractionation and mode of action study

II.2.3.1- Liquid - liquid partition and flash column chromatography

⬥ Principle

The basis of this technique is the distribution of sample molecules (compounds) between two immiscible liquid phases, a stationary phase and a mobile phase. Partition chromatography is achieved by holding one liquid phase on the surface of a chromatographic support, that is, the stationary phase, while the second liquid, that is, the mobile phase, is passed through the packed column, permitting intimate contact between the two phases

⬥ Procedure

The aqueous crude extract of the stem bark of *T. ivorensis* and the methanolic extract of *T. brownii* displaying good antiplasmodial activity and antimalarial efficacy were further fractionated using a liquid - liquid partition as previously described (Xie *et al.,* 2011) (**Figure 9)** and flash chromatography (**Figure 10**). Briefly, 90 g of *T. ivorensis* aqueous extract was suspended in water 95% - 5% MeOH and then successively extracted with n-hexane, dichloromethane and ethyl acetate. Each fraction was evaporated under reduced pressure at 45–55°C and then lyophilized. Three main residues were obtained and named as fractions $Ti^W Chl$ from dichloromethane [23.0 g, yield 23.0%], $Ti^W Ea$ from ethyl acetate [15.7 g, yield 15.7%] and the remaining aqueous residue ($Ti^W R3$) [48.5 g, yield 48.5 %]. Partitioning using hexane resulted in a nonquantifiable residue that was not investigated further. The methanolic extract of the stem bark of *T. brownii* did not dissolve in 5% MeOH/H_2O and was rather fractionated

using flash chromatography **(Figure 11)**. Briefly, 75 g of the extract was dissolved in methanol and then fixed with an equivalent mass of silica gel 230-400 MESH (MERCK). The dry mixture of crude extract-silica gel was further subjected to a silica gel (70–230 mesh, 60 Å, Aldrich) flash column chromatography (CC) eluting with Hex/Ea and Ea/MeOH in a gradient mode to yield 76 subfractions (ca. 250 mL each) which were combined into 5 main fractions [*Tb01 — Tb05*] based on their thin layer chromatography (TLC) profiles. Each of the afforded fractions from both plant extracts was tested for antiplasmodial activity.

Dried aqueous crude extract of *T. ivorensis* 90.0 g

Suspended in aqueous MeOH (5%) and extraction with hexane (5x200 mL)

Aqueous portion

n-Hexane fraction [$Ti^{W}Hex$] (0.8 g)

extraction with CH_2Cl_2 (5x200 mL)

CH_2Cl_2 fraction [$Ti^{W}Chl$] (23.0 g)

Aqueous portion

Extraction with Ethyl Acetate (5x200 mL)

Aqueous portion

freeze-dried

EtOAc fraction [$Ti^{W}Ea$] (15.7g)

Aqueous fraction [$Ti^{W}R3$] (48.5 g)
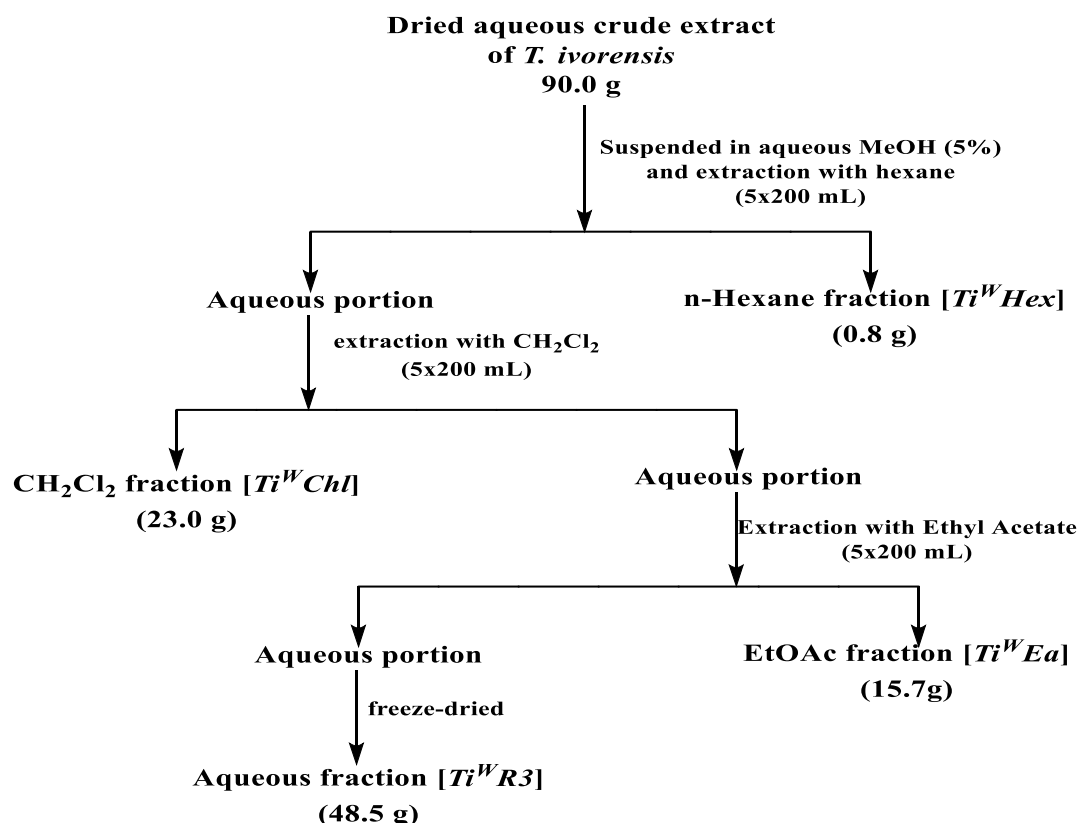
Figure 10: Fractionation procedure of *T. ivorensis* aqueous crude extract

Methanolic crude extract of *T. brownii* (75g)

Silica gel flash column chromatography using different solvent systems;

Collection of 76 sub-fractions (250 mL each) and combined into 5 main fractions based on TLC

Tb01 (6g)	*Tb02* (14g)	*Tb03* (19g)	*Tb04*(13g)	*Tb05* (20g)
Hex/Ea (1:3, v/v)	Hex/Ea (1:1, v/v)	Hex/Ea 3:1, v/v)	Hex/Ea (0:1, v/v)	Ea/MeOH (1:1, v/v)
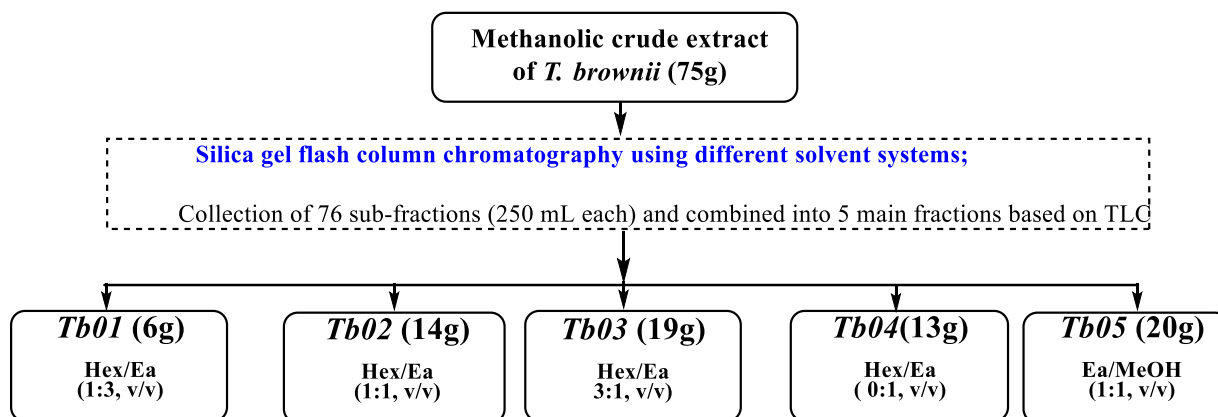
Figure 11: Fractionation procedure of *T. brownii* methanolic crude extract

II.2.3.2- Qualitative phytochemical profiling using UPLC-QTOF-MS

Based on their promising antiplasmodial activities, the ethyl acetate/methanol fraction codified as Tb05 (Ea/MeOH (1:1, v/v)) from the methanolic extract of *T. brownii* and the ethyl acetate fraction (Ti^{W}Ea) from the aqueous extract of *T. ivorensis* were subjected to phytochemical analysis using UPLC-MS.

II.2.3.2.1- Sample preparation for the fractions

The fractions were separately dissolved in HPLC-grade methanol and purified water at a ratio of 1:1. The samples were subjected to sonication and centrifugation before transfer to HPLC vials. Each sample (1 mg/ml) was prepared for UPLC - MS analysis.

II.2.3.2.2- UPLC–QTOF-MS analysis.

Principle

UPLC–MS works on van Deemter principle, which states that, the flow rate of smaller particles is much faster in compare with large particles as well as unfolding the correlation of flow rate and plate height (Ashraf et al., 2019).

Procedure

A Waters UPLC and Waters Synapt G2 QTOF Mass Spectrometer *System* including MassLynx v4.1 software was used for analysing the samples. For UPLC method development, the 1.7 µm *ACQUITY UPLC BEH C18* column (2.1 mm x 100 mm) was used. The gradient mobile phases used were A, water + 0.1% HCO_2H; and B, methanol + 0.1% HCO_2H. The elution flow rate was 0.300 mL/min. Elution started with 97% A and 3% B; and a linear gradient to 100% B until 14 minutes; isocratic from 14 to 16 minutes with 0% A and 100% B; a linear gradient from 16 to 20 minutes to reach 97% A and 3% B at completion. For mass detection, both positive and negative ionization modes were used.

MS ESI$^+$ parameters: source (capillary (kv) 2.6000, sampling cone [20.0000], extraction cone [4.0000]; temperature (source [120], desolvation [350]); gas flow (cone gas (L/h) [10.0], desolvation [650]; mass range (low mass [50], high mass [1200]).

MS ESI$^-$ parameters: source (capillary (kv) 2.0000, sampling cone [25.0000], extraction cone [4.0000]; temperature (source [120], desolvation [300]); gas flow (cone gas (L/h) [10.0], desolvation [600]; mass range (low mass [50], high mass [1200]).

II.2.3.2.3-Identification of phytoconstituent peaks

Compounds were tentatively identified by generating molecular formulas from MassLynx V 4.1 based on their iFit value, and by comparison of the MS/MS fragmentation

pattern with that of matching compounds from Waters UNIFI® Scientific Information System (version 1.9.2) accessing the Chinese Natural Products database. An ellagic acid (14668-50 MG) analytical standard was purchased from SIGMA-ALDRICH (Pty) LTD, South Africa, to confirm the presence of the compound in the plant extracts and fractions.

II.2.3.3- Fractionation of the most active and selective fractions by column chromatography

The EtOAc-soluble fraction (5.7 g) from *T. ivorensis* and 30.6 g of the EtOAc/MeOH (1:1 v/v) fraction from *T. brownii* which showed good antiplasmodial activity (IC$_{50}$PfDd2/Pf3D7=0.24/0.52 µg/mL) was further subjected to a silica gel column chromatography (CC) and eluted with EtOAc/MeOH in a gradient mode. Fraction from *T. ivorensis* yield to 105 subfractions (ca. 150 mL, each) which were combined into 5 main subfractions (Ti01–Ti05) based on their TLC profiles. The main subfraction SbTi01 (30.1 mg; EtOAc/MeOH 100:0→98:2 v/v) was obtained by combining subfractions 1–34 based on their almost similar TLC profile; after evaporation of the solvent and freeze-drying, 30.1 mg of a bank powder was obtained. In a similar grouping, SbTi02 (20.5 mg; EtOAc/MeOH 97:3→95:5 v/v) is a brown powder from the grouping of subfraction 35–50; SbTi03 (25.2 mg; EtOAc/MeOH 94:6→9:1 v/v) is an whitish powder from the grouping of subfraction 51–60; SbTi04 (100.0 mg; EtOAc/MeOH 9:1→85:15 v/v) is a brown powder from the grouping of subfraction 61-81; and SbTi05 (300.8 mg; EtOAc/MeOH 85:15 →1:1 v/v) is a yellow powder from the grouping of subfraction 82-105.

Fraction from *T. brownii* yield to 80 subfractions (ca. 300 mL, each) which were combined into 3 main subfractions (SbTb01–SbTb03) based on their TLC profiles. The main subfraction SbTb01 (2.2 g; EtOAc/MeOH/H$_2$O 95:4:1→90:9:1 v/v) was obtained by combining subfractions 1–20 based on their almost similar TLC profile; after evaporation of the solvent and freeze-drying, 30.1 mg of almost white powder was obtained. In a similar grouping, SbTb02 (12.5 g; EtOAc/MeOH/H$_2$O 90:9:1→80:18:2 v/v) is a brown powder from the grouping of subfraction 21–60; and SbTb03 (10.3 g; EtOAc/MeOH/H$_2$O 80:18:2 →2:1:1 v/v) is a yellow powder from the grouping of subfraction 61-80. Furthermore, the subfraction SbTb04 (5.5g; EtOAc/MeOH/H$_2$O 90:9:1→80:18:2 v/v) was separated on a Sephadex LH-20 column eluting with CH$_2$Cl$_2$–MeOH (4:6) to obtain compound **1** (Eschweilenol C; 6.0 mg; Yang *et al*., 1998) and a mixture of several inseparable compounds after several chromatographies spotted on silica gel and Sephadex LH-20.

Following column chromatography subfractions and isolated compounds were submitted to *in vitro* antiplasmodial activity against chloroquine-sensitive (*Pf*3D7), multiresistant (*Pf*Dd2) and mutant resistant (*Pf*Dd2-GNF156) strains of *P. falciparum* using *Pf*LDH-based assays and cytotoxicity as previously described. In addition, the transmission-blocking potential through the inhibition of transmissible gametocyte stages of *P. falciparum* was carried out using a luciferase-based assay.

II.2.3.4- Transmission blocking activity through inhibition of transmissible gametocyte stages of *P. falciparum*

II.2.3.4.1- Gametocyte induction and production

To produce gametocytes for anti-gametocidal assays, asexual blood-stage parasites were first synchronized by 5% D-sorbitol (wt/vol) treatment for 10 min at 37°C for two or more successive growth cycles. Synchronous parasites at 3% hematocrit were cultured in 100-cm^2 Petri dishes to 10% parasitemia (ring stage), at which point gametocytogenesis was induced by feeding cultures with 50:50 conditioned media (RPMI 1640 supplemented with 5.96 g/L HEPES, 2 g/L sodium bicarbonate, 50 mg/L hypoxanthine, 3.96 g/L glucose with 5% albumax II and 5% AB human serum). (Fivelman *et al.,* 2007; Muhia *et al.,* 2001)**.** The next day, trophozoite cultures were diluted fourfold and N-acetyl D-glucosamine (NAG; Sigma - Aldrich, Germany) was then added to a final concentration of 50 mM after all schizonts had ruptured. NAG treatment was maintained for the next two to three cycles of reinvasion to eliminate all asexual forms from the culture. Immature gametocytes (stages I and II) were magnetically purified by passage through a MACS CS column (Miltenyi Biotech) and transferred into 96-well plates at 2% hematocrit such that each well contained 2% gametocytes in a final volume of 150 μL. Giemsa-stained smears were examined daily to monitor gametocyte development.

II.2.3.4.2- Luciferase-based anti-gametocytocidal assays.

✚ Principle

A commonly used reporter gene is the luciferase gene from the firefly Photinus pyralis. This gene encodes a 61-kDa enzyme that oxidizes D-luciferin in the presence of ATP, oxygen, and Mg (++), yielding a fluorescent product that can be quantified by measuring the released light. (**figure 12**).
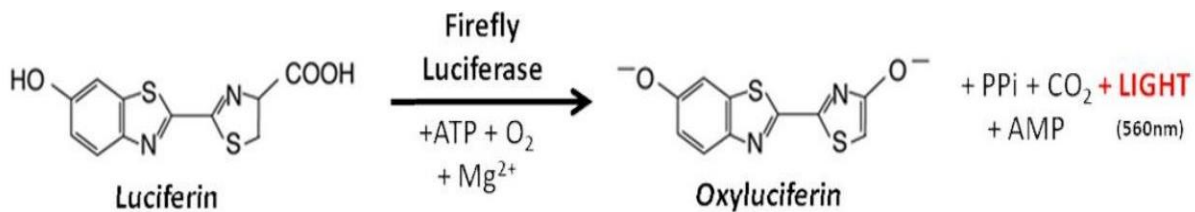
Figure 12: Biochemical reaction catalyzes by luciferase in presence of luciferin

✚ Procedure

Gametocytes were harvested daily for up to 12 days. Drug susceptibility assays were set up between days 12 and 16 (representing mature stage IV/V gametocytes) and carried out twice in triplicate at 2% gametocytemia and 2% hematocrit culture for 48 h of drug pressure in a gas chamber (90% N2, 5% O_2, and 5% CO_2) at 37 °C. Methylene blue and MMV390048 both served as a positive control for the inhibition of viability and the isolated compounds were screened at two concentrations (1 and 5 µg/ml). Following incubation, cells were lysed at room temperature in 3×Luciferin Lysis Buffer (15 mM DTT, 0.6 mM HSCoA, 0.45 mM ATP, 0.42 mg/mL luciferin, 10 mM $MgCl_2$, 10 mM Tris Base, 10 mM Tris·HCl, 0.03% Triton X-100). Luciferase activity was measured at 560 nm in a Victor luminescence plate reader (Perkin-Elmer). GFP expression from the different gametocyte-specific promoters was confirmed by fluorescence microscopy using a Nikon TiE PFS inverted microscope equipped with a CoolSNAP HQ2 monochrome camera.

II.2.3.4- Mode of action study of "hits" subfractions and isolated compounds.

II.2.3.4.1-Haemozoin inhibition assay

✚ Principle

In principle, the hemozoin inhibition assay is based on *in vitro* crystallization of heme or hematin (oxyhemoglobin) produced by living *P. falciparum* into soluble hemozoin which can be quantified at 400nm (**figure 13**).
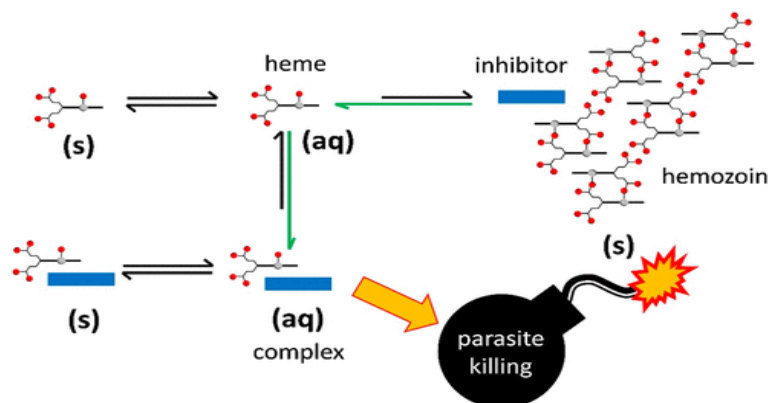
Figure 13: Biochemical mechanism of the inhibition of hemozoin formation

➕ Procedure

Hemozoin (β-hematin) inhibition by different subfractions and isolated compounds (Eschweilenol C) at their $IC_{50values}$ was assessed in *P. falciparum* cultures after 72h incubation (Akompong and Ghori, 2000). Following the incubation period, cultures were transferred to an Eppendorf tube and centrifuged (7 min, 1300 rpm; 4°C) to remove of the culture medium. Infected erythrocyte pellet (mingled with β-hematin and erythrocyte membranes) were exposed to 0.01% saponin lysis for 10 min at 25°C to lyse erythrocytes and release parasites. These released parasites were further washed three times with PBS for 5 min at 1500 rpm, resuspended in 2.5% sodium dodecyl sulfate buffer solution (SDS in PBS) and centrifuged at $20,000 \times g$ for 1 h. The supernatant was discarded and the insoluble hemozoin pellet was washed in 2.5% SDS in PBS and then dissolved in 20 mM NaOH. The hemozoin content was quantified by taking the absorbance at 400 nm and using a standard curve generated from β-hematin. The amount of hemozoin formed in relation to the negative control was calculated. All assays were performed in triplicate and repeated twice.

II.2.3.4.2- Time-course inhibition assay.

➕ Principle

It is based on the ability of inhibitors (extracts or compounds) to rapidly (within 24 hours) arrest *P. falciparum* proliferation in culture.

➕ Procedure

The relative speed of inhibition of the *Plasmodium* parasite by active subfractions and compounds was determined as previously described by (Manach *et al.,* 2013). Briefly, the growth of an asynchronous parasite culture in the presence of antimalarial compounds was assessed using a *Pf*LDH-based assay and expressed as IC_{50} values, as described above. For each compound, three exposure times were employed 72 (standard assay time), 48 and 24 h. The IC_{50} ratios, normalized to the 72h exposure were subsequently used to classify the compounds as fast or slow acting.

II.2.3.4.3- Stage-specific inhibition assay

➕ Principle

This assay is based on the ability of inhibitors (extracts or compounds) to arrest a specific stage (rings; trophozoites or schizonts) of *P. falciparum* in culture.

➕ Procedure

To investigate which stage of the *Plasmodium* parasite is inhibited by active subfractions (SbTi03, SbTi04) and Eschweilenol C, highly synchronized multiresistant strains

of *P. falciparum* (Dd2) rings, trophozoites and schizonts stages (2% parasitemia and 1% hematocrit) were treated with inhibitors at their IC_{99} for 48 h (rings), 24 h (trophozoites) and 12 h (schizonts) under normal culture conditions. Giemsa – stained thin smears were prepared at different intervals (6, 24 and 48 h for rings, 6 and 24 h for trophozoites and 12 h for schizonts) for microscopic evaluations to determine the compound's effect on parasite growth and stage transition (Roberts *et al.,* 2017). After the respective incubation periods, the drug was removed by washing the culture three-times with a complete RPMI medium and drug-free cultures were resuspended in a complete culture medium and maintained under normal growth conditions for a total of 48 h (rings), 24 h for (trophozoites) and (schizonts). After this incubation period, thin smears were prepared from control and treated wells and processed for Giemsa staining. The percentage of stage-specific inhibition by each compound was calculated in comparison to the corresponding drug-free control by counting 3000 cells (10 – 12 fields) for each parasite stage. Parameters such as stage-specific growth inhibition, cytostatic or cytocidal effects, and the postdrug exposure growth suppression were evaluated. Parasites with pycnotic morphology were considered nonviable cells.

II.2.3.4.4- Antioxidants activities

II.2.3.4.4.1- DPPH scavenging activity assay

🞣 Principle

This method is based on the capacity of antiplasmodial substances to supply protons to 2, 2-Diphenyl-1-picrylhydrazyl (DPPH) free radicals. DPPH radical is unstable and when it reacts with an antioxidant compound it becomes more stable. The decolorization of the purple-colored DPPH solution reveals this reducing power of the substances. A decrease in absorbance at 517 nm is proportional to the antioxidant potential of the substances.
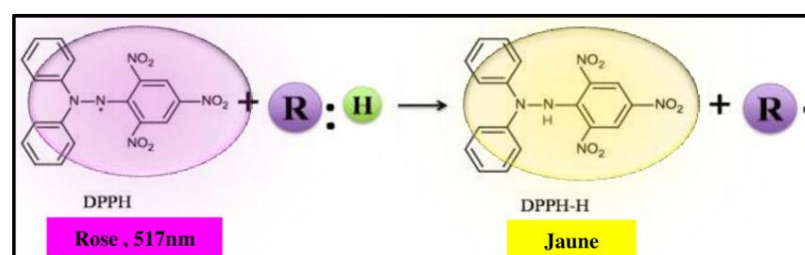
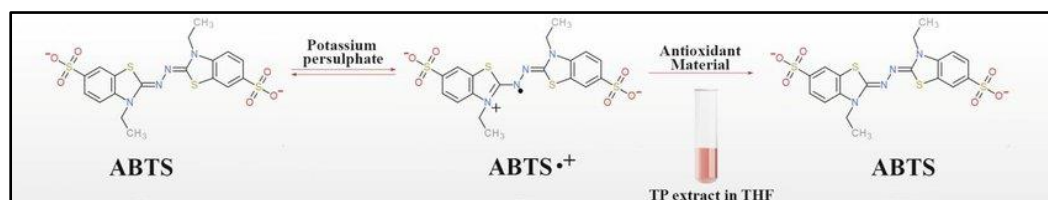**Figure 14**: Biochemical reaction of the reduction of DPPH free radical by antioxidant agents

🞣 Procedure

The free radical scavenging activity of the potent subfractions and Eschweilenol C was determined using the DPPH assay. The drugs along with the positive control (gallic and ascorbic acid) were reconstituted in methanol to obtain an initial starting concentration of 400

µg/mL and were then mixed with 90 mM of methanolic DPPH to form final drugs and positive control concentrations ranged from 100 to 0.7812 µg/mL in a 96 well microtiter plate. After that, the plates were incubated for 30 min in the dark at 25°C and the absorbance was read at a wavelength of 517 nm using an Infinite M200 microplate reader (TECAN). DPPH inhibitory Percent was calculated following the formula below:

DPPH scavenging percent (%) =. [Control A0 -. sample A1/control A0.] × 100

II.2.3.4.4.2-ABTS radical scavenging activity

✦ Principle

This method is based on the capacity of the extract's constituents or compounds to reduce the blue-green 2, 2'-azino bis-(3-ethylbenzothiazoline-6-sulphonic acid) (ABTS$^+$) radical to the colorless ABTS by donating its H$^+$. An increase in absorbance measured by spectrophotometry at 734 nm is proportional to the antioxidant concentration of the extracts/compounds.

Figure 15: Biochemical reaction of the reduction of ABTS free radical by antioxidant agents

✦ Procedure

The determination of the free radical scavenging activity of the potent antiplasmodial drug and ascorbic acid (positive control) was performed by the ABTS assay. ABTS cation radical production was accomplished by combining 10 mg of ABTS$^+$ and 2 mg potassium persulfate in distilled water. The solution was kept in the dark at room temperature for approximately, 12–16 h before use. ABTS solution (1 mL) was then diluted with 60 mL of methanol. After that, the experiment was conducted as described for the DPPH assay. Experiments were carried out in triplicate. The percentage of inhibition evidenced by absorbance at 734 nm was calculated using the formula stated by (Rock and Brunswick, 2005).

ABTS scavenging percent (%) =. [Control A0 -. sample A1/control A0. ×] 100

II.2.3.4.4.3- Ferric reducing antioxidant power (FRAP) activity

✦ Principle

The principle of his method is based on the reduction of Fe^{3+} to Fe^{2+} by components of the extracts. Fe^{2+} in the presence of 1, 10-phenanthroline forms a brown-colored complex that absorbs at 505 nm. The intensity of the coloration is proportional to the amount of Fe^{3+} converted.
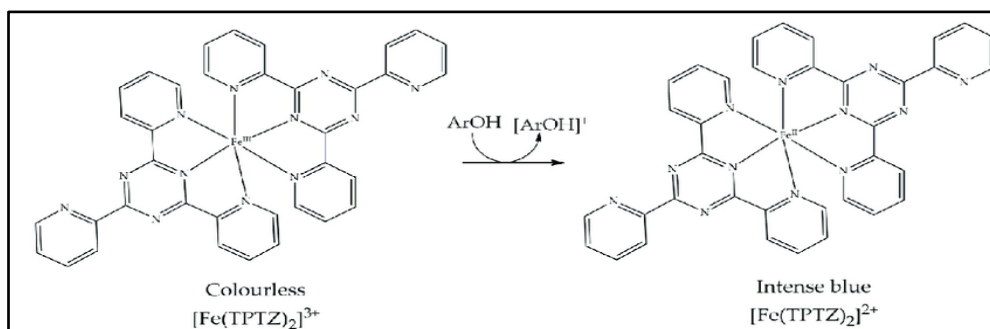
Figure 16: Biochemical reaction of the reduction of Fe3+ to Fe2+ by antioxidant agents

Procedure

This method measures the ability of antioxidant agents to reduce ferric iron (Fe^{3+}) as described by (Benzie and Strain, 1996). It is based on the reduction of the complex of ferric iron (Fe^{3+}) and orthophénanthroline to the ferrous (Fe^{2+}) form. This reduction was monitored by measuring the change in absorption at 505 nm, using a spectrophotometer. The Fe^{3+} solution was prepared by dissolving 60 mg of $FeCl_3$ in 50 mL of distilled water followed by homogenization to obtain a proportion of 100 µg of iron in 120 µl of solution and the ortho-phenanthroline solution was used to measure the amount of Fe^{2+} formed at 0.2% by dissolving 200 mg of powder in 100 ml of ethanol. The concentration of subfractions, Eschweilenol C and positive control ranged from 100 to 0.7812 µg/ml in a 96-well microtiter plate. Experimentally, 25 µl of subfractions, Eschweilenol C and positive control were mixed with 25 µL of Fe^{3+} solution followed by an incubation of 15min at room temperature in the dark. After that, 50 µL of orthophénanthroline was added to the different wells of the microtiter plate followed by another incubation period of 15 min under the same conditions. The absorbance was read at 505 nm using an Infinite Microplate reader (M200).

Reducing power percent (%) =. [sample A1 -. Control A0/ sample A1] * 100 where control **A0** and sample **A1** are absorbances of $FeCl_3$ without drugs and FeCl3 with drugs respectively for IC_{50} value calculation. Reducing power percent (%) was plotted against the logarithm of concentration to determine the median inhibitory concentrations (IC_{50}) through sigmoidal dose - response curves using GraphPad Prism V5.0.

II.2.4-Statistical Analysis

The results are presented as the mean ± SD of triplicate assays compared using a one-way analysis of variance (ANOVA). Data from the percentage of inhibition were normalized to percent control activity and median inhibitory concentrations (IC_{50s}) were calculated using Prism 8.0 software (GraphPad) with data fitted by nonlinear regression to the variable slope

sigmoidal dose - response formula y = $100/[1+ 10^{(\log IC50-x)\,H}]$, where H is the Hill coefficient or slope factor. XLSTAT (Addinsoft, New York, NY, USA) was used to achieve the Pearson correlation analysis and principal components analysis (PCA) for PfLDH assay validation and antioxidant studies and the difference was considered significant at $p < 0.05$. For inhibition of haemozoin production, GraphPad Prism statistics version 8.0 was used for data analysis using a one-way ANOVA with significant data given at ***$p < 0.0001$.

RESULTS AND DISCUSSION

CHAPTER III

III-RESULTS AND DISCUSSION

III-1- Establishment and validation of malaria *Pf*LDH-based colorimetric assay.

III.1.1- Sensitivity and linearity of *Pf*LDH detection

Assay performance was evaluated for linearity, detection range, reproducibility, assay screening window coefficient (Z'-factor) and interassay reproducibility via %CV. The equivalence between the absorbance signal from the *Pf*LDH-enzymatic reaction and parasitemia was confirmed by the linear correlation between parasitemia determined through microscopic examination of Giemsa-stained malaria parasites and the absorbance value measured (**Fig 17**). Of note**,** the linear relationship between absorbance and parasitaemia was displayed regardless of the *Pf*LDH content of the parasites, which varies dramatically during their intraerythrocytic life cycle and is mostly expressed at the highly metabolically active trophozoite stage. In addition to the strong correlation between *Pf*LDH parasitemia and absorbance, there were acceptable linearity profiles of $r^2 = 0.97$ and 0.92 for *Pf*3D7 and *Pf*Dd2, respectively **(Fig 17)**. Additionally, the detection limit (DL) and quantification limit (QL) were also examined to determine the level of assay sensitivity. DL and QL parameters are related but have distinct definitions and should not be confused. The intended purpose of this study was to define the lowest parasitaemia level that can be detected with no guarantee about the bias or imprecision of the assay result, the concentration at which quantitation as defined by bias and precision goals is feasible, and finally the parasitaemia at which the malaria parasite can be quantitated with a linear response (Armbruster and Pry, 2008). Therefore, the QL for this *Pf*LDH-based method was equivalent to the lowest parasitaemia that can be significantly differentiated from the next lower one tested. The DL based on the trophozoite stage of the parasite was 0.09%, while QL was determined to be 0.4% parasitemia for both sensitive (*Pf*3D7) and resistant (*Pf*Dd2) strains.
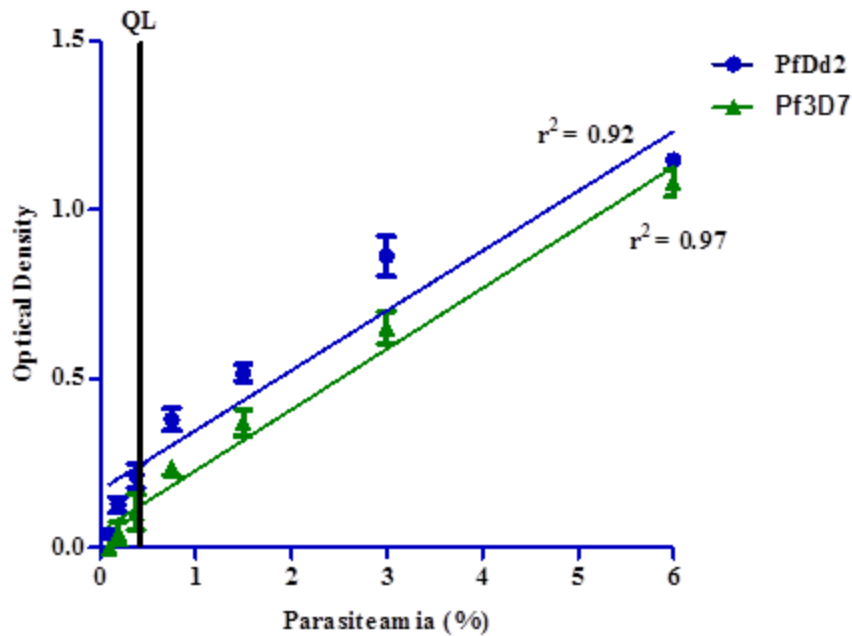
Figure 17: Assessment of *Pf*LDH absorbance linearity.

Cultures of *Plasmodium falciparum* Dd2 and 3D7 strains at their metabolically active trophozoite stages were diluted with RPMI 1640 culture medium to yield different dilutions of parasitemia ranging from 0 to 6% and constant hematocrit of 2% followed by the addition of LDH reagents. Absorbance was thereafter recorded at 650 nm in a Tecan M200 microplate reader. The data were analysed by linear regression and each data point shows the mean of at least triplicate analyses ± the standard deviation. Data are from a representative experiment of two independent experiments.

Table 4: Assay quality, reproducibility and the assay screening window coefficient (Z-factor) of the *Pf*LDH assay.

Assay performance for *Pf*LDH-based assay				
	Assay 1	**Assay 2**	**Assay 3**	**Average**
Z-factor (Z')	0.76	0.76	0.79	0.77 ± 0.01
S/N (Signal to Noise ratio)	49.1	35.85	189.6	91.51 ± 85.20
S/B (Signal to Background ratio)	3.73	4.37	3.87	3.99 ± 0.33
%CV (Coefficient of Variation)	5.5%	9.41%	1.51%	5% ± 0.03

Cultures of *P. falciparum* Dd2 and 3D7 strains at their trophozoite stages were diluted with RPMI 1640 culture medium to yield different dilutions of parasitemia ranging from 0 to 6% and a constant haematocrit of 2% followed by the addition of LDH reagents. The absorbance was then recorded at 650nm in a Tecan M200 microplate reader. All parameters of assay quality were calculated from at least three independent experiments for each assay, each time performed in triplicate.

The robustness and quality performance of the assay for high-throughput screening was calculated by using the statistical measure of Z' (Zhang *et al.,* 1999) For high-throughput screening, the assay is acceptable when the Z-factor displays a value between 0.5 and 1 and is more favourable as it approaches 1. The assay quality was proven, as the Z-factor varied between 0.76 and 0.79 with an acceptable average Z-factor of 0.77 between the independent assays (**Table 3**). The average interassay reproducibility via %CV was 5.47 between independent experiments. The results highlighted a strong reproducibility between the different assays, which is acceptable at < 20% (Iversen et al., 2012) and therefore supported the use of the developed *Pf*LDH assay in the antiplasmodial drug screening cascade (**Table 3**).

II.1.2- Validation of *Pf*LDH assay

III.1.2.1-Determination of IC$_{50}$ with and without edge effect on *Pf*LDH assay for four antimalarial drugs.

To verify the suitability of the *Pf*LDH assay for drug screening, a set of four antimalarial drugs (artemisinin, mefloquine, 2-aminopyridine and MMV00130) was screened on the multidrug-resistant strain (Dd2) of *P. falciparum* at different concentrations reported killing the asexual blood stage of *P. falciparum.* Hence, edge effects were also evaluated to check for suitable distribution of microplates and the effect of evaporation from certain well contents, which can cause variation in the IC$_{50}$ value. More precisely, edge effects can contribute to variability, and spotting them can be a helpful troubleshooting technique. Edge effects are sometimes due to increased evaporation from outer wells that are incubated for either short or long periods or by plate stacking. These conditions allow the edge wells to reach the desired incubation temperature faster than the inner wells. **Table 4** shows the results from a representative experiment that illustrates the lack of a significant edge effect on drug IC$_{50}$ determination following a 72 h incubation period in the *Pf*LDH assay. The data acquired indicated that similar results were obtained for different drugs at 72 h of incubation, suggesting no significant ($p < 0.05$) edge effect on the IC$_{50}$ values. Additionally, the coefficients of correlation from the determination of the IC$_{50}$ with or without the edge of each drug averaged ~0.97, highlighting the goodness of the assay.

Table 5: Edge effect on *Pf*LDH-based IC$_{50}$ determination for four antimalarial standards after 72 h incubation.

Antimalarial Drugs	Complete row of micro-plate		(p < 0.05)	*Row without edge of miro-plate	
	IC$_{50}$ (nM)	r^2		IC$_{50}$ (µg/mL)	r^2
MMV000006	14.57 ± 3.92	0.99		19.67 ± 3.60	0.98
MMV000015	15.99 ± 3.75	0.97		43.14 ± 3.64	0.98
MMV390048	47.54 ± 3.42	0.96		53.83 ± 11.81	0.96
MMV000130	877.05 ± 160	0.96		763.3 ± 3.43	0.97

. The four standard antimalarials were tested against *P. falciparum* Dd2 in the culture at a parasitemia and hematocrit of 2% and 1% respectively while taking into account the complete row of microplates and excluding columns 1 and 12 of the 96-well microtiter plate. Data were normalized to percent control activity and median inhibitory concentrations (IC50s) were calculated using Prism 8.0 software (GraphPad) with data fitted by nonlinear regression to the variable slope sigmoidal dose - response formula y = 100/[1+ 10(logIC50-x)H], where H is the Hill coefficient or slope factor.

III.1.2.2- Correlation between SyBr Green, Microscopy and *Pf*LDH after 72 h of incubation.

To validate the results obtained using the *Pf*LDH assay, we compared the *Pf*LDH-based IC$_{50}$ values of the antimalarial drugs towards the *Pf*Dd2 strain to those obtained using microscopy and SyBr Green fluorescence assays. **Table 5** shows the drug IC$_{50}$s determined using microscopy, and *Pf*LDH and SyBr Green assays. The results indicated little variation in IC$_{50}$ profiles for individual test drugs highlighting a good correlation for the 4 compounds across all three methods. Interestingly, artemisinin showed a similar activity profile across the three methods (IC$_{50}$ ranging from 13.18 to 14.57 nM), providing an extent of validation for the *Pf*LDH assay. In addition, the other drugs showed eclectic IC$_{50}$ profiles across the three methods. Indeed, mefloquine exerted the strongest activity (IC$_{50}$ of 15.99 nM) when tested using the *Pf*LDH assay compared to Sybr Green (IC$_{50}$ of 53.57 nM) and microscopy (IC$_{50}$ of 32.94 nM). Similar activity profiles were obtained for MMV390048 when using the *Pf*LDH assay and microscopy (IC$_{50}$ of 45.54-47.54 nM), against an IC$_{50}$ of 74.08 nM for the SYBR Green assay. Finally, the activity (IC$_{50}$) of MMV000130 was less correlated when using the *Pf*LDH assay (IC$_{50}$ of 877.05 nM), SyBr Green assay (IC$_{50}$ of 350.17 nM) and microscopy (IC$_{50}$ of 283.95 nM).

Table 6: Comparison (p < 0.05) of IC50 values determined using SyBr Green, microscopy and PfLDH at 72 h of incubation against the multiresistant strain of *P. falciparum* Dd2.

	†Mean IC$_{50}$ (nM) ± SD (*pIC50*)		
	*Pf*LDH assay	SyBr Green assay	Microscopy assay
Drugs			
Artemisinin	14.6 ± 3.9 (*7.8*)	13.29 ± 4.2 (*7.8*)	13.2 ± 3.3 (*7.8*)
Mefloquine	16.0 ± 3.8 (*7.7*)	53.6 ± 6.5* (*7.2*)	32.9 ± 17.6* (*7.4*)
MMV390048	47.5 ± 3.4 (*7.3*)	74.08 ± 18.2* (*7.1*)	45.5 ± 3.0 (*7.3*)
MMV000130	877.1 ± 160* (*6.0*)	350.2 ± 138.3 (*6.4*)	284.. ± 75.9 (*6.5*)

The standard antimalarials were tested against *P. falciparum* Dd2 in the culture at a parasitemia and hematocrit of 2% and 1% respectively. After that, each independent plate was revealed using *Pf*LDH, SyBr Green and Microscopy methods. For each method, data were normalized to percent control activity and median inhibitory concentrations (IC50s) were calculated using Prism 8.0 software (GraphPad) with data fitted by nonlinear regression to the variable slope sigmoidal dose - response formula y = 100/[1+ 10(logIC50-x)H], where H is the Hill coefficient or slope factor. †Mean IC50 values of experiments run on different days using *Pf*LDH and SyBr Green-based assays and microscopy. *p < 0.05. pIC50 is given as the negative log10 of IC$_{50}$ in a molar.

However, the global goodness of fit (r^2 values) between the *Pf*LDH, microscopy and SyBr Green-based assays was 0.99 and 0.98, respectively, and therefore showed a strong correlation between *Pf*LDH and microscopy; *Pf*LDH and SyBr Green assays for the four standard antimalarials investigated (**Figure 18A and 18B**).
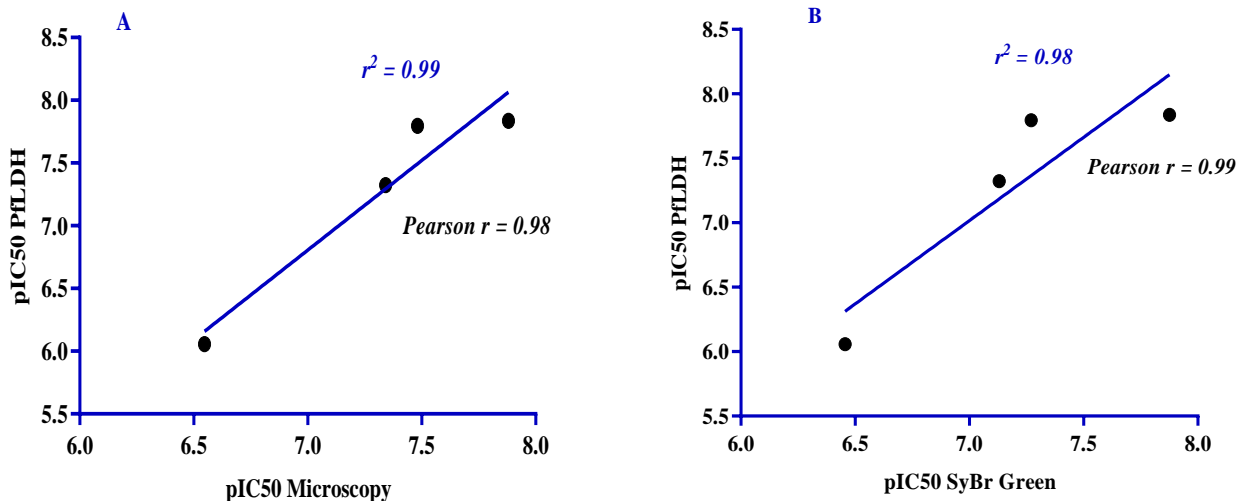
Figure 18: Global correlation of drug pIC50s determined by PfLDH versus microscopy (A) and PfLDH versus SyBr Green (B) assays. IC_{50}s of artemisinin, mefloquine, 2-aminopyridine and MMV000130 were obtained on a multiresistant strain (Dd2) of *P. falciparum* using *Pf*LDH, microscopy and SyBr. Green assays. pIC_{50} represents the negative log10 of IC_{50} in a molar.

II.1.3- Assay confirmation

To further confirm the suitability of the *Pf*LDH assay implemented in our laboratory for drug screening against malaria parasites, 19 MMV compounds were comparatively screened on *Pf*Dd2 in culture using both *Pf*LDH and SyBr Green assays. Then, the global goodness of fit (r^2 values) between the *Pf*LDH and SyBr Green-based assays was assessed to directly determine the correlation and linear regression between the IC_{50} values obtained from both methods following 72 h of incubation (**Figure 19**). The results achieved indicated goodness of fit for *Pf*LDH versus SyBr Green of $r^2 = 0.93$ and therefore confirmed a correlation of IC_{50}s obtained from both the *Pf*LDH and SyBr Green assays. Out of the 19 compounds screened for antiplasmodial activity confirmation using both *Pf*LDH and SyBr Green assays, only five (chloroquine, lumefantrine, 2-aminopyridine, quinine sulfate dihydrate and MMV000130) (**Table 7**) exhibited significant differences (at *p < 0.05; ***p < 0.001) between the IC_{50} obtained across both assays, highlighting the suitability of the *Pf*LDH-based method for antimalarial drug screening. A linear trend was observed between the outcomes from the SyBr Green and *Pf*LDH assays, with limited variability around the model line (**Figure 19**). Moreover, only 3 compounds outside the first confidence interval [-1.96, 1.96] (**Figure 19**) were noted, but none were outside the second confidence interval, underlining the strong relationship between the two methods. In addition, the regression

of PfLDH by SyBr Green was very close to the validation set, indicating that there will not be a significant difference in the IC$_{50}$ of a given compound when using PfLDH or SyBr Green methods in the antimalarial drug screening cascade. The Pearson correlation analysis showed a positive correlation between the SyBr Green and PfLDH assays with a coefficient of $r=$ 0.96 (**Table 6, Figure 20**). Moreover, correlation maps (**Figure 20**) showed a strong correlation between the two methods, as the colour scale was red. The results from the graph matrix and scatter plot (**Figure 20A**) showed that the PfLDH method has a very strong linear relationship with the SyBr Green method. To assess the suitability of PfLDH for antiplasmodial screening using a statistical approach, IC$_{50}$ values from antiplasmodial assays were subjected to principal component analysis (PCA) using XLSTAT. Furthermore, to determine the correlations between assays, factor analysis was performed on the IC$_{50s}$ obtained using both methods for each compound. This accounted for the total covariance of the compounds; thus, for two-factor loadings, a factor rotation using the Varimax method was performed (Erkan and Saban, 2011). **Figures 21A&B** show variance on the F1 and F2 axes to be 98.43% and 1.57%, respectively, indicating a strong correlation and nonsignificant difference between the IC$_{50s}$ obtained by both methods. Principal component analysis (PCA) for antiplasmodial activity using both PfLDH and SyBr Green assays indicated that compounds are closely loaded to the F1 axis rather than F2, denoting a nonsignificant difference between the IC$_{50}$ values of investigated compounds when using both methods.

Table 7: Results of Pearson correlation for the *in vitro* antiplasmodial assay using SyBr Green and PfLDH.

Methods	SyBr Green	PfLDH
SyBr Green	1	
Pf**LDH**	0.969	1

Associations between IC50 values from both SyBr Green and PfLDH methods were determined using Pearson's correlation coefficient and a significance level of 0.05 (p > 0.05)

Table 8: Inhibition of *P. falciparum* proliferation in cultures of 19 MMV compounds using *Pf*LDH and SyBr Green-based assays.

Compounds	*IC$_{50}$ ± SD (nM) (pIC$_{50}$)*	
	*Pf*LDH method	Sybr Green method
Dihydroartemisinin)	4.8 ± 0.1(*8.3*)	4.3 ± 0.8 (*8.3*)
Artemisinin	17.2 ± 1.0 (*7.7*)	23.8 ± 3.6 (*7.6*)
Chloroquin	398.9 ± 21.6 (*6.3*)	265.5 ± 23.7***(*6.5*)
Lumefantrine	197.5 ± 0.8 (*6.7*)	64.9 ± 0.9***(*7.1*)
Mefloquine	41.7 ± 2.3(*7.3*)	39.5 ± 0.7(*7.4*)
Piperaquine	107.5 ± 3.1(*6.9*)	162.0 ± 2.6 (*6.7*)
Primaquine	>1000 (*ND*)	>1000 (*ND*)
Pyrimethamine	>1000 (*ND*)	>1000 (*ND*)
Artemisone	6.8 ± 0.6 (*6.9*)	4.1 ± 0.5 (*6.7*)
Tafenoquine	>1000 (*ND*)	>1000 (*ND*)
Atovaquone	2.0 ± 0.0 (*8.6*)	1.4 ± 0.2 (*8.8*)
MMV390048	57.8 ± 0.8 (*7.2*)	121.0 ± 14.9* (*6.9*)
MMV000052	>1000 (*ND*)	>1000 (*ND*)
Quinine sulfate dihydrate	308.7 ± 75.9 (*6.5*)	223.3 ± 2.2***(*6.6*)
Methylene blue	11.2 ± 0.2 (*7.9*)	10.1 ± 0.6 (*7.9*)
MMV000147	1.9 ± 0.1 (*8.7*)	3.4 ± 0.1 (*8.4*)
MMV018912	52.9 ± 10.0 (*7.2*)	46.2 ± 3.2 (*7.3*)
MMV642943	45.7 ± 1.4 (*7.3*)	65.2 ± 3.7 (*7.1*)
MMV000130	827.3 ± 38.7 (*6.0*)	533.9 ± 22.8***(*6.2*)
Chloroquine	240.6 ± 22.9 (*6.6*)	180.8 ± 69.7 (*6.7*)
Artemisinin	15.3 ± 3.0 (*7.8*)	17.3 ± 0.3 (*7.7*)

Compounds were tested on *P. falciparum* Dd2 in culture at a parasitemia and hematocrit of 2% and 1% respectively using both SyBr Green and *Pf*LDH methods. Data were normalized to percent control activity and median inhibitory concentrations (IC50s) calculated using Prism 8.0 software (GraphPad) with data fitted by nonlinear regression to the variable slope sigmoidal dose - response formula y = 100/[1+ 10(logIC50-x)H], where H is the Hill coefficient or slope factor.. *Mean IC50 values ± SD (standard deviation) from triplicate experiments using *Pf*LDH and SyBr Green assays. Data were compared using one-way analysis of variance (ANOVA) with GraphPad Prism statistics version 5.0. Significant differences are given at *p < 0.05 and ***p < 0.001. pIC$_{50}$ is the negative log10 of IC$_{50}$ in molar. ND: Not Determined
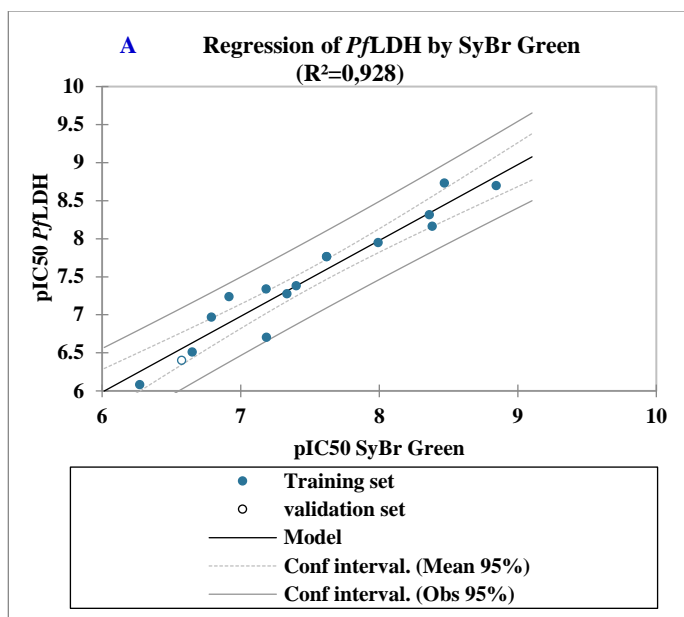
Figure 19: Linear regression of *Pf*LDH by SyBr Green.

The chart allows us to visualize the data, the regression line (the fitted model), and two confidence intervals: the confidence interval on the mean of the prediction for a given IC_{50} value of the SyBr Green methods is the one closer to the line. The other is the confidence interval on a single prediction for a given value of the SyBr Green methods.
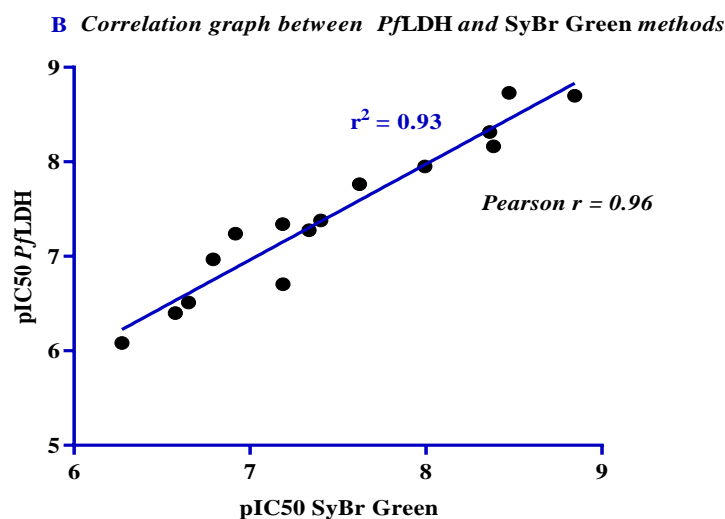
Figure 20: Global Pearson correlation of *Pf*LDH-assay and SyBr Green-assay.

Compounds were tested on multiresistant strains of *P. falciparum* using the *Pf*LDH and SyBr Green methods. n =The experiment was performed in triplicate. The data are presented as the mean ± SD. Significant data are given as ***p < 0.0001.
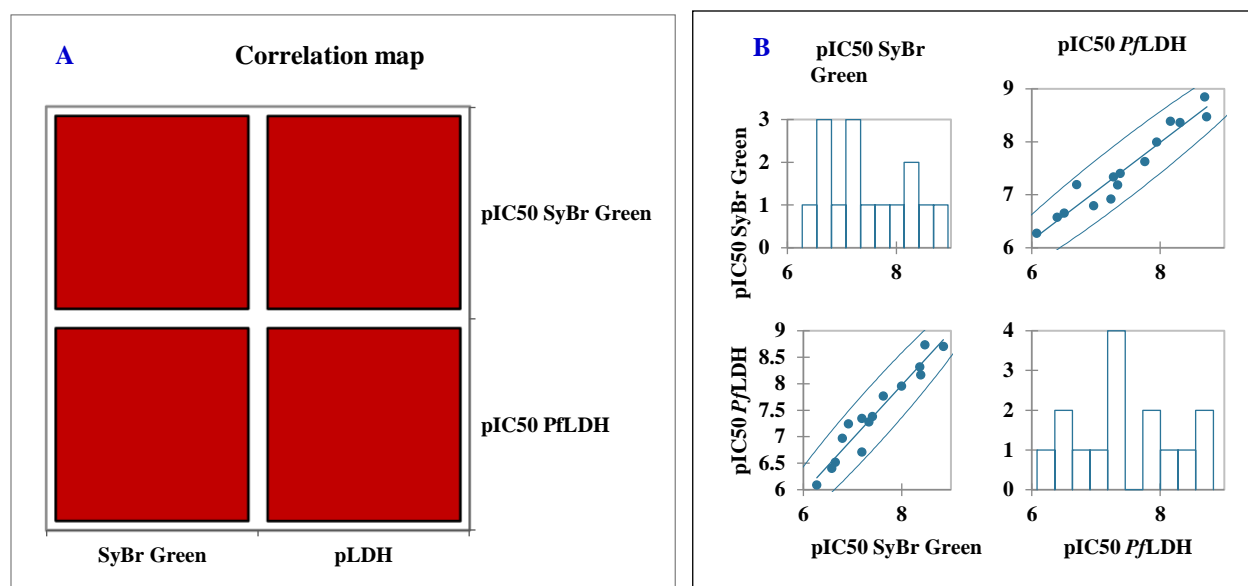
Figure 21: Correlation maps between *Pf*LDH and SyBr Green methods.

A: The correlation is depicted with a colour scale from blue to red (cold-hot scale). The blue colour corresponds to a negative correlation close to -1, and the red colour corresponds to a positive correlation close to 1. The red colour indicates a strong correlation between *Pf*LDH and the SyBr Green method. **B**: Scatter plot and graph matrix of *Pf*LDH and SyBr Green. The Y-axis and X-axis represent the negative log10 of IC_{50} (pIC50) of the different compounds in each method. The graph matrix displays one histogram per variable (on the diagonal), revealing the characteristics of the variable distribution. The scatter plot shows possible pairs for all variables, reflecting the sign characterized by the colour of the dots as well as the slope of the regression line, and the strength of a correlation is depicted by the dispersion of the dots around the line.
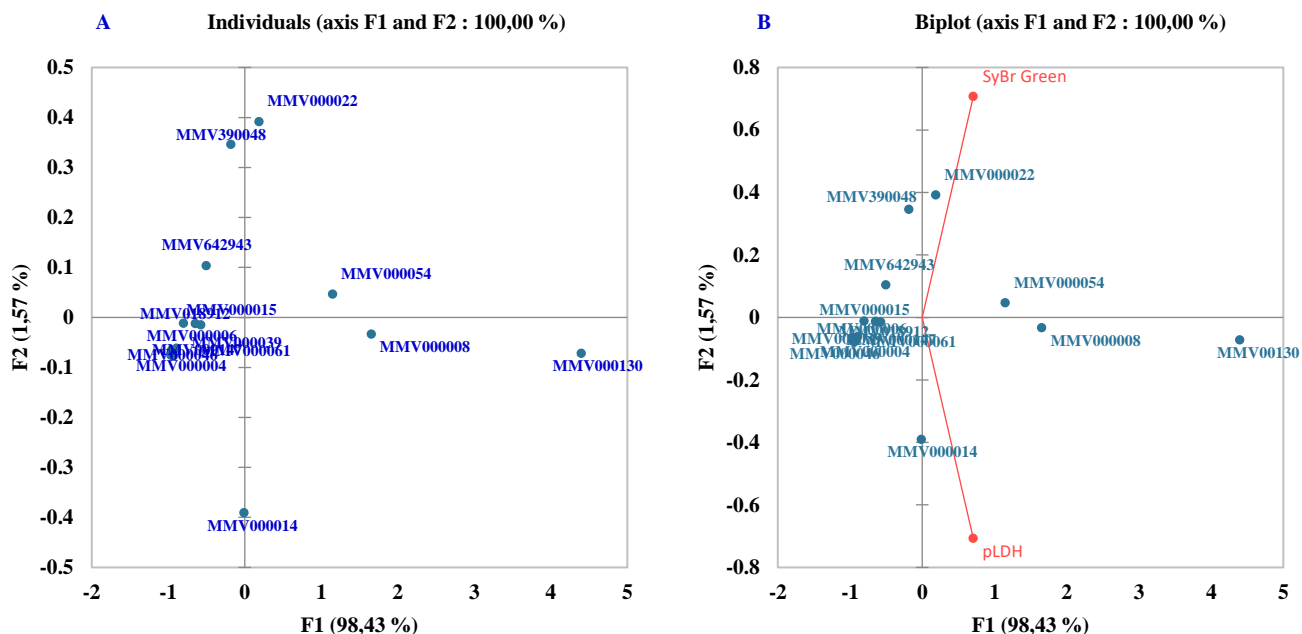
Figure 22: Correlation between *Pf*LDH-based and SyBr Green-based methods in antiplasmodial drug screening using XLSTAT 2021.1.1.1088 – Correlation tests and principal components analysis (PCA). **A**: distribution of the compounds around the F1 and F2 axes; **B**: projection of the compounds and tests around the F1 and F2 axes.

II.1.4-Discussion

In vitro assays against *P. falciparum* asexual stages are essential steps for the identification and further scrutiny of promising anti-plasmodial chemotypes with the potential to be developed into antimalarial drugs. Drug screening platforms exploit the eventual inhibition of different critical genomic and metabolic functions of *Plasmodium,* such as 1) nongenome-coded targets (Bell 2011; Fong and Wright; 2013; Sullivan, 2013) [inhibition of heme detoxification-Intraerythrocytic *P. falciparum* ingests and degrades hemoglobin amassed within the red blood cell (RBC) to obtain amino acids essential for its growth and maturation. This breakdown of hemoglobin in the food vacuole releases toxic free haem, which, left to accumulate insoluble form, could damage biological membranes and inhibit a variety of parasite enzymes. 2) Genome-coded enzymes/biosynthetic pathways [example a) Inhibition of histone deacetylase (HDAC) and histone acetyltransferase that together control the total level of acetylation of histones (proteins that package DNA into nucleosomes)- This results in the accumulation of hyperacetylated histones,

which in turn are implicated in altered gene expression, cell differentiation and cell cycle arrest. Example b) Inhibition of glycolytic enzymes- Unlike most tissues of the mammalian host, *P. falciparum* lacks a functional citric acid cycle and is instead entirely dependent on glycolysis for energy generation. Consequently, compounds that selectively inhibit the parasite's ATP-generating machinery or by using other metabolic pathways would therefore constitute potential antimalarial agents. Such drugs may interact by either inhibiting the activity of a specific enzyme or disturbing the microorganization of consecutive enzymes in a metabolic pathway (Okombo and Chibale, 2016). However, one of the major drawbacks that are encountered includes assay reproducibility and robustness. Hence, implementation and continuous validation of novel or available easy-to-use methods remain paramount in the process of standardized antimalarial drug discovery, particularly in resource-constrained laboratories of low- and middle-income countries of Africa. In that regard, the enzymatic-based lactate dehydrogenase (*Pf*LDH) antiplasmodial assay has been shown to be of interest for this purpose. Hence, the present report describes the implementation, examination of assay conditions and validation of a *Pf*LDH-based assay for routine use in antimalarial drug screening in our laboratory. This assay is based on the observation that the lactate dehydrogenase enzyme of *P. falciparum* has the ability to rapidly use 3-acetyl pyridine NAD (APAD) as a coenzyme in the glycolysis reaction, leading to the formation of pyruvate from lactate. The presence of *P. falciparum* at parasitemia levels of 0.02% from *in vitro* cultures can be detected by measuring the development of APADH (Kalra *et al.,* 2006). In fact, the enzyme isoform (*Pf*LDH) expressed by *P. falciparum* is a key enzyme for energy generation through anaerobic glycolysis and thus is among the Achilles heels for *P. falciparum* parasite survival.

As previously reported by Makler and Hinrichs (1993), there is a linear increase in *Pf*LDH absorbance that correlates with the increase in the content of the parasitic enzyme lactate dehydrogenase. Based on this rationale, we evaluated *Pf*LDH-absorbance linearity, detection range, reproducibility, assay screening window coefficient (Z-factor) and interassay reproducibility via %CV in drug susceptibility testing. We showed that the *Pf*LDH assay allowed linear detection of *P. falciparum* parasites regardless of their LDH content, which was corroborated by a high correlation between absorbance and plasmodial enzyme LDH. The detection limit (DL) for the *Pf*LDH assay was 0.09% for both the multiresistant (Dd2) and sensitive (3D7) strains of *P. falciparum*. This consistent DL was shown to be strongly linked to *Plasmodium*

asexual stages investigated. In fact, *Plasmodium* lactate dehydrogenase (*Pf*LDH) is produced during the cycle of asexual replication (ring-trophozoite-schizont) but is more highly expressed at the metabolically active trophozoite stage. Therefore, using a 72-hour *Pf*LDH antiplasmodial drug screening assay format led to enhanced sensitivity in enzyme activity detection owing to significantly increased *Pf*LDH content at the trophozoite stage when compared to the ring and schizont stages. No significant variation was observed in the detection and quantitative limits when using multiresistant (Dd2) and sensitive (3D7) strains of *P. falciparum,* highlighting the suitability of the *Pf*LDH assay for antiplasmodial drug screening when targeting both parasite strains. Drug screening assays using the *Pf*LDH approach showed robustness and sensitivity, resulting in a high signal-to-noise ratio (S/N) and a reasonable limit of quantification. This assay exhibited good intra-assay reproducibility (average Z-factor 0.77) as well as high sensitivity (average S/N of 91.51) and percent coefficient of variation (%CV) of 5% (which was far below the upper acceptable limit of 20%). Furthermore, edge effects are important to monitor antimalarial drug screening and reproducibility, as small changes in the reported IC_{50} values can mislead the resistance profile for a study population (drugs) in a malaria-endemic region, with an impact on treatment regimen due to misdiagnosis of their parasite resistance index (Johnson et al., 2007). The edge effect has been linked to environmental assay conditions such as temperature changes during the handling of culture plates and the addition of LDH assay reagents. However, in this study, no edge effect was observed, highlighting the *Pf*LDH assay's suitability for high-throughput (HTS) screening of potential antimalarial drugs.

The validation of an assay includes determining the Z-factor (Z'), which weighs the error associated with the absolute difference between the assay's positive and negative values (Zhang *et al.,* 1999). From testing compounds using the LDH assay, our results showed that the assay quality, defined as the Z-factor, varied between 0.76 and 0.79, with an acceptable average Z-factor of 0.77 regardless of the culture conditions or parasite strain used. The obtained Z-factor was very close to that of SyBr Green antiplasmodial assay validation ($0.73 \leq Z' \geq 0.95$) (Zhang *et al.,* 1999). The assay appeared consistent and reproducible, as there was no significant difference in assay performance (indicated by the Z-factor values) across assays and time. In preliminary validation assays, we used a set of four antimalarial drugs (artemisinin, mefloquine, 2-aminopyridine, MMV000130) to assess antiplasmodial activity using *Pf*LDH, SyBr Green, and microscopy. We found no significant variation in the IC_{50} values of artemisinin across the three assays. In addition,

no significant ($p < 0.05$) differences were observed among the three assays. Of note, the IC_{50} values for artemisinin exhibited a strong correlation between *Pf*LDH and microscopy (global r2=.0.99; Fig 15A) and between *Pf*LDH and SyBr Green (global r2=0.98; Fig 15B). Furthermore, the IC_{50} of mefloquine was significantly different ($p < 0.05$) when *Pf*LDH- was used rather than microscopy and SyBr Green. These discrepancies could be attributed to the different metabolic pathways targeted by each assay as well as the assay sensitivity. Moreover, there was no significant difference at $p < 0.05$ in the IC_{50} values of 2-aminopyridine when using *Pf*LDH and microscopy. Because microscopy assays are more specific than parasite metabolic activity assays, we can allude that the *Pf*LDH assay is less sensitive than the other methods as long as the microscopy methods are no longer suitable for MTS and HTS drug discovery. Principal component analysis (PCA) with a larger set of compounds revealed a strong correlation between the *Pf*LDH and SyBr Green methods that target parasite proteins and nucleic acids, respectively. The achieved findings support the use of the *Pf*LDH assay in antiplasmodial drug screening in our laboratory and elsewhere.

III-2- *In vitro* antiplasmodial activity and *in vivo* antimalarial efficacy of crude extract from *T. ivorensis* and *T. brownii*

III.2.1- *In vitro* antiplasmodial activity and selectivity of crude extracts on normal cells and erythrocytes

III.2.1.1-Plant collection and extraction

Table 9: Extraction yields *T. ivorensis* and *T. brownii* extracts and fractions

Species	Plant part	solvent of extraction	Extract's Codes	Yields (%)
T. ivorensis	Stem bark	Water	Ti^W	1.49
		Ethanol	Ti^E	3.81
		Hydro-Ethanol	Ti^H-E	11.92
		Methanol	Ti^M	11.06
		Ethyl-Acetate	Ti^Ea	1.78
T. brownii	Stem bark	Water	Tb^W	5.48
		Ethanol	Tb^E	8.57
		Hydro-Ethanol	Tb^H-E	7.37
		Methanol	Tb^M	5.46
		Ethyl-Acetate	Tb^Ea	3.50

The stem bark of *T. ivorensis* and *T. brownii* were collected and macerated with water, ethanol, hydroethanol, methanol and ethyl acetate**.** The extraction yield ranged from 1.49% to 11.92% and 3.50% to 8.75% for *T. ivorensis* and *T. brownii* respectively (**Table: 8**). However, the highest extraction yield was obtained with hydroethanol and ethanol for *T. ivorensis* and *T. brownii* respectively.

III.2.1.2- Prior overview of the hemolytic potential of extracts

The potential of crude extracts from *T. ivorensis* and *T. brownii* to elicit hemolysis was assessed on erythrocytes. The results revealed no hemolytic effect at up to 250 µg/mL. Therefore, the activity detected at concentrations below this threshold was consistent with the effect of inhibitors alone. In addition, these results highlight the ability of crude extracts from both plants to target the parasites without damaging the host to ascertain that the observed antiplasmodial activity is attributed to their specific activity against *P. falciparum* and not to erythrocyte damage.

III.2.1.3-*In vitro* antiplasmodial activities of crude extracts from *T. ivorensis* and *T. brownii*.

A total of 10 plant extracts from *T. brownii* and *T. ivorensis* were tested against chloroquine-sensitive (*Pf*3D7) and multiresistant (*Pf*Dd2) strains of *P. falciparum*. Overall, all the extracts inhibited the growth of both parasite strains with median inhibitory concentrations (IC$_{50}$) ranging from 0.13 µg/mL to 10.59 µg/mL, except for the hydroethanol extract of *T. ivorensis* that preferentially inhibited *Pf*Dd2 (IC$_{50}$= 0.85 µg/mL), but with IC$_{50}$ > 100 µg/mL against *Pf*3D7 (**Table 9, Figure 23**). Based on the antiplasmodial activity classification criteria by Muganza et al**.** (2016), 8 extracts out of the 10 tested (Ti^E; Ti^{H-E}; Ti^{M,}, Ti^{EA} from *T. ivorensis* and Tb^E; Tb^M, Tb^{W,} Tb^{H-E} from *T. brownii* showed highly potent activities against both *P. falciparum* strains with IC$_{50}$ values below 3 µg/mL (**Table 9**). In addition, two hits' extracts (Ti^W and Tb^M) exhibited a higher inhibitory effect on both *Pf*3D7 and *Pf*Dd2 with IC$_{50}$ < 1 µg/mL, coupled with higher selectivity indices (SI) ranking from > 252 to > 1925 relatives to Vero and Raw cell lines and erythrocytes. These activity parameters make the two extracts more attractive for further investigation.

The resistance indices (RI= IC$_{50}$*Pf*Dd2/IC$_{50}$*Pf*3D7) for the frontrunner extracts were 7.53 and 5.46 (**Table 9**), indicating fundamental differences in the biology of both *P. falciparum* strains used in this study.

Table 10: Antiplasmodial activity and cytotoxicity parameters of *T. ivorensis* and *T. brownii* crude extracts.

| Species | Code | Antiplasmodial activity | | | **Cell Cytotoxicity | | *Selectivity index | | | |
| | | *$IC_{50} \pm SD$ (µg/mL) | | | VC | RC | (SI_{VC}) | | (SI_{RC}) | |
		*Pf*3D7	*Pf* Dd2	RI	$CC_{50} \pm SD$ (µg/mL)		*Pf*3D7	*Pf*Dd2	*Pf*3D7	*Pf*Dd2
	Ti[W]	0.13 ± 0.02	0.98 ± 0.06	7.53	> 250	> 250	> 1923	> 255	> 1923	> 255
	Ti[E]	0.83 ± 0.01	1.44 ± 0.11	1.73	> 250	> 250	> 301	> 173	> 301	> 173
T. ivorensis	Ti[H-E]	> 100	0.85 ± 0.10	-	> 250	> 250	> 2.5	> 294	> 2.5	> 294
	Ti[M]	0.86 ± 0.01	1.02 ± 0.05	1.18	> 250	> 250	>291	>245	>291	>245
	Ti[Ea]	1.74 ± 0.06	1.04 ± 0.07	0.5	198.3 ± 0.10	108.8 ± 0.05	114	191	62	105
	Tb[W]	1.07 ± 0.01	1.07 ± 0.09	1	> 250	> 250	> 233	> 233	> 233	> 233
	Tb[E]	0.96 ± 0.02	2.23 ± 0.12	2.32	> 250	> 250	> 260	> 112	> 260	> 112
T. brownii	Tb[H-E]	0.91 ± 0.02	0.93 ± 0.03	1.02	> 250	> 250	> 274	> 268	> 274	> 268
	Tb[M]	0.13 ± 0.00	0.71 ± 0.02	5.46	> 250	> 250	> 1923	> 352	> 1923	> 352
	Tb[Ea]	10.59 ± 0.30	6.28 ± 0.95	0.59	> 250	116.1 ± 2.97	> 23	> 39	11	18
Reference Drugs	Artemisinin (nM)	3.38 ± 0.066	14. 47 ± 0.02	4.3						
	Chloroquine (Nm)	7.55 ± 0.01	133 ± 0.02	17.61						

*Inhibitors were tested against parasites in culture. IC_{50}: Median inhibitory concentration, CC_{50}: Median cell cytotoxic concentration; **Cytotoxicity of compounds was tested against normal mammalian cells. Data are the mean values of triplicate experiments; ***Selectivity values represent the ratio of CC_{50} to IC_{50}; RI: IC_{50}*Pf*Dd2/IC_{50}*Pf*3D7; *Ti: Terminalia ivorensis; Tb*: *Terminalia brownii;***W**: Water; **E:** Ethanol; **H-E**: Hydro-Ethanol; **M:** Methanol; **Ea**: Ethyl acetate; **Art**: Artemisinin; **CQ**: Chloroquine; **RC:** Raw Cells, **VC:** Vero cells, **SD:** Standard Deviation, **SI:** Selectivity Index, **RI:** Resistance Index
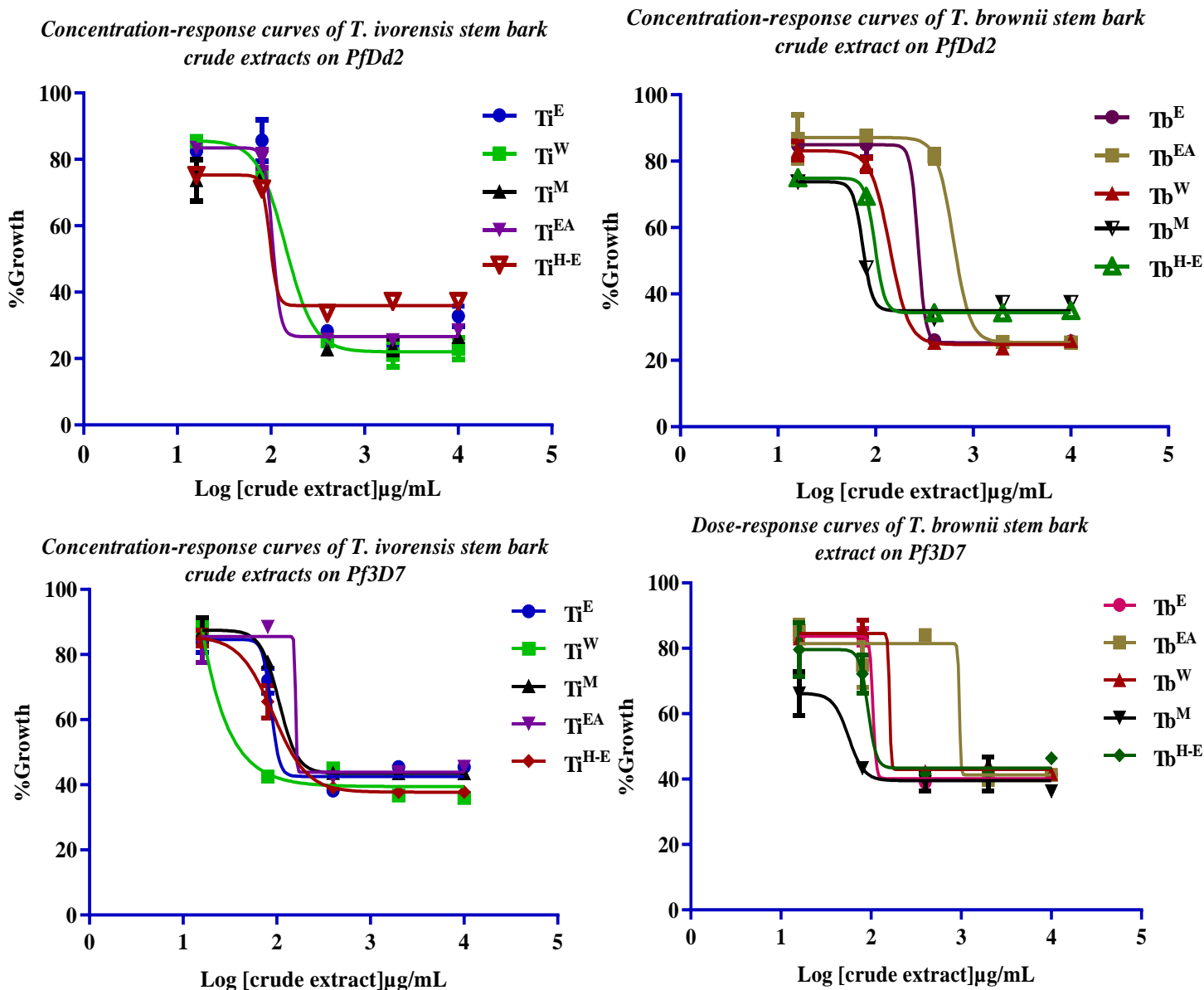
Figure 23: Dose - response curves of *Terminalia ivorensis* and *Terminalia brownii* crude extracts on *P. falciparum* Dd2 and 3D7 using the *Pf*LDH assay.

Data were normalized to percent control activity and median inhibitory concentrations (IC$_{50}$s) calculated using Prism 8.0 software (GraphPad) with data fitted by nonlinear regression to the variable slope sigmoidal dose - response formula y = 100/[1+ 10$^{(logIC50-x)H}$], where *H* is the Hill coefficient or slope factor. Ti^{W}: aqueous extract of *T. ivorensis*; Ti^{E}: ethanol extract of *T. ivorensis*; Ti^{H-E}: hydroethanol (70%) extract of *T. ivorensis*; Ti^{M}: methanol extract of *T. ivorensis*; Ti^{Ea}: ethyl acetate extract of *T. ivorensis*; Tb^{W}: aqueous extract of *T. brownii*; Tb^{E}: ethanol extract of *T. brownii*; Tb^{H-E}: hydroethanol (70%) extract of *T. brownii*; Tb^{M}: methanol extract of *T. brownii;* Tb^{Ea}: ethyl acetate extract of *T. brownii*.

III.2.2-*In vivo* antimalarial activity of aqueous and methanolic stem bark extracts of *T. ivorensis* and *T. brownii*

III.2.6.1-*In vivo* acute toxicity

The results showed that oral administration of Ti^W and Tb^M at a dose of 2000 mg/kg did not cause mortality or major behavioural changes among the experimental groups of animals indicating that the LD_{50} values of Ti^W and Tb^M were greater than 2000 mg/kg in BALB/c mice. Therefore, according to the OECD's Globally Harmonized System of Classification (OECD, 2002), both extracts (Ti^W and Tb^M) can be classified as category 5 and considered nontoxic once administered orally. Additionally, recording of body weight during 14 days of observation showed no significant change in treated animals compared to the normal group. Ti^W and Tb^M progressed to *in vivo* antimalarial efficacy using a 4-day suppressive test and were used in the following experiments at a fixed dose of 100 mg/kg
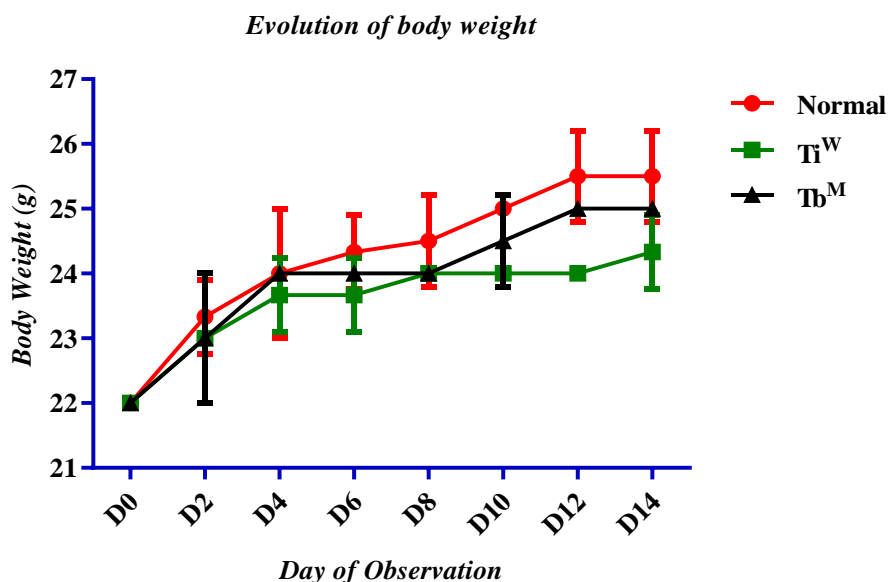
Figure 24: Evolution of body weight of mice-treated with extract and distilled water for 14 days.

III.2.6.2-*In vivo* antimalarial efficacy

III.2.6.2.1-*In vivo* antimalarial efficacy of aqueous and methanolic stem bark extracts of *T. ivorensis* and *T. brownii.*

The antimalarial efficacy of *T. ivoresnsis* and *T. brownii* was studied in *P. berghei*-infected mice using a 4-day suppressive test. The results showed that 4-day administration of aqueous and

methanolic stem bark extract of *T. ivoresnsis* and *T. brownii* suppressed *Plasmodium berghei* multiplication by 100% and 68.67% respectively (**Table 10 & Figure 25A**) compared to the group of mice that received distilled water (vehicle). Interestingly, there were no significant differences between the chloroquine treated group and the Ti^W-treated group (***P < 0.0001) following 4-days of treatment while a significant difference was observed between the chloroquine treated group and Tb^M. On Day 8, Ti^W and Tb^W treatment resulted in parasite suppression of 87.91% and 94.47% respectively compared to the group of mice treated with distilled water (vehicle) (**Table 10 & Figure 25B**). Conversely, chloroquine treatment abolished *Plasmodium berghei* multiplication over the entire period of observation.

Table 11: Percentage of *Plasmodium berghei* suppression by aqueous and methanolic extracts of *T. ivorensis* and *T. brownii*.

	% Of Parasite suppression	
	At Day 4	**At Day 8**
Chloroquine	100 ± 0.00	100 ± 0.00
Ti^W	100 ± 0.00	87.91 ± 0.51***
Tb^M	68.67 ± 1.36***	94.47 ± 0.25*

Percentages of parasite suppression according to the treatment, calculated by comparison to H$_2$O treated mice. ***P < 0.0001, *P < 0.05 between the TiH$_2$O and TbMeOH groups and to H$_2$O group.

A *Parasiteamia at D4 post infection*

Treatment groups
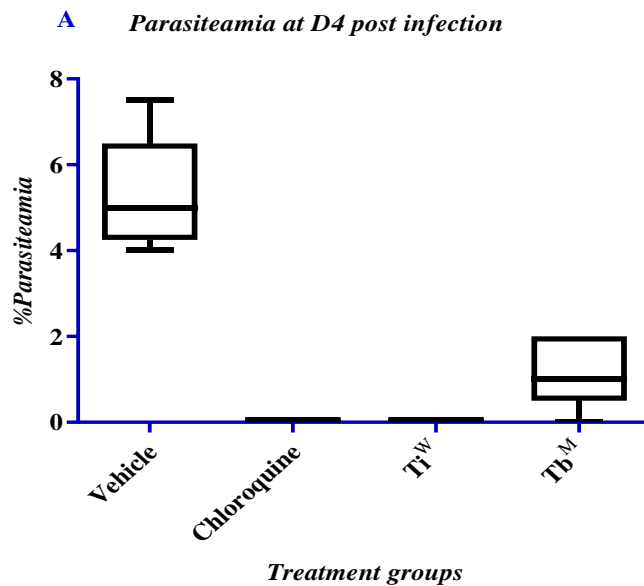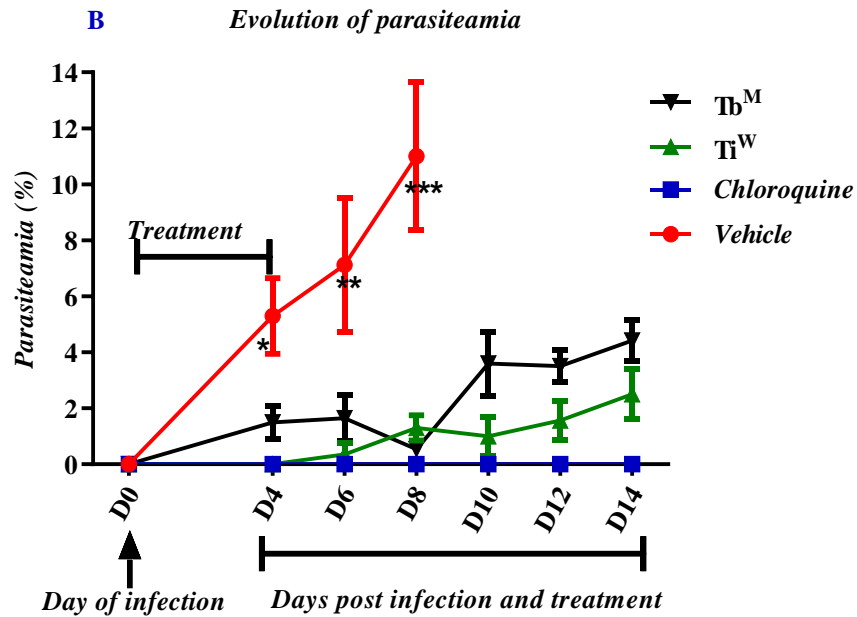
Figure 25: *In vivo* antimalarial efficacy of *T. ivoresnsis* and *T. brownii* in the *P. berghei* model. BALB/c mice were infected with *P. berghei* NK65 and treated 2 h later with chloroquine (10 mg/kg), aqueous and methanolic stem bark extracts of *T. ivoresnsis* and *T. brownii* (100 mg/kg) respectively or water (25 mL/kg) following intraperitoneal infection (10^6 *Plasmodium*/mice) from Day 0 to Day 3. Parasite densities (parasitaemia) were measured every 48 h from D4 to D14. (**A**) Effects of chloroquine; Ti^W and Tb^M on the parasitemia of infected mice on day 4. (**B**) Evolution of parasitaemia on the day post-infection. Parasitemia was compared according to treatment received (($*P < 0.05$; $**P < 0.005$ or $***P < 0.001$)) and extract and CQ treatment were compared to vehicle.

III.2.6.2.2-Effect of aqueous and methanolic stem bark extracts of *T. ivorensis* and *T. brownii* treatment on survival following *Plasmodium infection* in mice.

Treatment of mice with *T. ivorensis* and *T. brownii* greatly improved survival as chloroquine did. Comparisons of survival rates between groups at D9 postinfection showed a critical effect of Ti^W and Tb^M treatments on survival (**Figure 26**). At D9, all mice that received the vehicle died whereas 5 of the 6 mice (83.3%) treated with Ti^W and Tb^M, survived (**Figure 26**). In the CQ treatment group, 100% of infected mice survived at D9. At D15, the survival rates of Ti^W and Tb^M treated mice were similar to those of CQ-treated mice (5/6 and 5/6 for Ti^W and Tb^M versus 6/6 for CQ, see **Figure 26**)
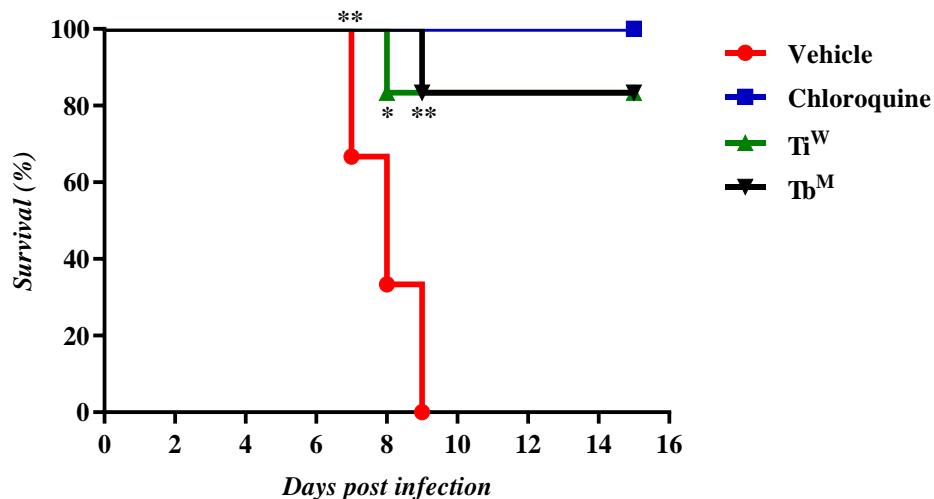
Figure 26: Percentage of survival following infection in mice.

Survival was measured daily and compared according to treatment received at D9 (**P < 0.005). Ti^W; Tb^M and CQ treatments were compared to vehicle, (**P < 0.05).

III.2.6.2.3-Effect of aqueous and methanolic stem bark extracts of *T. ivorensis* and *T. brownii* on mouse body weight after *Plasmodium infection* in mice.

To evaluate the effect of Ti^W and Tb^M stem bark extracts on body weight following infection, analysis was first focused on weight differences between the initial weight (D0) and D4 according to the Peters' test. Second, weight differences between D0 and D9 (peak of death in the *P. berghei* model) were studied. Chloroquine; Ti^W and Tb^M -treated mice lost weight as well as those treated with the vehicle at D4 **(Table 11)**. However, there were no significant differences in weight loss between vehicles and mice treated with CQ and extracts (P < 0.05). Surprisingly, the highest weight loss was observed in CQ-treated mice at D4. At D9, when all mice that received vehicle had died, there were no significant differences between the bodyweight of mice treated with CQ and those receiving extracts **(Table 11)**.

Table 12: Differences in body weight of *Plasmodium*-infected BALB/c mice before (D0) and after infection and administration of the aqueous stem bark extracts of *T. ivorensis* (Ti^W) and methanolic stem bark extract *T. brownii* (Tb^M) at 4- and 9-days postinfection.

Infection Group	Treatment group	n	D4-D0 ± SD	D9-D0 ± SD
P. berghei NK65	Vehicle	6	-0.8 ± 1.30	-
	Chloroquine (CQ) (10mg/mL)	6	-0.2 ± 0.44	-0.4 ± 1.14
	Ti^W (100mg/mL)	6	-1 ± 1.00	0.25 ± 1.70
	Tb^M (100mg/mL)	6	-0.8 ± 0.83	0 ± 1.14

Chloroquine (CQ) was used as the positive control, **SD***:* Standard Error; comparisons of mice treated with CQ or extracts were performed by one-way analysis of variance (ANOVA) followed by the means multiple comparison method of Bonferroni–Dunnett. The Mann–Whitney U- test was used for two-by-two comparisons. Differences were considered significant if P < 0.05.

III.2.3-Discussion

The Plant Kingdom stands as an infinite resource for the discovery of novel chemotypes and pharmacophores, and scaffolds for amplification into efficacious drugs for a multitude of disease indications. Plants remain an important source of novel pharmacologically active compounds with many blockbuster drugs being derived directly or indirectly from plants. Despite the current move with synthetic chemistry as a vehicle to discover and manufacture drugs, the contribution of plants to disease treatment and prevention is still enormous. Even at the dawn of the 21st century, 11% of the 252 drugs considered basic and essential by the WHO were exclusive of flowering plant origin (Veeresham, 2012). For drug discovery, profiling the chemical composition of plant extracts is of utmost importance and fundamentally orients the unveiling of new chemical scaffolds with the potential to provide a novel or diverse range of promising drugs to control many diseases, including malaria. Hence, this part of the study investigated the *in vitro* antiplasmodial activity and *in vivo* antimalarial efficacy of *T. ivorensis* and *T. brownii,* two traditionally used Cameroonian medicinal plants. Almost all the extracts from both plants displayed a highly potent antiplasmodial inhibitory effect against the chloroquine-sensitive (3D7) and multiresistant (Dd2) strains of *P. falciparum* and good selectivity against normal cells and erythrocytes. Activity data generated from this investigation confirmed the antiplasmodial potential and selectivity of extracts from *Terminalia* species as previously reported. For instance,

Wande and Babatunde, (2017) reported the antiplasmodial IC_{50} of *T. ivorensis* methanolic leaf extract to be 2.58 mg/mL using the β-hematin synthesis inhibitory assay. This finding further suggests that antiplasmodial metabolites are secreted from the metabolic performance in different parts of this plant. Likewise, using the thin blood films approach, Annan *et al.,* (2012) reported the antiplasmodial activity of the ethanolic extract from the stem bark of *T. ivorensis* against *P. falciparum* 3D7 with an IC_{50} of 6.94 µg/mL, suggesting that antiplasmodial metabolites are diversely and readily extracted from *T. ivorensis* by the solvent of varying relative polarities (Ethyl-acetate-0.228, Ethanol-0.654, Methanol-0.762, Water-0.991-1.000). Of note, the values for relative polarity are normalized from measurements of solvent shifts of absorption spectra (Reichardt, 2003). Notably, the ethanolic extract from the stem bark of the Cameroonian *T. ivorensis* investigated in the present study exerted 4.81-8.36-fold more potency against *P. falciparum* 3D7 and Dd2 strains than the extract from the Ghanaian species against *P. falciparum* 3D7. This discrepancy in activities further indicates that the geographical origin of the plant might play a critical role in the quality of bioactive secondary metabolites present in the crude extract (Demain and Fang, 2000). Moreover, the 4-8-fold shift in the activity of the *T. ivorensis* extract between this study and the report by Annan et al. (2012) denotes the impact of the adopted screening procedures that undoubtedly influence the displayed activity parameters. Indeed, Annan et al., (2012) used the microscopic technique to assess the antiplasmodial activity while the *Pf*LDH-based assay was used in this study. From a wider perspective, plant extracts from the *Terminalia* genus have consistently shown antiplasmodial activity. Recently, Mbouna et al., (2018) reported the antiplasmodial activity of the stem bark and leaf extracts of *T. mantaly* and *T. superba* with potent activities (IC_{50}: 0.26–1.26 µg/mL) and selectivity (SI > 158) against resistant INDO and sensitive 3D7 strains of *P. falciparum*. Additionally, water decoction extracts of leaf of *T. catappa* L. and leaf and bark of *T. mantaly* H. Perrier showed antiplasmodial activities with IC_{50} values of 6.41/8.10 µg/mL, 2.49/1.90 µg/mL and 3.70/2.80 µg/mL respectively against the 3D7/INDO strains of *P. falciparum*. Additionally, reports indicated that *T. avicennioides* leaf and stem bark aqueous, methanol, butanol, ethyl acetate and dichloromethane extracts showed antiplasmodial activity with IC_{50} values ranging from 1.60 to 7.40 µg/mL against The *P. falciparum* K1 strain (Ouattara *et al.,* 2014; Sanon *et al.,* 2013). Taken together, these previous studies on *Terminalia* species support and confirm the strong *anti-Plasmodium* activity of both investigated plants.

In vivo validation of antimalarial safety and efficacy mostly for *T. ivorensis* has never been achieved. Hence, to further confirm and validate the antimalarial efficacy of aqueous and methanolic stem bark extracts of both plants, their safety in healthy mice and efficacy in a murine malaria model were investigated. The results of the acute toxicity tests indicate that administration of up to 2000 mg/kg of aqueous and methanolic stem bark extract of *T. ivorensis* and *T. brownii* is safe in BALB/c mice. Thus, the dose tested in this study (100 mg/kg) was safe, and it can be assumed that the antimalarial activities observed are not due to the extract's toxicity. *In vivo* efficacy using 4-day suppressive tests was achieved in experimental models for malaria based on *P. berghei* infections in BALB/c mice. The results showed that Ti^W and Tb^M -treated mice displayed 100% and 68.67% chemo-suppression of parasite multiplication at D4 (Day 4) and 87.91% and 94.47 at D8 (Day 8) respectively when the peak of parasitemia was reached in untreated (vehicle) mice. This significant result reflects an inhibitory activity on parasite replication in this model. In addition, daily control of parasitemia from D4 until D14 to evaluate the reversibility of the extract's effect showed that a resurgence of *P. berghei* multiplication in Ti^W-treated mice after 0% parasite growth at D4 was observed. At D9, all untreated mice died whereas 100% and 83.33% of mice that received Ti^W and Tb^M survived, respectively. This result indicates a very interesting ability of both extracts to extend survival in this model characterized by a high mortality rate. However, survival to *P. berghei* infection was not related to parasite elimination in Ti^W and Tb^M -treated mice because daily observation and parasitemia control showed the presence of parasites at low density compared to untreated mice. Hence, this survival could be explained by the fact that, in the *P. berhei* model, death is due to neuroinflammation related to the influx of myeloid immune cells to the brain, oxidative stress, blood - brain barrier permeability and neurodegeneration (Isah and Ibrahim 2014; Howland *et al.,* 2015)**.** Moreover, the recrudescence of the parasite observed during daily observation and post drug exposure could be explained by the fact that, latent *P. berghei* merozoite escapes the extract's effect by "hiding" in macrophages and neutrophils (Landau *et al.*, 1995; Landau *et al.,* 1999). The results from the body of infected animals suggest that aqueous and methanolic stem bark extracts of *T. ivorensis* and *T. brownii* might not reduce the deleterious effect of the parasite in this model at a critical time for survival. In fact, i*n vivo* studies of some *Terminalia* species have been reported in the literature. For instance, Camara et al. (2019) reported that *P. berghei* (ANKA strain) infected mice treated with *Terminalia albida* methanol extract significantly decreased parasitemia by 100% on Day 4

and 89% on Day 7 postinfection and extended animal survival by 50% on Day 20. Tali *et al.,* (2020) reported that *T. mantaly* aqueous stem bark extract was safe in mice with a median lethal dose (LD_{50}) higher than 2000 mg/kg of body weight and also exerted a good antimalarial efficacy *in vivo* with an ED_{50} of 69.50 mg/kg and had no significant effect on biochemical, hematological, and histological parameters**.** Biruk *et al.,* (2020) also reported that 80% methanol and aqueous extract from *T. brownii* did not cause mortality in healthy mice when administered at a dose up to 2000 mg/kg and significantly suppress parasite (ANKA strain) multiplication in *P. berghei* infected mice with a maximum level of chemo-suppression of 60.2% and 51.1% at 400 mg/kg dose for 80% methanol extract and aqueous extract respectively. Comparatively, our study reports for the first time the *in vivo* antimalarial efficacy of methanol extract of *T. brownii* on lethal *P. berghei* NK65 form with significant chemo-suppression of 68.67% and 94.47% at the dose of 100 mg/kg at Day 4 and Day 8 respectively. In addition, our studies also demonstrate the ability of methanol extract from *T. brownii* to extend survival in *P. berghei* NK65-infected mice by 83.33% on day 14 postinfection. More interestingly, our study also reports for the first time the safety in healthy mice and *in vivo* antimalarial efficacy of *Terminalia ivorensis* stem bark extract. Taking together, the findings from this study and the previous study emphasize the potential of *Terminalia* species to produce secondary metabolites with potent and safe antimalarial efficacy.

III.3-Dual-step activity guided fractionation and biological mode of action of promising substances

III.3.1-First step fractionation and *in vitro* antiplasmodial activities of fractions from *T. ivorensis* and *T. brownii* crude extracts

Fractionation of both extracts led to three (03) main fractions ($Ti^{W}_{chl,}$ Ti^{W}_{Ea} and Ti^{W}_{R3}) from Ti^{W} and five (05) fractions (Tb01, Tb02, Tb03, Tb04 and Tb05) from Tb^{M}. All obtained fractions were subsequently tested for antiplasmodial activity and cell cytotoxicity (**Table 12, Figure 27**). Overall, two fractions from *T. ivorensis* [Ti^{W}_{Ea}; Ti^{W}_{R3}] and two from *T. brownii* [Tb01; Tb05]) exhibited a highly potent inhibitory effect on both *P. falciparum* strains with IC_{50} values ranging from 0.15 to 1.88 µg/ml and high selectivity (SI > 133). The three fractions exhibiting the highest antiplasmodial potency against both strains of *P. falciparum* were the ethyl acetate fraction (Ti^{W}_{Ea}) of *T. ivorensis* aqueous extract (IC_{50} *Pf*3D7 0.52 µg/mL; IC_{50} *Pf*Dd2 0.24 µg/mL), and fractions Tb01 (IC_{50} *Pf*3D7 0.15 µg/mL; IC_{50} *Pf*Dd2 1.73 µg/mL) and Tb05 (IC_{50} *Pf*3D7 0.94 µg/mL; IC_{50}

*Pf*Dd2 0.95 µg/mL) from the *T. brownii* methanolic extract. The three highly potent fractions also showed high selectivity (SI > 144), serving as an indicator of their safety towards human cells and their promise as a source of nontoxic drug candidates for malaria control. Two other fractions, Tb03 and Tb04 displayed moderate (IC$_{50}$ 10 - 20 µg/mL) to low (IC$_{50}$ 20 – 40 µg/mL) antiplasmodial activity against *P. falciparum* strains. Of note, the methylene chloride fraction (Ti$^{W}_{chl}$) from Ti^{W} and the Hex/Ea (1:1, v/v) fraction (Tb02) from Tb^{M} were inactive against the chloroquine-sensitive *Pf*3D7 strain but showed activity against the multiresistant *Pf*Dd2 strain of *P. falciparum* (IC$_{50}$ values of 23.71 µg/mL and 6.74 µg/mL respectively).

Table 13: Antiplasmodial activity and cytotoxicity parameters of fractions obtained from T. ivorensis and T. brownii aqueous and methanolic crude extracts

Plants	Crude extract code	Solvent	Fraction code	Antiplasmodial activity $*IC_{50} \pm SD$ (µg/mL)			Cell cytotoxicity $**IC_{50} \pm SD$ (µg/mL)		***Selectivity index SI_{VC}		SI_{RC}	
				Pf3D7	PfDd2	RI	VC	RC	Pf3D7	PfDd2	Pf3D7	PfDd2
T. ivorensis	Ti^W	Methylene Chloride	Ti^W_{chl}	> 100	23.71 ± 0.34	> 0.23	> 250	171.6 ± 0.05	-	> 10	-	7.23
		Ethyl acetate	Ti^W_{Ea}	0.52 ± 0.01	0.24 ± 0.06	0.46	> 250	> 250	>480	>1041	> 480	>1041
		-	Ti^W_{R3}	1.88 ± 0.16	1.46 ± 0.08	0.77	> 250	> 250	>132	>171	>132	>171
T. brownii	Tb^M	Hex:Ea 1:3	Tb01	0.15 ± 0.00	1.73 ± 0.09	11.53	> 250	> 250	>1666	>144	>1666	> 144
		Hex:Ea 1:1	Tb02	> 100	6.74 ± 0.07	> 0.06	> 250	> 250	-	>37	-	> 37
		Hex:Ea 3:1	Tb03	18.30 ± 0.64	17.24 ± 0.08	0.94	> 250	161.7 ± 0.02	>14	>14.50	8.83	9.37
		Hex:Ea 0:1	Tb04	17.27 ± 0.08	25.04 ± 0.02	1.44	> 250	> 250	>14.47	>10	>14	> 10
		MeOH:Ea (1:1)	Tb05	0.94 ± 0.00	0.95 ± 0.01	1.01	> 250	> 250	>265	>263	>265	>263
Reference Drugs			Artemisinin (nM)	3.38 ± 0.066	14. 47 ± 0.02	4.3						
			Chloroquine (nM)	7.55 ± 0.01	133 ± 0.02	17.61						

*Inhibitors were tested against parasites in culture. IC_{50}: Median inhibitory concentration, CC_{50}: Median cell cytotoxic concentration; **Cytotoxicity of compounds was tested against normal mammalian cells. Data are mean values of triplicate experiments; ***Selectivity values represent the ratio of CC_{50} to IC_{50}; RI: $IC_{50}Pf$Dd2/$IC_{50}Pf$3D7; **Art**: Artemisinin; **CQ**: Chloroquine; **chl**: Methylene chloride; **MeOH**: Methanol; **Hex**: Hexane, **Ea**: Ethyl acetate; **Ti**: *Terminalia ivorensis;* **Tb**: *Terminalia brownii;* **W***: Water;* **R3***: Residue. **RC***: Raw Cells, **VC***: Vero cells, **SD***: Standard Deviation, **SI***: Selectivity Index, **RI***: Resistance Index.*
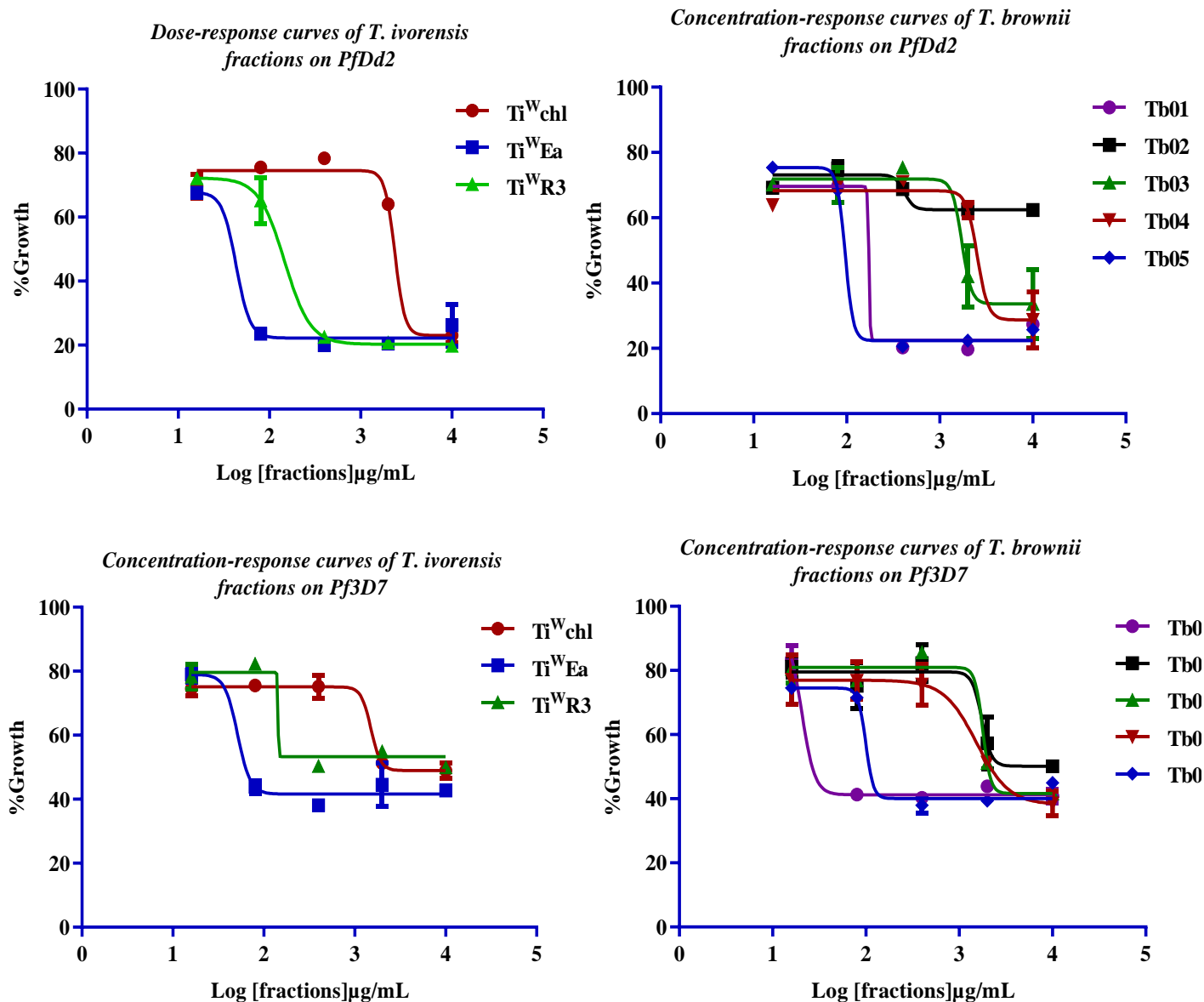
Figure 27: Dose - response curves of fractions from *Terminalia. ivorensis* and *Terminalia brownii* aqueous and methanolic crude extracts on P. falciparum Dd2 and 3D7 using *Pf*LDH-based assay.

Data were normalized to percent control activity and median inhibitory concentrations (IC$_{50}$S) calculated using Prism 8.0 software (GraphPad) with data fitted by nonlinear regression to the variable slope sigmoidal dose - response formula y = 100/[1+ 10$^{(logIC50-x)H}$], where *H* is the Hill coefficient or slope factor. Ti^{w}Ea: ethyl acetate fraction derived from the aqueous extract of *T. ivorensis*; Ti^{w}chl: dichloromethane fraction deriving from the aqueous extract of *T. ivorensis*; Ti^{w}R3: aqueous residue derived from the aqueous extract of *T. ivorensis*; Tb01: Hex/Ea (1:3, v/v) fraction derived from the methanol extract of *T. brownii*; Tb02: Hex/Ea (1:1, v/v) fraction deriving from the methanol extract of *T. brownii*; Tb03: Hex/Ea (3:1, v/v) fraction derived from the methanol extract of *T. brownii*; Tb04: Hex/Ea (0:1, v/v) fraction derived from the methanol extract of *T. brownii*; Tb05: Ea/MeOH (1:1, v/v) fraction derived from the methanol extract of *T. brownii*.

III.3.2- Qualitative chemical profiling of promising fractions

Analysis of the UPLC - MS of fractions from aqueous and methanol extracts of *T. ivorensis* (Ti^WEa) and *T. brownii* (Tb05) led to the identification of ellagic acid (**1**) and papyriogenin D (**3**) in fraction Ti^WE and ellagic acid (**1**) and leucodelphidin (**2**) in fraction Tb05 (**Figure: 28-29; Table: 13**). Since ellagic acid (**1**) appeared in both active fractions, we suspected it to be responsible for the observed activity. Hence, this compound was purchased for both UPLC MS analysis and antiplasmodial activity. *In vitro*, ellagic acid showed significant activity on both multiresistant (*Pf*Dd2; IC_{50} = 0.59 ± 0.08 µM) and chloroquine-sensitive (*Pf*3D7; IC_{50} =2.68 ± 0.08 µM) strains of *P. falciparum*. UPLC-QTOF-MS analysis of the standard of ellagic acid confirmed the presence of the compound in the bio-active fractions (**Table:14**).
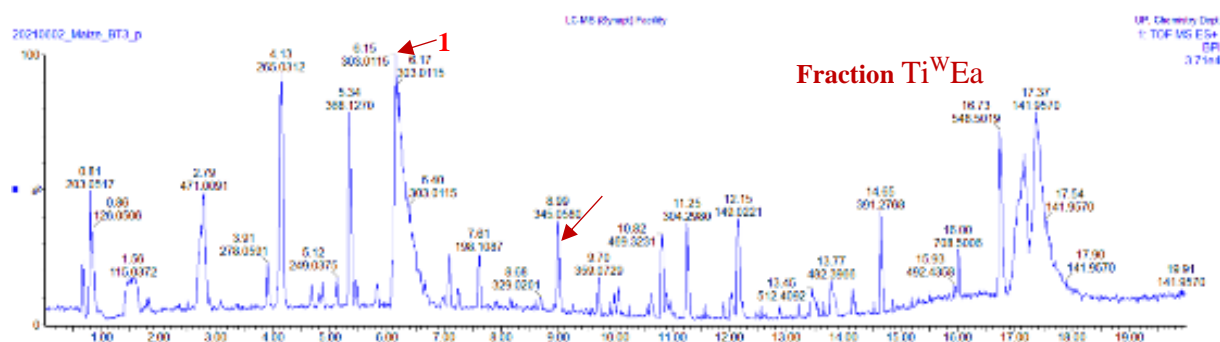
Figure 28: UPLC-MS chemical profiles (positive mode) of fractions Ti^WEa from aqueous stem bark extract from *T. ivorensis*.
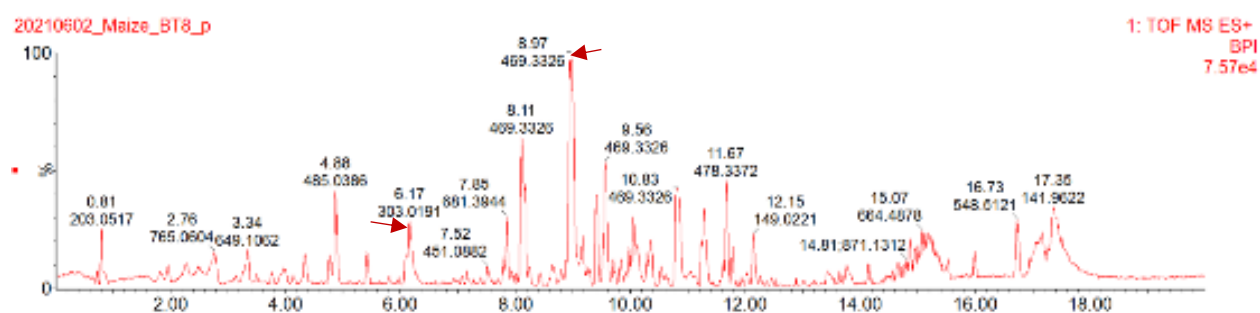
Figure 29: UPLC - MS chemical profiles (positive mode) of hits fractions Tb05 from crude methanol extract of *T. brownii*.

Table 14: Compounds identified in the hit fractions from *T. brownii* and *T. ivorensis*

Peak	Retention time	Acquired [M+H]$^+$ m/z	Exact mass	Molecular Formula	Name of compound
1	6.17	303.0191	302.006270	$C_{14}H_6O_8$	Ellagic acid
2	8.99	345.0560	322.068870	$C_{15}H_{14}O_8$	Leucodelphidin Leucodelphinidin Gallocatechin-4-beta-ol
3	8.97	469.3309	468.323960	$C_{30}H_{44}O_4$	Papyriogenin D

Compounds were tentatively identified by generating molecular formulas from MassLynx V 4.1 based on their iFit value, and by comparison of the MS/MS fragmentation pattern with that of matching compounds from Waters UNIFI® Scientific Information System (version 1.9.2) accessing the Chinese Natural Products database.

Table 15: Comparison of UPLC - MS data of ellagic acid (1) from analysis of the purchased standard and fractions from *T. ivorensis* and *T. brownii*.

Sample	Retention time	Acquired [M+H]$^+$ m/z	Molecular Formula	MS/MS data (fragments)
Ellagic acid fractions from *T. ivorensis* and *T. brownii*	6.15	303.0191	$C_{14}H_6O_8$	257.0141 201.0214 173.0293
Standard ellagic acid	6.14	303.0182	$C_{14}H_6O_8$	257.0129 201.0199 173.0278

Compounds were tentatively identified by generating molecular formulas from MassLynx V 4.1 based on their iFit value, and by comparison of the MS/MS fragmentation pattern with that of matching compounds from Waters UNIFI® Scientific Information System (version 1.9.2) accessing the Chinese Natural Products database.

Ellagic acid

Leucodelphidin (Flavonoids)

Papyriogenin D (Triterpenes)
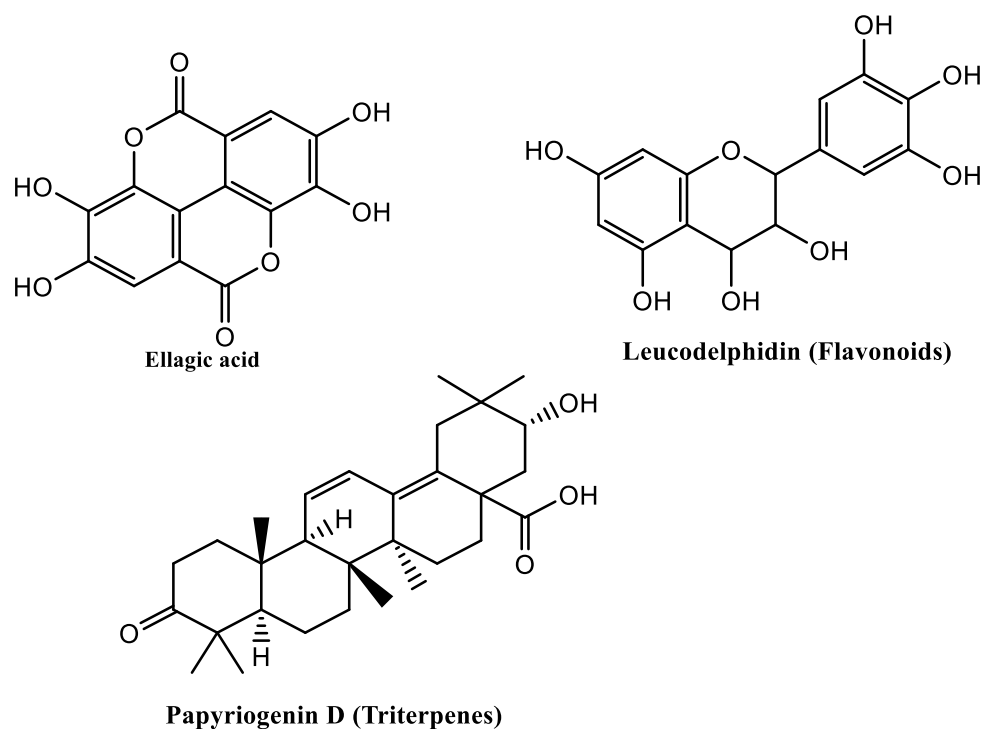
Figure 30: Chemical structures of secondary metabolites identified from the antiplasmodial "hit" fraction from *Terminalia ivorensis* and *Terminalia brownii*.

III.3.3-Second chromatography fractionation of the potent fractions.

III.3.3.1- Structural characterization of the isolated compound.

Eschweilenol C (4-α-rhamnopyranosyl ellagic acid) is a poorly soluble compound in most common solvents except DMSO. Obtained as a light-yellow amorphous powder, it was isolated from *T. brownii* for the first time. However, the presence of this compound in this species is not surprising as plants of the *Terminalia* genus are rich sources of ellagic acid derivatives. The structure of this compound was determined using 1D and 2D NMR data in comparison with the literature (Rodrigues et al., 2019). Indeed, in its ^{1}H-NMR spectrum, five oxymethine protons were observed (**Table 15**), along with a doublet methyl signal (δ 1.14) indicating the existence of one 6-deoxysugar (Yang et al., 1998) and only two singlets (δ 7.74 and 7.48) in the aromatic region indicating the ellagic acid derivative (Rodrigues et al., 2019). The glycoside was easily determined to be rhamnose through analysis of the chemical shifts and coupling patterns of its proton signals and by comparison with the literature, which was connected by a COSY spectrum. Although the aglycon bears only two singlets (δ 7.72 and 7.46) in the aromatic region, there are 14 carbon signals in the low field region of its ^{13}C-NMR spectrum, including two carbonyl esters and 12 aromatic carbons of which 6 are oxygenated. This information indicated that the main skeleton consisted of an ellagic acid moiety and a

rhamnose unit whose signals were at $\delta_{C/H}$ (100.6/5.46 (d, J=1.2, 1H)) and are typical of the anomer. This proposed assignment was supported by the following HMBC evidence. From this spectrum, both vinyl proton signals (H-5 and H-5′) had similar patterns for their long-range correlations, which were to carbons with signals at δ 114.9 (C-1), 141.6 (C-3), 146.8 (C-4), 107.9 (C-6), 159.5 (C-7) and 112.2 (C-1′), 140.1 (C-3′), 149.1 (C-4′), 108.5 (C-6′), and 159.4 (C-7′), respectively. The location of the rhamnose substituent was confirmed by the observation of the HMBC correlation between H-5 (δ 7.74) and C-4′ (δ 146.8) which can be distinguished from other oxygenated carbons by comparison with literature data (**Table 15**). The anomeric configuration was confirmed as **R** by the small coupling constant of the anomeric proton (J=1.2 Hz). All this information allowed us to assign the structure of eschweilenol C (4-α-rhamnopyranosyl ellagic acid) to the isolated compound without ambiguity.
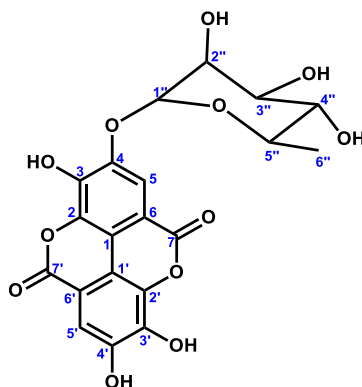
Figure 31: Chemical structures of the isolated compound (Eschweilenol C) with numbering.

Table 16: NMR data of eschweilenol C in CD3OD (δ in ppm/J in Hz).

Pos.	^{13}C (125 MHz)	^{1}H (500 MHz)	HMBC	^{13}C (150 MHz)	^{1}H (600 MHz)
	δ_C (mult.)	δ_H	$^{2}J_{C\text{-}H}$ and $^{3}J_{C\text{-}H}$	$\delta_{C\,Lit*}$	$\delta_{H\,Lit*}$
1	114.9 (C)			114.4	
2	136.8 (C)			136.3	
3	141.6 (C)			141.1	
4	146.8 (C)			146.3	
5	111.9 (CH)	7.74 (s,1H)	107.9 (C-6), 114.9 (C-1), 141.6 (C-3), 146.8 (C-4), 159.5 (C-7)	111.5	7.75 (s,1H)
6	107.9 (C)			107.4	
7	159.5 (C)			158.9	
1′	112.2 (C)			111.7	
2′	137.1 (C)			136.6	
3′	140.1 (C)			139.7	
4′	149.1 (C)			148.6	
5′	110.7 (CH)	7.48 (s,1H)	108.5 (C-6′), 112.2 (C-1′), 140.1 (C-3′), 149.1 (C-4′), 159.4 (C-7′)	110.2	7.49 (s,1H)
6′	108.5 (C)			107.9	
7′	159.4 (C)			158.8	
1″	100.6 (CH)	5.46 (d, J=1.2, 1H)	70.3 (C-2″), 146.8 (C-4)	100.1	5.46 (brs, 1H)
2″	70.3 (CH)	4.00 (m, 1H)	72.2 (C-4″)	69.7	4.00 (d, 1H)
3″	70.5 (CH)	3.84 (dd, J= 9.4, 3.3, 1H)	72.2 (C-4″)	70.0	3.85 (dd, 1H)
4″	72.2 (CH)	3.30 (m, 1H)	18.3 (C-6″), 70.3 (C-2″), 70.4 (C-5″)	71.6	3.33 (dd, 1H)
5″	70.4 (CH)	3.57 (m, 1H)	18.3 (C-6″), 72.2 (C-4″)	69.8	3.70 (ddq, 1H)
6″	18.3 (CH$_3$)	1.14 (d, J= 6.2, 1H)	70.4 (C-5″), 72.2 (C-4″)	18.0	1.14 (d, 3H)

* (Rodrigues et al., 2019)

III.3.3.2- *In vitro* antiplasmodial activity and selectivity of subfractions and isolated compound (Eschweilenol C).

Overall, eight subfractions were obtained from both plant species, five (05) from *T. ivorensis*; three (03) from *T. brownii* and one isolated compound characterized as eschweilenol C from the ethyl acetate/methanol fraction of methanolic extract of *T. brownii*. Subfractions and eschweilenol C were screened against asexual-blood stages of multiresistant (Dd2*)* and sensitive (3D7*)* strains of *P. falciparum* in culture using a *Pf*LDH-based assay. The classification of anti-plasmodial activity of tested substances was performed according to the criteria adopted by Muganza *et al.,* (2016). Hence, subfractions SbTi02; SbTi03; SbTi04 and SbTi05 from ethyl acetate fraction of *T. ivorensis* aqueous extract and SbTb01; SbTb04 and eschweilenol C displayed pronounced antiplasmodial activity with IC$_{50}$ < 5 µg/ml against both sensitive and multiresistant strains of *P. falciparum*. Interestingly, three top hit inhibitors, two from *T. ivorensis* (SbTi03; SbTi04) and one from *T. brownii* (eschweilenol C) displayed a very

good antiplasmodial profile with $IC_{50} < 1$ µg/ml and $SI > 10$. Together, these results suggest that SbTi03; SbTi04 and eschweilenol C are promising new starting points for the development of new antimalarial drugs. Motivated by the need for the discovery of panreactive anti-malarial agents, subfractions and eschweilenol C were also screened against mutant-resistant strains of *P. falciparum* Dd2 (PfDd-GNF156) with a novel mechanism of resistance. Out of the eight (08) subfractions screened, six (SbTi02, SbTi03, SbTi04, SbTi05, SbTb01) and eschweilenol C showed good antiplasmodial profiles with IC_{50} value ranging from 0.20 to 8.34 µg/ml. Fractions SbTi03, SbTi04, and compound eschweilenol C showed the same inhibitory profile ($IC_{50} < 1$ µg/ml) against *Pf*Dd-GNF156. Overall, subfractions SbTi03, SbTi04 and eschweilenol C showed no spontaneous reduction in potency which could be attributed to their novel mode of action. The screening (1 and 5 µg/ml) of eight subfractions and eschweilenol C *in vitro* against the late gametocyte stage (IV/V) indicated dose-dependent inhibition (**Table 17**; **Figure 33**) but were inactive with inhibition percentages ranging from 0 to 16.9%.

Table 17: Antiplasmodial activity and selectivity of *T. ivorensis* and *T. brownii*-derivatives.

Subfractions/Compounds	*Inhibition of Plasmodium proliferation*				**Cytotoxicity**		***Selectivity Indices**			
	IC$_{50}$ ± SD (μg/ml)				IC$_{50}$ ± SD (μg/ml)					
	*Pf*Dd2	*Pf*3D7	*Pf*Dd2-*GNF-156*	RI (IC$_{50}$*Pf*Dd2/ IC$_{50}$*Pf*3D7)	VC	RC	SI (VC)		SI (RC)	
							PfDd2	*Pf3D7*	*PfDd2*	*Pf3D7*
SbTi01	> 25	> 25	> 25	-	> 100	> 100	185	95	-	-
SbTi02	5.73 ± 0.09	1.05 ± 0.01	8.34 ± 0.00	5.45	> 100	> 100	204	667	>185	95
SbTi03	0.54 ± 0.04	0.15 ± 0.02	0.20 ± 0.00	3.6	> 100	77.03 ± 0.09	30	270	157	514
SbTi04	0.49 ± 0.08	0.37 ± 0.05	0.20 ± 0.00	1.32	> 100	80.34 ± 0.08	23	48	24	217
SbTi05	4.52 ± 0.06	2.10 ± 0.40	1.16 ± 0.02	2.15	> 100	> 100	20	21	28	48
SbTb01	3.53 ± 1.15	4.67 ± 0.00	7.74 ± 0.00	0.75	> 100	67.95 ± 0.07	18	83	14	15
SbTb02	4.94 ± 0.25	1.21 ± 0.07	> 25	4.08	> 100	> 100	455	83	18	83
SbTb03	5.49 ± 0.51	> 25	> 25	-	> 100	> 100	244	588	455	-
Eschweilenol C	0.22 ± 0.01	0.17 ± 0.01	0.21 ± 0.00	1.29	> 100	53.73 ± 0.14	185	95	131	316
Artemisinin (nM)	0.04085 ± 0.00	0.0095 ± 0.00	0.051817 ± 0.00	4.3	-	-	-	-	-	-
Chloroquine (nM)	0.042542 ± 0.00	0.002415 ± 0.00	> 3.1987	17.61	-	-	-	-	-	-

*Compounds were tested against parasites in culture. IC$_{50}$: Median inhibitory concentration, CC$_{50}$: Median cell cytotoxic concentration; **Cytotoxicity of subfractions and eschweilenol C was tested against normal mammalian cells. Data are mean values of triplicate experiments ± standard deviation; ***Selectivity values represent the ratio of CC$_{50}$ to IC$_{50}$; RI: IC$_{50}$*Pf*Dd2/IC$_{50}$*Pf*3D7; **Art:** Artemisinin; **CQ**: Chloroquine, **Sb**: Subfraction, *RC: Raw Cells, VC: Vero cells, SD: Standard Deviation, SI: Selectivity Index, RI: Resistance Index*
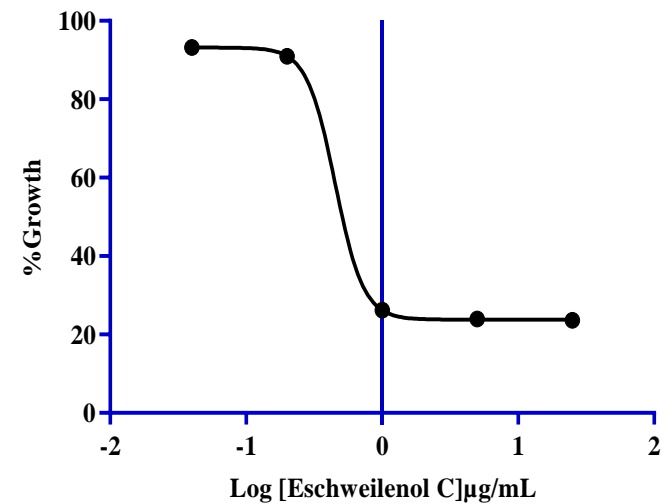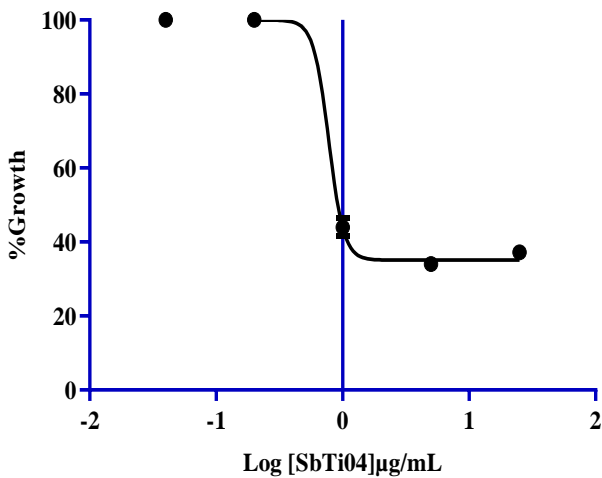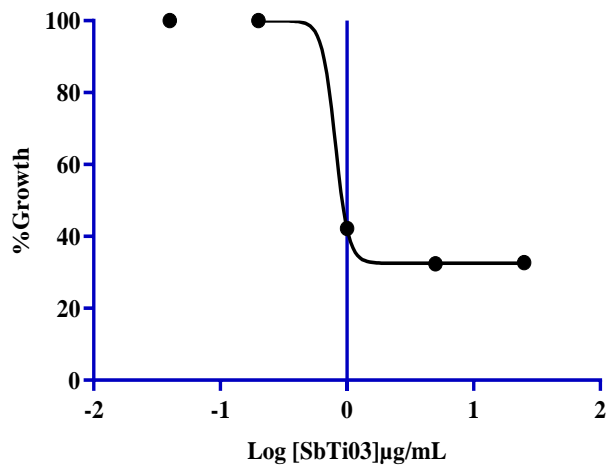
Figure 26A: *Concentration - response curves of the most potent subfractions (IC_{50} < 1 µg/mL) on P. falciparum Dd2.*

Figure 32: Dose - response curves of the hit subfractions and eschweilenol C on sensitive (3D7), multiresistant (Dd2) and mutant (Dd2-GNF156) strains of *P. falciparum*.

Table 18: Dual point inhibition of late-stage gametocyte (IV/V) proliferation at 1 and 5 µg/ml using the luciferase-based assay

	Inhibition of *P. falciparum* late stages gametocytes									
Drugs	SbTi02	SbTi03	SbTi04	SbTi05	SbTb01	SbTb02	SbTb03	Eschweilenol C	MB (µM)	MMV390048(µM)
IC$_{50}$ (µg/mL)	> 5	> 5	>5	> 5	> 5	> 5	> 5	> 5		6.43 ± 0.43

Legend: MB: Methylene Blue, IC$_{50}$: Inhibitory Concentration 50, MMV: Medicine for Malaria Venture
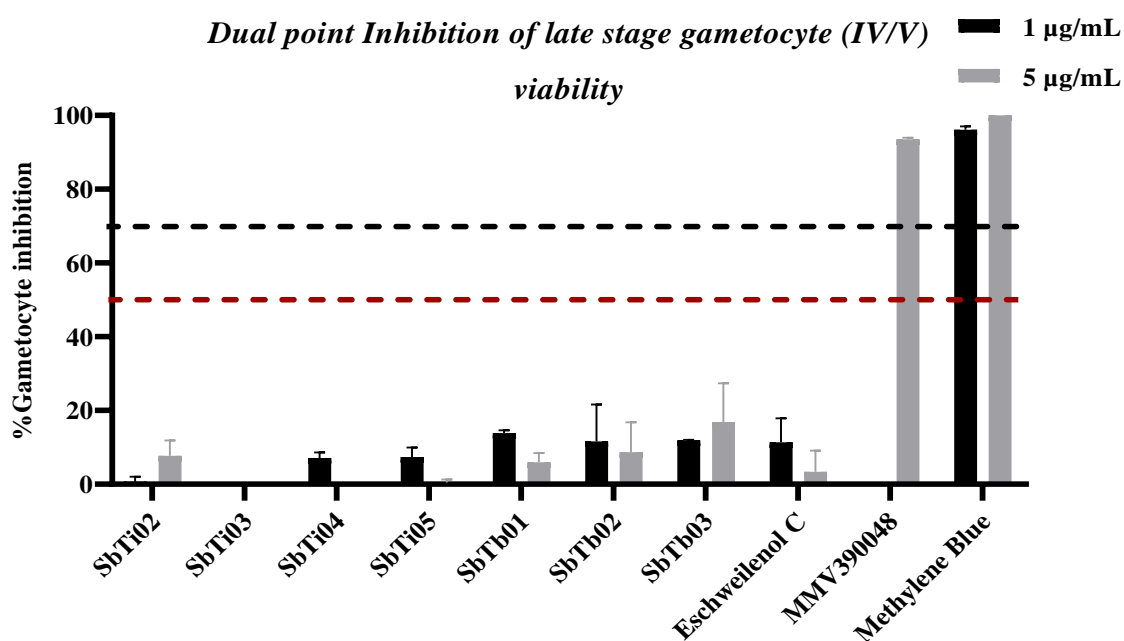
Figure 33: Inhibition of in vitro viability of late-stage gametocytes (2% gametocytaemia, n=3) of *P. falciparum* (NF54-Mal8p1.16-GFP-Luc) by *T. ivorensis* and *T. brownii* derived subfractions and Eschweilenol C.

III.3.3.3-Effect of potent subfractions and eschweilenol C on hemozoin production

The quantity of hemozoin produced is directly related to the level of hemoglobin digestion. Hence, to quantify the amount of hemozoin in response to drug exposure as a possible mode of action, the UV - Visible spectra of β-hematin dissolved in NaOH (20 mM) were first recorded at different concentrations and a calibration graph was constructed (**Figure 34**) which was used to quantify the maximum amount of β-hematin (hemozoin) produced by *Plasmodium* in the presence of different subfractions, eschweilenol C and the positive control. Data for hemozoin production by *Plasmodium* in the effect of artemisinin; chloroquine, Eschweilenol C and the two hit subfractions (SbTi03 and SbTi04) are presented in **Figure 35**. The level of

hemozoin production in response to treatment with SbTi03; SbTi04 and Eschweilenol C was not significantly different when compared to chloroquine and artemisinin. However, those subfractions and eschweilenol C showed significant (***p < 0.0001) inhibition of hemozoin production when compared to the control (**Figure 35**).
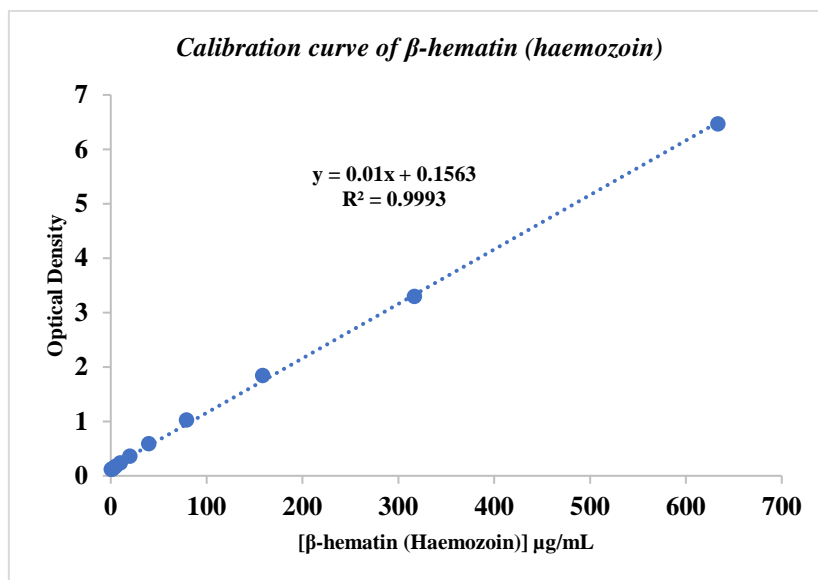
Figure 34: Calibration curve for β-hematin (hemozoin) (Sigma - Aldrich) at different concentrations.

β-hematin was prepared at 633.49 µg/ml in NaOH (20 mM) and geometrically diluted in 2-fold serial dilution. After that, the absorbance was recorded at 405 nm.
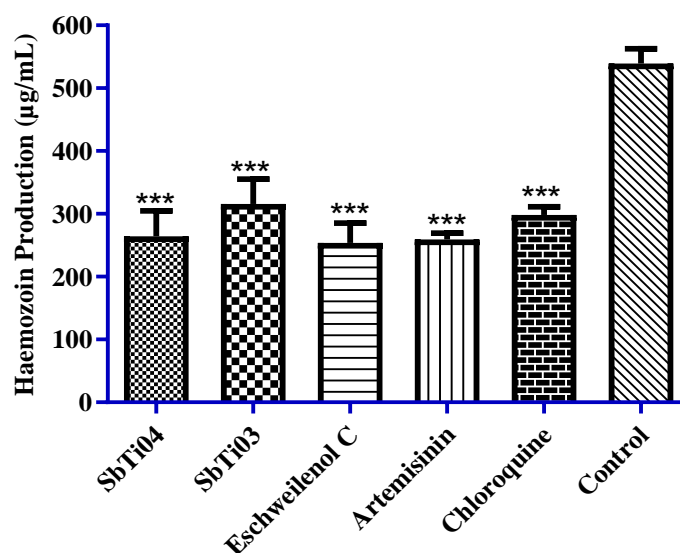
Figure 35: Amount of hemozoin produced (µg/mL).

n = the experiment was performed in triplicate. Data are presented as the mean ± SD and were compared using one-way analysis of variance (ANOVA). GraphPad Prism statistics version 9.0 was used for data analysis. Significant data are given as ***p < 0.0001.

III.3.3.4- Time-kill kinetics

The *in vitro* speed of action of SbTi03; SbTi04 and eschweilenol C was determined according to the method developed by Le Manach *et al.,* (2013), which classifies drugs as slow or fast-acting based on a relative *in vitro* speed of action. To this end, growth inhibition assays were performed, using asynchronous cultures of multiresistant *Pf*Dd2, and parasite growth was assessed after drug exposure for 24, 48 and 72 h. The ratio of 24 hours IC_{50} values to 72-hour IC_{50} values for the tested subfractions and eschweilenol C could not be determined as IC_{50} could not be reached within 24 hours. For comparative reasons, artemisinin was analysed in parallel. The IC_{50} ratios of SbTi03; SbTi04 and eschweilenol C were independent of the exposure time ((> 25, 0.24 ± 0.04 and 0.13 ± 0.00); (> 25, 0.12 ± 0.06 and 0.13 ± 0.06); (> 25, 0.25 ± 0.03, 0.59 ± 0.00) for 24, 48 and 72 h of drug exposure, respectively) indicating a slow-acting action. Similarly, the exposure time did not affect the IC_{50} ratios of artemisinin (17.91 ± 0.04, 10.29 ± 0.00 and 12.12 ± 0.00 for 24, 48 and 72 h of treatment, respectively) indicating its fast-acting action during the inhibition of *P. falciparum* proliferation in culture.

Table 19: Data overview of IC_{50} speed assay.

Subfractions	IC_{50} Speed assay (µg/ml)				
	P. falciparum Dd2 Strain				
	IC_{50} 24 h	IC_{50} 48 h	IC_{50} 72 h	Ratio of IC_{50} 24 h / IC_{50} 72 h	Conclusion
SbTi03	> 25	0.24 ± 0.04	0.13 ± 0.00	ND	Slow-acting
SbTi04	> 25	0.12 ± 0.06	0.13 ± 0.06	ND	Slow-acting
Eschweilenol C	> 25	0.25 ± 0.03	0.59 ± 0.00	ND	Slow-acting
Artemisinin (nM)	17.91 ± 0.04	10.29 ± 0.00	19.04 ± 0.00	0.94	Fast-acting
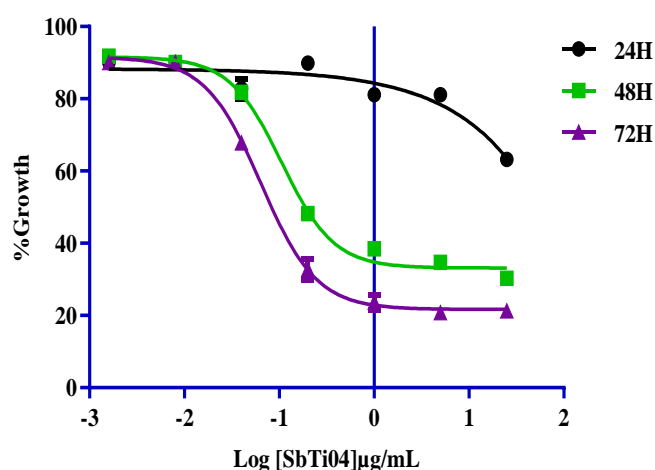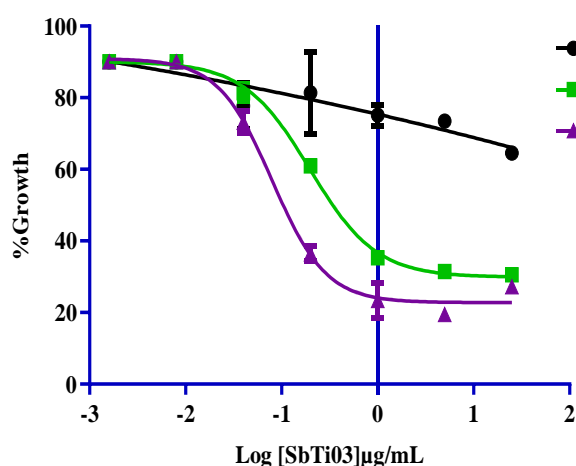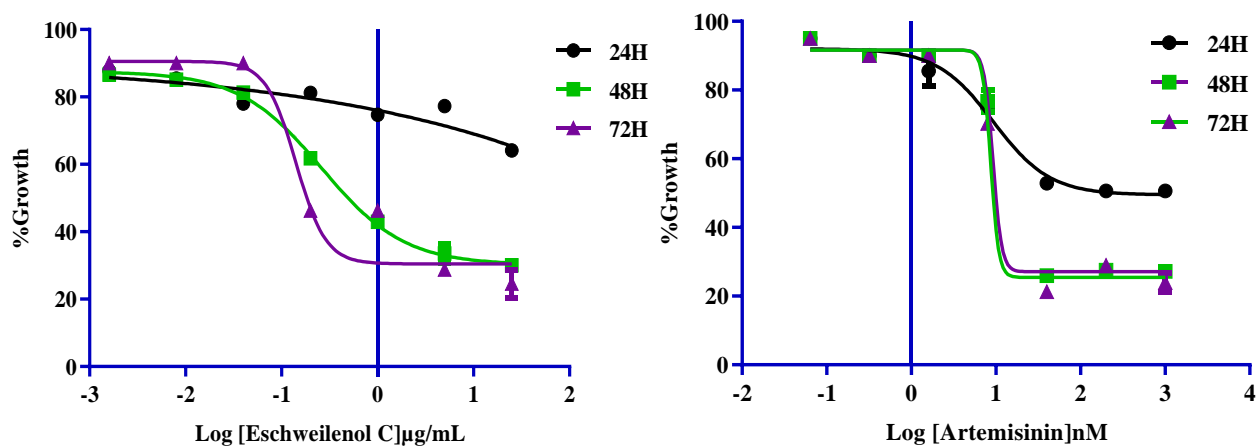
Figure 36: Sigmoidal curve of the time-course analysis of subfractions Ti03; Ti04; eschweilenol C and artemisinin on *P. falciparum* Dd2.

Effect of subfractions SbTi03, SbTi04; eschweilenol C and artemisinin on unsynchronized cultures of *P. falciparum* Dd2 at 24 h, 48 h and 72 h. IC_{50} could not be reached within 24 hours for the hit subfractions and for eschweilenol C. SbTi03; SbTi04 and eschweilenol C reached the IC_{50} by 48 hours. Error bars represent the standard error of the experiments performed twice with each concentration of compound tested in triplicate.

III.3.3.5- Stage-specific study of parasitostatic *vs* parasiticidal actions of subfractions and eschweilenol C.

As drugs that eliminate multiple stages of the parasite life cycle will be critical components in global efforts to eliminate malaria (Spangenberg *et al.,* 2013), we were interested in knowing if there was stage specificity in the action of hit subfractions (SbTi03, SbTi04) and Eschweilenol C. The results showed that, compared to the untreated cultures, SbTi03; SbTi04 and Eschweilenol C rapidly (6 hpi) inhibited parasite development from the early ring and trophozoite (**Figure 37**). Additionally, at 6 hpi, the two subfractions and Eschweilenol C arrested parasite rings to trophozoite stage transition are highlighted by the presence of a pyknotic form of the parasite in the treated culture compared to the control (**Figure 37**). Following 48 h (rings) and 24 hpi (trophozoite), the parasite inhibition ranged from 73.33% (SbTi03) to 82.13% (Eschweilenol C) for ring stages and from 72.95% (SbTi03) to 85.01% (Eschweilenol C) for trophozoite stages. However, we observed low inhibition of schizont stages ranging from 41.59% (SbTi03) to 58.88% (Eschweilenol C) (**Table 19 & Figure 38**). Overall, SbTi03, SbTi04 and Eschweilenol C were not active in blocking merozoite egress and erythrocyte invasion as revealed by the presence of ring stages in the treated cultures compared to the untreated culture after 12 hours of drug exposure (**Figure 37**). Overall, all tested drugs were found to preferentially inhibit *P. falciparum* ring and trophozoite stages with a slight effect on schizont stages.

Following drug pressure, treated and untreated cultures were washed free of drugs and grown in drug-free media for a total of 48 h for rings, 24 h for trophozoites and schizonts. Outputs of stage-specific growth inhibition, parasitostatic, parasiticidal, and postdrug exposure growth suppression are summarized (**Table 19 & Figure 39**). Further drug withdrawal and culture maintenance in drug-free medium showed no increase in parasitaemia (SbTi03$_{86.15\%}$; SbTi04$_{80.89\%}$; Eschweilenol C$_{80.09\%}$ for the ring and SbTi03$_{97.10\%}$; SbTi04$_{86.50\%}$; Eschweilenol C$_{90.97\%}$) (**Table 19 & Figure 39**) in culture treated with SbTi03, SbTi04 and Eschweilenol C and were classified as parasiticidal for ring and trophozoite. Microscopic data showed that the rings and trophozoite stages of malaria parasites treated with subfractions and eschweilenol C failed to revive during drug-free incubations (**Figure 39**). In addition, all subfractions and eschweilenol C were parasitostatic for schizonts (SbTi03$_{58.38\%}$; SbTi04$_{48.42\%}$; Eschweilenol C$_{57.89\%}$) clarified by no reduction in parasitemia following drug withdrawal and did not prevent merozoite egress and invasion as shown in the microscopy data (**Figure 38 & 39**).

Table 20: Stage-specific inhibition and postdrug effect suppression of different compounds.

Subfractions (IC$_{99}$)	Stage-specific growth inhibition (%)			Post-drug inhibition (%)		
	Ring	Trophozoite	Schizont	Ring	Trophozoite	Schizont
SbTi03	73.33	72.95	41.59	86.15	97.10	58.38
SbTi04	74.22	79.57	51.63	80.89	86.50	48.42
Eschweilenol C	82.13	85.01	58.88	80.09	90.97	57.89
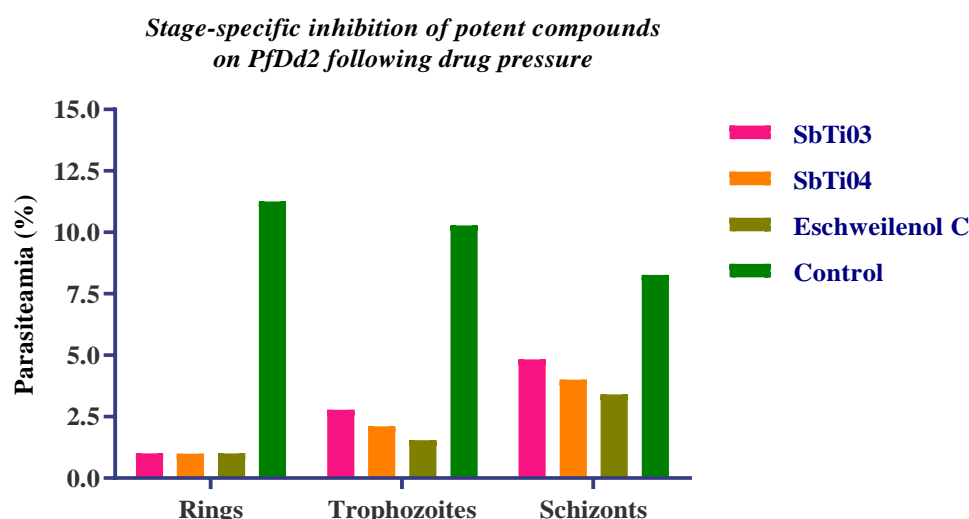
Figure 37: Stage-specific parasitaemia calculated by microscopic observation of Giemsa-stained blood smears of different compounds versus negative control following 24 h (Trophozoites), 48 h (Rings) and 12 h (Schizonts) of drug pressure.
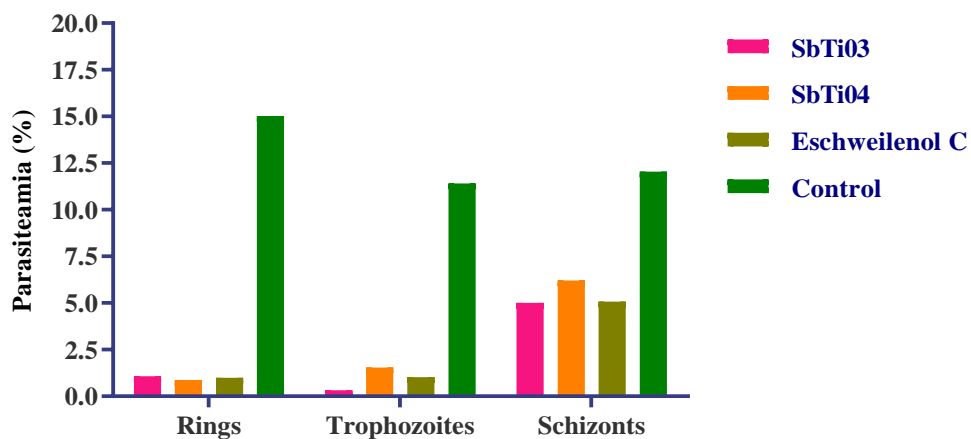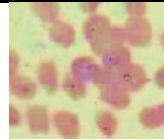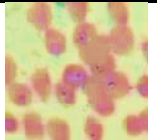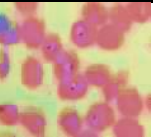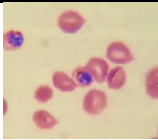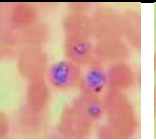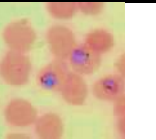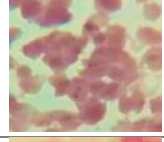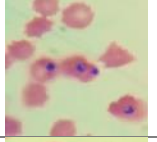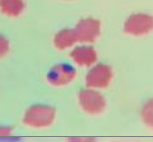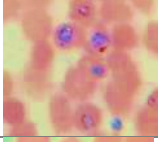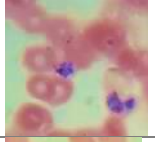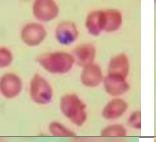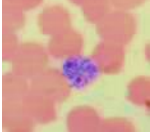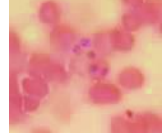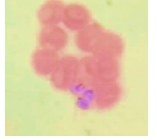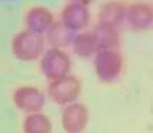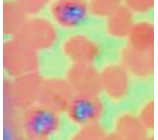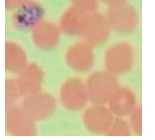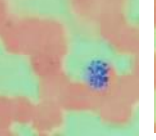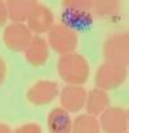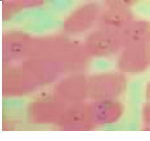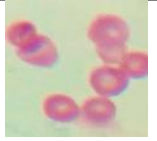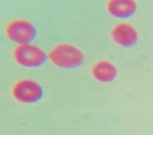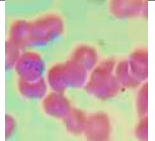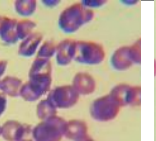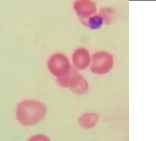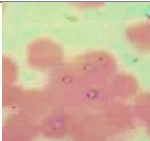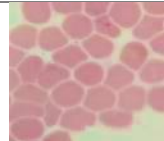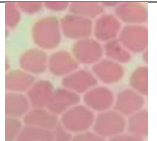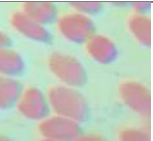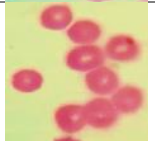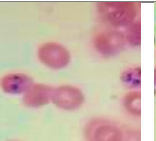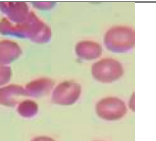
Figure 38: Stage-specific parasitaemia after drug withdrawal calculated by microscopic observation of Giemsa-stained blood smears of different compounds versus negative control.

	Ring-stage specific inhibition					Trophozoites-stage specific inhibition			
Exposure time	Control	SbTi03	SbTi04	Eschweilenol C	Exposure time	Control	SbTi03	SbTi04	Eschweilenol C
0hpi					0hpi				
6hpi					6hpi				
24hpi					18h				
48hpi					24hpi				
48h-Post drug effect					24h-Post drug effect				

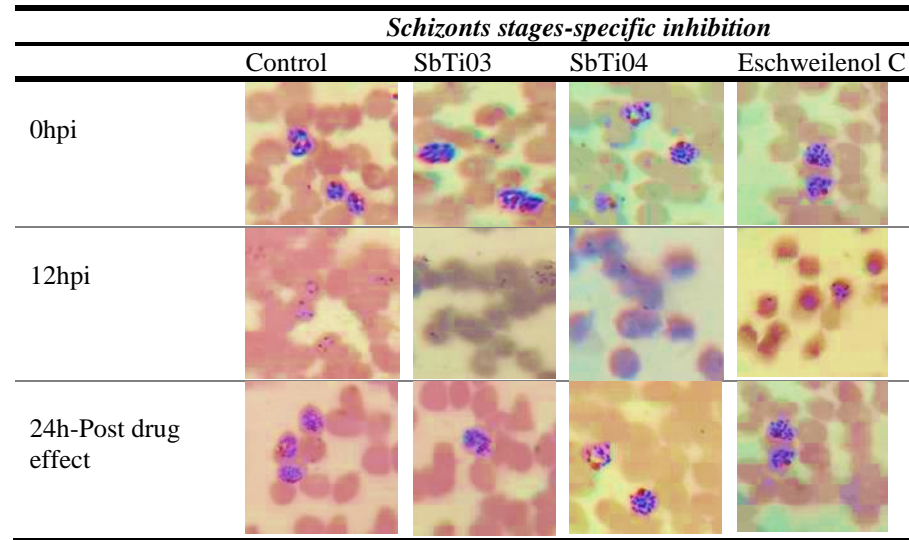|	Schizonts stages-specific inhibition			
	Control	SbTi03	SbTi04	Eschweilenol C
0hpi				
12hpi				
24h-Post drug effect				

Figure 39: *In vitro* stage-specific analysis of « hit » subfractions (SbTi03; SbTi04) and Eschweilenol C on intraerythrocytic stages of *Pf*Dd2.

Synchronized ring, trophozoite and schizont stage cultures of *Pf*Dd2 were treated with IC_{99} of subfractions for different times (0, 6, 24 and 48 h for rings, 0, 6, 18 and 24 h for trophozoites and 12 h for schizonts). In each case, the drug was withdrawn and the cells were washed and incubated in a drug-free medium for a total of 96 h (rings), 72 h (trophozoites) and 36 h (schizonts). Representative microscopic images of Giemsa-stained smears at different time points of ring, trophozoites and schizonts.

III.3.3.6-Antioxidant studies

III.3.3.6.1- DPPH scavenging activity assay

The DPPH radical scavenging potential of the different subfractions and eschweilenol C were evaluated and the results are presented in **Table 20**. From this table, all subfractions and eschweilenol C showed a scavenging activity against DPPH free radicals. The median inhibitory concentration (IC_{50}) ranged from 4.18 ± 0.05 µg/mL to 36.32 ± 0.06 µg/mL. Eschweilenol C displayed the highest and most significant ($p < 0.05$) scavenging effect with an IC_{50} of 10.23 ± 0.07 µg/mL.

III.3.3.6.2-ABTS radical scavenging activity

The $ABTS^{+}$ scavenging potential of the subfractions and eschweilenol C are presented in **Table 20**. All subfractions and eschweilenol C showed a strong scavenging activity with IC_{50} $< 5 \mu$g/mL (**Figure 40B**). The subfractions SbTi03 were the most active with the lowest IC_{50} of 2.07 ± 0.30 µg/mL.

### III.3.3.6.3- Ferric reducing antioxidant power (FRAP) activity

The reducing potential evidence by IC_{50} is presented in **Table 20** which shows that the reducing power of Fe^{3+} to Fe^{2+} at different concentrations (100 to 0.781 µg/mL) was dose-dependent (**Figure 40C**) with IC_{50} value ranging from 10.66 to 91.00 µg/mL. Interestingly, eschweilenol C was the most active with a lower IC_{50} indicating a higher antioxidant potential.

**Table 21:** Antioxidant activities of the "hit" subfractions.

	Anti-Oxidants activities		
	$IC_{50} \pm SD$ (µg/mL)		
Drugs	**DPPH**	**ABTS^{+}**	**FRAP**
SbTi03	36.32 ± 0.06	2.07 ± 0.30	91.00 ± 2.02
SbTi04	32.24 ± 0.00	3.42 ± 0.07	30.36 ± 0.17
Eschweilenol C	10.23 ± 0.07	4.34 ± 0.09	10.66 ± 0.13
Gallic Acid	4.58 ± 0.02	2.69 ± 0.02	> 100
Ascorbic Acid	4.18 ± 0.05	4.47 ± 0.14	3.48 ± 0.14

IC$_{50}$: Inhibitory Concentration 50; **DPPH**: 1,1 diphenyl-2-picrylhydrazyl; ABTS: **FRAP**: Ferric Reducing Antioxidant Power. Values are expressed as the mean ± SD (n = 3).

Concentration-response curves of subfractions, Eschweilenol C and positive control
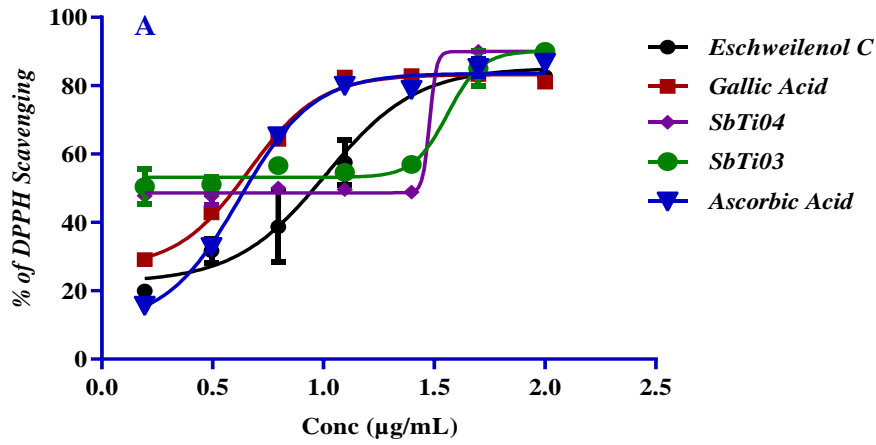
A

% of DPPH Scavenging vs Conc (µg/mL)

Legend:
- Eschweilenol C
- Gallic Acid
- SbTi04
- SbTi03
- Ascorbic Acid

Concentration-responses curve of subfractions, Eschweilenol C and positive control

B

%ABTS$^+$ Scavenging vs Conc (µg/mL)

Legend:
- Ascorbic Acid
- Gallic Acid
- SbTi03
- SbTi04
- Eschweilenol C

Concentration-responses curve of subfractions, Eschweilenol C and positive control

C

% of Fe^{3+} Scavenging vs Conc (µg/mL)

Legend:
- Ascorbic Acid
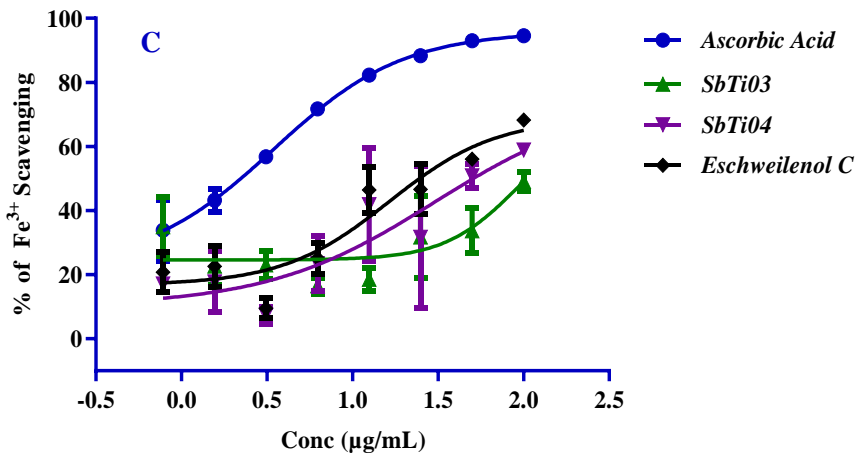- SbTi03
- SbTi04
- Eschweilenol C
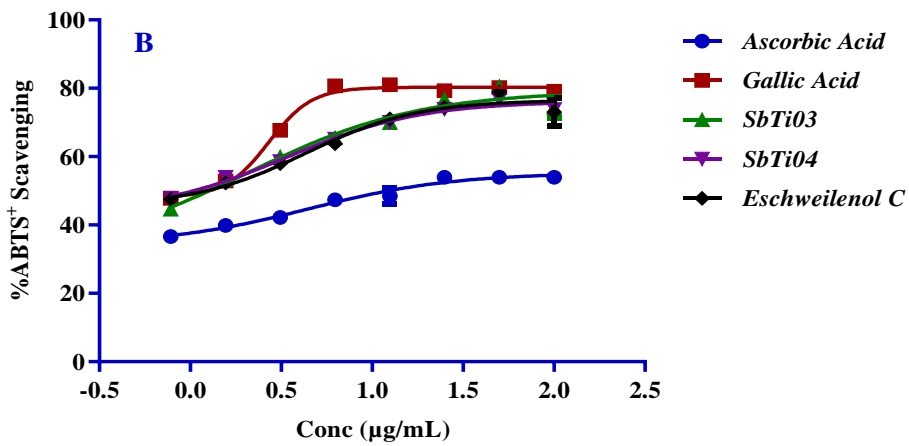
Figure 40: Concentration - response curve of subfractions and positive control (gallic and ascorbic acid) on DPPH (A), ABTS+ scavenging activity (B) and ferric antioxidant reducing Power (FRAP) activity (C).

Data were normalized to percent control activity and median inhibitory concentrations ($IC_{50}s$) calculated using Prism 8.0 software (GraphPad) with data fitted by nonlinear regression to the variable slope sigmoidal dose - response formula y = 100/[1+ 10$^{(logIC50-x)\ H}$], where H is the Hill coefficient or slope factor.

III.3.3.6.4-Correlation studies between the DPPH scavenging activity; ABTS$^+$ radical scavenging activity and ferric reducing antioxidant power activity

A positive correlation between the DPPH scavenging potential and FRAP was observed (**Table: 21**). In fact, SbTi03, SbTi04 and eschweilenol C demonstrated a positive correlation between DPPH scavenging activity and ferric reducing antioxidant power (FRAP) with a coefficient of 0.78 (**Table 21**). Unfortunately, a negative correlation was found between DPPH scavenging activity and FRAP and ABTS$^+$ radical activity with a correlation coefficients of -0.88 and -0.98 respectively. The correlation obtained between DPPH and FRAP supports the fact that, the investigated subfractions and eschweilenol C can scavenge free radicals by protecting cellular macromolecules from cells membranes oxidative damage. To overcome misunderstandings regarding the choice of the most effective antioxidative inhibitors between SbTi03, SbTi04 and eschweilenol C *in vitro* and to help report the most reliable antioxidant activity order of investigated inhibitors based on a statistical approach, principal component analysis (PCA) was applied to the antioxidant assay data. Hence, factor analysis was performed on the data obtained for SbTi03, SbTi04 and eschweilenol C. A factor rotation using the Varimax method was performed for two-factor loadings to see the correlations between assays that accounted for the total covariance of the subfractions (Erkan and Saban, 2011). In **Figure 41**, the variances caused by F1 and F2 were found to be 94.26% and 5.68% respectively. As seen in the PCA graph, the results from DPPH scavenging activity and FRAP activity are respectively closely loaded to F2. In contrast, the ABTS assay results appear to be loaded very close to F1 indicating a strong correlation and nonsignificant difference between the DPPH and FRAP methods.

Table 22: Results of Pearson correlation for *in vitro* antioxidant assays.

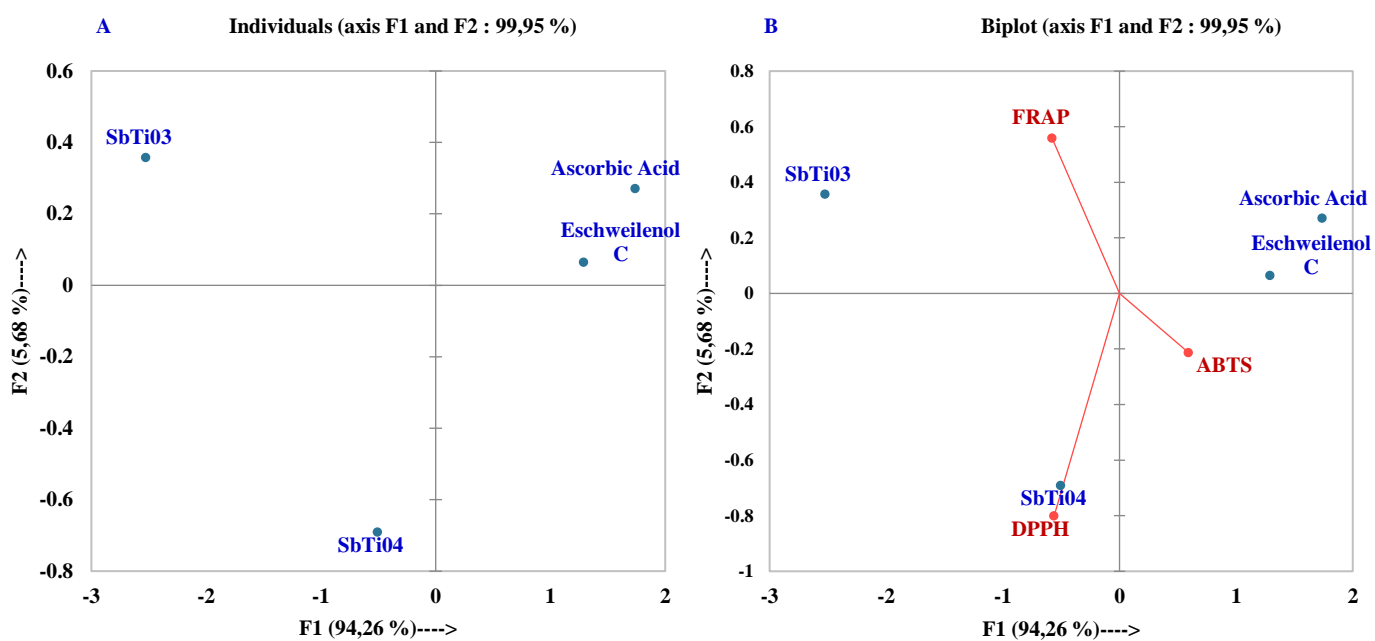| Antioxidants Assay	DPPH	ABTS	FRAP
DPPH	1		
ABTS	-0.884	1	
FRAP	0.788	-0.984	1

Figure 41: Correlation between antioxidant capacity of different subfractions investigated. ABTS: ABTS radical scavenging test; DPPH: DPPH radical scavenging test; FRAP: Ferric Reducing Antioxidant Power test. **A**: distribution of the samples around the F1 and F2 axes; **B**: projection of the samples and tests around the F1 and F2 axes.

III.2.5-Discussion

The discovery of antimalarial drugs that hit novel targets and are rapidly active against multiple asexual blood stages, including transmissible gametocyte stages with novel mechanisms of action is urgently needed. Hence, the third part of this work provides the first report on the extent of the multistage potential mode of inhibition of metabolites from *T. ivorensis* and *T. brownii* derivatives including an understanding of their biological mode of action. Therefore, promising extracts Ti^w and Tb^M ($IC_{50} < 1\,\mu g/mL$; $SI > 250$) were fractionated by liquid - liquid partition for the aqueous extract of *T. ivorensis* and by flash column chromatography for the methanolic extract of *T. brownii* and the resulting fractions were tested for antiplasmodial activity and cytotoxicity. The results indicated that two of the resulting fractions displayed similar antiplasmodial activity ($IC_{50} < 1\,\mu g/mL$; $SI > 250$) on both sensitive and resistant strains of *P. falciparum* when compared to parent crude extracts (Ti^wEa vs Ti^w and Tb05 vs Tb^M). This result could tentatively indicate that fractionation concentrated the active principle(s) within the potent fractions from the parent crude extracts, potentially acting

synergistically as previously reported (Rasoanaivo et al., 2011). Indeed, previous studies showed that fractionation of an extract positively or negatively changes its biological properties by concentrating active ingredients into a fraction, or by sharing them between the various ones (Nwodo et al., 2010). The most active and selective ethyl acetate: methanol (1:1) fraction Tb05 from the methanolic extract of *T. brownii* (Tb^M) and the ethyl acetate fraction Ti^{W}Ea from the aqueous extract of *T. ivorensis* (Ti^W) were submitted to UPLC - MS analysis and led to the identification of three (03) phytocompounds including ellagic acid, flavonoid (Leucodelphidin), terpenoids (Papyriogenin D). These secondary metabolites are likely to be responsible for the elicited antiplasmodial activity, as similar compounds have previously been implicated in such bioactivity (Kamkumo *et al.,* 2012; Malterud, 2017; Zofou *et al.,* 2012).

To the best of our knowledge, the antiplasmodial activities of leucodelphidin (flavonoids) and papyriogenin D (terpenoids) have not yet been reported making those fractions more attractive for further investigation. Therefore, we hypothesized that the inhibition of *Plasmodium* proliferation by the Tb05 fraction could be attributed to the different constituents detected through UPLC - MS analysis. Of note, ellagic acid was previously reported to selectively display significant antiplasmodial activity with IC$_{50}$ values ranging from 105 to 330 nM regardless of the chemosensitivity of the *P. falciparum* strain tested and to exhibit significant antimalarial efficacy (suppressive, curative and prophylactic) in *Plamodium vinckei-*infected mice (Soh et al., 2012). The preferential targets of action of this compound were reported to be the trophozoite and schizont stages of the *Plasmodium* intraerythrocytic life cycle (Soh et al., 2008). Within the scope of this work, the reported activity profile of ellagic acid was corroborated through the investigation of a commercially sourced compound that displayed IC$_{50}$ values of 0.59 µM and 2.68 µM against *Pf*Dd2 and *Pf*3D7. This finding further validated the active input of ellagic acid to the displayed antiplasmodial activity of fractions from both *Terminalia* species. Similarly, Machumi et al. (2013) previously reported a phytochemical investigation of the ethyl acetate-soluble fraction from the stem bark of *T. brownii* collected in Kenya, leading to the isolation of a new oleanane-type triterpenoid, along with seven known triterpenoids, seven ellagic acid derivatives, and 3-*O*-β-D-glucopyranosyl-β-sitosterol. Among these natural products, two ellagic acid derivatives bearing a galloyl group (4-*O*-(3´´,4´´-di-*O*-galloyl-α-L-rhamnopyranosyl and 23-galloylarjunic acid) were found to be moderately active against the chloroquine-sensitive (D6) and chloroquine-resistant (W2) strains of *P. falciparum* with IC$_{50}$ values ranging from 2.8 to 4.7 µg/ml. Of note, the compounds identified in this study from the methanolic extract of *T. brownii* stem bark (ellagic acid, leucodelphidin and papyriogenin D) were not reported by Machumi et al. (2013) while investigating the ethyl

acetate extract. On the other hand, the biological mechanisms of action of ellagic acid were previously reported to include DNA topoisomerase inhibition, the induction of cell cycle arrest, and the activation of apoptotic pathways (Constantinou et al., 1995). In addition, its strong antiplasmodial activity has been attributed to the inhibition of Plasmepsin II, the reduction of glutathione content inside the *Plasmodium* parasite and impairment of beta-hematin formation (Constantinou et al., 1995; Dell'Agli et al., 2003; Sturm et al., 2009). From this rationale, we can hypothesize that part of the antiplasmodial activity displayed by fractions from both *Terminalia* spp. may be attributable to ellagic acid, which elicits bioactivity through the inhibition of molecular targets of critical importance to *Plasmodium* survival.

In addition, to ellagic acid, other interesting phytochemical constituents such as flavonoids (Leucodelphidin) and triterpenoids (Papyriogenin D) have been identified. Previous studies revealed that flavonoids are known to interface and prohibit the action of *P. falciparum* cysteine protease (falcipain), a vital enzyme involved in the hemoglobin digestion inside the acidic food vacuole of the intraerythrocytic parasite (Sinha *et al.,* 2019). Sinha *et al.;* (2019) showed that flavonoids hinder plasmodial hemozoin formation in culture suggesting that they act on this pathway leading to the death of the *P. falciparum* parasite. In the same direction, terpenoids such as the antimalarial drug artemisinin (a sesquiterpene lactone) are reputed to inhibit the biosynthesis of both dolichol and the isoprene side chain of ubiquinones and the isoprenylation of proteins in the intraerythrocytic stages of *P. falciparum* leading to the dead parasite (Goulart *et al.,* 2004). Moreover, they have also been reported to inhibit β-hematin formation in *P. falciparum* (Ns *et al.,* 2013) **.** Previous investigations also showed that terpene molecules are activated by heme to generate free radicals, which in turn damage proteins required for parasite survival (Tilley *et al.,* 2016; Wang *et al.,* 2015). Overall, the mode of action of the identified class of compounds could well explain the strong antiplasmodial activity observed with both "hit" fractions. Given the promising antiplasmodial profile of Tb05 and Ti^{W}Ea, the unidentified phytoconstituents are of potential interest for further investigation.

Based on a previous study conducted on fractions from *Terminalia ivorensis* and *Terminalia brownii* and their key interest as a source of new antimalarial drug lead, we carried out a second activity-guided fractionation of both "hit" fractions (Ti^{W}Ea and Tb05) using silica gel column chromatography. After that, the derived subfractions and eschweilenol C were assessed *in vitro* for their activity against asexual-blood stages of multiresistant (*Pf*Dd2), chloroquine-sensitive (*Pf*3D7) and mutant resistant (*Pf*Dd2-GNF156) strains of *P. falciparum*. Out of the eight subfractions obtained, five showed good antiplasmodial activity across all strains of *Plasmodium* used. Interestingly, two (02) subfractions (SbTi03; SbTi04) and

eschweilenol C exhibited strong inhibition ($IC_{50} < 1$ µg/mL) against multiresistant (*Pf*Dd2) and sensitive (*Pf*3D7) strains of *P. falciparum* and showed no reduction in its potency when tested against mutant resistant (*Pf*Dd2-GNF156) strains of *P. falciparum*. Hence, these results suggest that SbTi03 and SbTi04 contain antimalarial drugs leading to a novel mechanism of action. Our study also highlights for the first time the isolation of 4-α-rhamnopyranosyl ellagic acid (eschweilenol C) from *Terminalia brownii* together with its strong antiplasmodial potency. As a derivative of ellagic acid, we can hypothesize that, 4-α-L-rhamnopyranosyl ellagic acid could exhibit the same mechanism of *Plasmodium* growth inhibition as ellagic acid and therefore explain its high activity. The difference in activity between eschweilenol C and ellagic acid reported in the literature could be explained by the presence of sugars. In fact, the presence of sugars as attachments to the core structure has been known to increase solubility and hydrogen binding (Fontaine *et al.,* 2017). Hence, this work suggests that the appended sugars do not simply modulate compound solubility, and therefore the ability to reach the cellular target(s), but instead indicate that the sugars may make key interactions with cellular components, thereby decreasing antiplasmodial activity compared to ellagic acid. All subfractions and eschweilenol C had no sterilizing effect against mature gametocytes of *falciparum* at the tested concentration ($IC_{50} > 5$ µg/mL). Of note, a study conducted by Sore *et al.,* 2018 showed that ethanol and methanol leaf extracts of *Terminalia macroptera* exhibited activity against mature gametocyte stages of *P. falciparum* at 32.47 and 36.34 µg/mL (IC_{50}) (Soré *et al.,* 2018) respectively justifying the results observed in this study and highlighting the fact that *Terminalia species* and their derivatives might exert their sterilizing effect on mature gametocyte stages of *P. falciparum* at the highest concentration.

The measurements of hemozoin quantify the parasite's ability to detoxify reactive free heme through hemozoin formation in response to the drug, where an increase in free heme corresponds to a decrease in parasite survival. Hence, we carried out an inhibition of hemozoin formation assay to provide an understanding of the mode of action of potent subfractions and eschweilenol C. As expected, the results obtained suggest that eschweilenol C and two hit subfractions (SbTi03; SbTi04) display a similar mechanism of inhibition as chloroquine and artemisinin. The stage-specific action of potent subfractions and Eschweilenol C were also evaluated and the results suggest that *Terminalia ivorensis* and *Terminalia brownii*-derived subfractions (SbTi03, SbTi04) and Eschweilenol C are stage-specific, arresting the parasites' life cycle at the ring and trophozoite stage and therefore, inhibiting their transition into schizont stages. Schizont maturation and merozoite invasion of uninfected erythrocytes seemed microscopical not to be affected by the treatment. Of note, the effect of that plant-derivative on

trophozoites can be justified by its effect on hemoglobin catabolism through the inhibition of haemozoin formation or haem polymerization as revealed. However, the former first-line antimalarials chloroquine and sulfadoxine-pyrimethamine mainly affect trophozoites by inhibiting the hemoglobin catabolism pathway that provides nutrients for the parasite and the folate biosynthesis pathway that delivers the building blocks for DNA synthesis, respectively (Blasco *et al.,* 2017). A study conducted by (Mbouna *et al.,* 2022) showed a stage-specific action of *Terminalia mantaly* derived subfractions with preferential action on ring, trophozoite, merozoite egress and invasion. Hence, belonging to the same species, we can hypothesize that, *Terminalia ivorensis* and *Terminalia brownii* are promising sources of new antimalarial drugs leading to a novel mode of action against malaria parasites as long as they specifically inhibit rings, trophozoite and schizont stages of malaria parasites by interfering with hemoglobin catabolism.

During the *Plasmodium* erythrocytic life cycle, *Plasmodium* digests haemoglobin within its acidic food vacuole and releases toxic ferriprotoporphyrin IX (FP) and reactive oxygen species (ROS) (Postma *et al.,* 1996). Therefore, finding antimalarial drug that can scavenge ROS or stimulate the production of ROS to contribute to *P. falciparum* death will be very important in the malaria drugs discovery pipeline. In addition to antimalarial activity, the antioxidant properties of promising subfractions (SbTi03, SbTi04) and eschweilenol C were also investigated using DPPH, ABTS$^+$ and FRAP and the results showed that SbTi03; SbTi04 and eschweilenol C exhibited good antioxidants activity with eschweilenol C being the most active across the three assays. The lower IC$_{50}$ obtained with eschweilenol C in the DPPH assay can be explained by the richness of the phenolic compound with a hydroxyl group. Additionally, our results demonstrated that the ABTS$^+$ scavenging potential of the investigated subfractions and eschweilenol C are strongly linked to the plant's content or the nature of the compound. Overall, we can suggest that the nature of the compound present in these subfractions or the phenolic nature of eschweilenol C allow them to act as reducing agents by converting free radicals into stable molecules. These results correlate with the statement that the IC$_{50}$ of the samples is inversely proportional to its antioxidant power thus to the substance's nature.

III.2.6-General Discussion

The research work "Validation of *Plasmodium falciparum* lactate dehydrogenase-based assay and bio-guided search for *Plasmodium falciparum* inhibitors from *Terminalia ivorensis* and *Terminalia brownii*" combines two key aspects of malaria research: the validation of an

assay platform and the search for potential anti-malarial compounds from natural sources. The first part of the research involves the validation of a *Plasmodium falciparum* lactate dehydrogenase (*Pf*LDH) based assay. *Pf*LDH is an enzyme critical for the survival and replication of the malaria parasite, *Plasmodium falciparum*. Therefore, it is widely used as a target for antimalarial drug discovery. The validation of the assay platform involves assessing its accuracy, precision, sensitivity, reproducibility, and reliability. This step ensures that the assay can reliably detect and quantify the activity of *Pf*LDH and can be used effectively in subsequent experiments.

The second aspect of the research focuses on the bio-guided search for *Plasmodium falciparum* inhibitors from *Terminalia ivorensis* and *Terminalia brownii*, which are two plant species known for their medicinal properties. We aim to identify inhibitors from these plants that can inhibit the growth or activity of *Plasmodium falciparum*. Our search involves the extraction of bioactive extracts and compounds from the plants using a double step activity guided fractionation, followed by a series of tests to determine their potential as anti-malarial agents. This bio-guided approach involves using the malaria parasite as a guide to identify the most promising extracts; fractions or compounds. By combining the validation of an assay platform with the search for novel anti-malarial compounds, this research aims to contribute to the development of effective tools for antimalarial drug screening. The validation of the *Pf*LDH assay will ensure its accuracy in detecting the presence of *Plasmodium falciparum* culture, which is crucial for timely and accurate identification of novel antimalarial chemotypes. Additionally, the search for new anti-malarial compounds from *Terminalia ivorensis* and *Terminalia brownii* may lead to the discovery of novel drugs or drug leads that could be developed into effective malaria treatments.

Overall, this research topic addresses important challenges in malaria research and has the potential to contribute to the development of improved strategies for malaria diagnosis and treatment.

CONCLUSION AND PERSPECTIVES

CONCLUSIONS AND PERSPECTIVES

This study was designed to validate *Pf*LDH-based assay and search for inhibitors of *P. falciparum* from *Terminalia ivorensis* and *Terminalia brownii* endowing a novel mode of action that could contribute to the next generation of malaria treatment. At the end of this work, the following conclusions were obtained:

- The validation of the *Pf*LDH-based assay was successful and exhibited reliability, robustness and reproducibility.

- Crude extracts from *T. ivorensis* and *T. brownii* exhibited very good antiplasmodial potential on both multi-resistant (Dd2) and chloroquine-sensitive (3D7) strains of *P. falciparum* (IC$_{50}$ ranging from 0.13 µg/ml to 10.59 µg/ml) with good selectivity toward normal (Vero and Raw) cells and erythrocytes. In addition, aqueous and methanolic extracts were nontoxic in an animal model with good antimalarial efficacy in *P. berghei* NK65 infected mice.

- Double-step activity-guided fractionation led to eight (08) subfractions and eschweilenol C as validated antiplasmodial "hit" compounds. Subfractions SbTi03; SbTi04 and Eschweilenol C exhibited preferential killing of trophozoites and schizont stages by interfering with hemozoin formation or heme polymerization and parasite oxidative stress.

The results achieved in this study are of utmost scientific interest as they report for the first time the *in vivo* validation of *T. ivorensis* stem bark extract and the isolation of eschweilenol C from *T brownii*. This is a significant finding regarding *T. ivorensis* and *T. brownii* as it implies that SbTi03, SbTi04 and eschweilenol C are active across all asexual-blood stages of the malaria parasite found in the human host, marking them as potential hits for the malaria drug discovery pipeline. Given the vision of malaria eradication worldwide, eschweilenol C and *T. ivorensis*-derived subfractions could certainly play a crucial role and deserve more attention.

Thus, we intend to:

- Identify and isolate novel anti-asexual blood stage potential leads from subfractions SbTi03 and SbTi04 using a modern LCMS-based dereplication strategy.

- Determine the effect of "hit" compounds on transmissible gametocytes and their ability to block gamete ex-flagellation and zygote development in mosquitoes.

- Determine the effect of dual-active "hits" on *Plasmodium* liver stages *in vitro*.

- Determine the microsomal stability of triple-acting compounds and *in vivo* transmission-blocking activity.

REFERENCES

REFERENCES

Akompong, T., Ghori, N., 2000. In Vitro Activity of Riboflavin against the Human Malaria Parasite *Plasmodium falciparum. Antimicrobial agents and chemotherapy*, *44*(1), 88–96. https://doi.org/10.1128/AAC.44.1.88-96.2000.

Amexo, M., Tolhurst, R., Barnish, G., Bates, I., 2004. Malaria misdiagnosis : effects on the poor and vulnerable. *Lancet (London, England)*, *364*(9448), 1896–1898. https://doi.org/10.1016/S0140-6736(04)17446-1.

Amir Ashraf, S., Nazir, S., Adnan, M., & Rashid Azaz Ahmad Azad, Z. (2021). UPLC-MS: An Emerging Novel Technology and Its Application in Food Safety. IntechOpen. doi: 10.5772/intechopen.92455

Amorati, R.; Valgimigli, L. Advantages and limitations of common testing methods for antioxidants. 346 *Free Radic. Res*. **2015**, *49*, 633–649.

Amorati, R.; Foti, M. C.; Valgimigli, L. Antioxidant Activity of Essential Oils. *J. Agric. Food Chem.* **2013**, *61*, 10835-10847

Niki, E. Assessment of Antioxidant Capacity in vitro and in vivo. *Free Radic. Biol. Med.* **2010**, *49*, 358 503–51

Annan, K., Sarpong, K., Asare, C., Dickson, R., Amponsah, K., Gyan, B., Ofori, M., Gbedema, S.Y., 2012. In vitro anti-plasmodial activity of three herbal remedies for malaria in Ghana: Adenia cissampeloides (Planch.) Harms., Termina liaivorensis A. Chev, and Elaeis guineensis Jacq. *Pharmacognosy Research* 4, 225–229. https://doi.org/10.4103/0974-8490.102270.

Armbruster, D.A., Pry, T., 2008. Limit of Blank , Limit of Detection and Limit of Quantitation. *The Clinical biochemist. Reviews*, *29 Suppl 1*(Suppl 1), S49–S52.

Ashley, E.A., Ashley, E.A., 2018. Drugs in Development for Malaria. *Drugs* 78, 861–879. https://doi.org/10.1007/s40265-018-0911-9.

Atanasov, A.G., Waltenberger, B., Pferschy-Wenzig, E.M., Linder, T., Wawrosch, C., Uhrin, P., Temml, V., Wang, L., Schwaiger, S., Heiss, E.H., Rollinger, J.M., Schuster, D., Breuss, J.M., Bochkov, V., Mihovilovic, M.D., Kopp, B., Bauer, R., Dirsch, V.M., Stuppner, H., 2015. Discovery and resupply of pharmacologically active plant-derived natural products: A review. *Biotechnology Advances*. https://doi.org/10.1016/j.biotechadv.2015.08.001.

Asua, V., Conrad, M.D., Aydemir, O., Duvalsaint, M., Legac, J., Duarte, E., Tumwebaze, P., Chin, D.M., Cooper, R.A., Yeka, A., Kamya, M.R., Dorsey, G., Nsobya, S.L., Bailey, J., Rosenthal, P.J., 2021. Changing Prevalence of Potential Mediators of Aminoquinoline ,

Antifolate , and Artemisinin Resistance Across Uganda 223. https://doi.org/10.1093/infdis/jiaa687

Barnes, K.I., Durrheim, D.N., Little, F., Jackson, A., Mehta, U., Allen, E., Dlamini, S.S., Tsoka, J., Bredenkamp, B., Mthembu, D.J., White, N.J., Sharp, B.L., 2005. Effect of artemether-lumefantrine policy and improved vector control on malaria burden in KwaZulu-Natal, South Africa. *PLoS Medicine*. https://doi.org/10.1371/journal.pmed.0020330

Baruah, U.K., Gowthamarajan, K., Vanka, R., Venkata, V., Reddy, S., Selvaraj, K., Jojo, G.M., Ã, U.K.B., Gowthamarajan, K., Ã, R.V., Venkata, V., Reddy, S., Selvaraj, K., Jojo, G.M., 2017. Malaria treatment using novel nano-based drug delivery systems Malaria treatment using novel nano-based drug delivery systems 2330. https://doi.org/10.1080/1061186X.2017.1291645

Becker, K., Tilley, L., Vennerstrom, J.L., Roberts, D., Rogerson, S., Ginsburg, H., 2004. Oxidative stress in malaria parasite-infected erythrocytes : host – parasite interactions. *International journal for parasitology*, *34*(2), 163–189. https://doi.org/10.1016/j.ijpara.2003.09.011

Behl, C., 2005. Oxidative stress in Alzheimer's disease: implications for prevention and therapy. *Sub-cellular biochemistry*. https://doi.org/10.1007/0-387-23226-5_3

Bell, A., 2011. Antimalarial Peptides : The Long and the Short of It. *Current pharmaceutical design*, *17*(25), 2719–2731. https://doi.org/10.2174/138161211797416057.

Benzie, I.F.F., Strain, J.J., 1996. The ferric reducing ability of plasma (FRAP) as a measure of "antioxidant power": The FRAP assay. *Analytical Biochemistry* 239, 70–76. https://doi.org/10.1006/abio.1996.0292

Berkley, J., Mwarumba, S., Bramham, K., Lowe, B., Centre, K.M., 1999. Bacteraemia complicating severe malaria in children. *Transactions of the Royal Society of Tropical Medicine and Hygiene*, *93*(3), 283–286. https://doi.org/10.1016/s0035-9203(99)90024-x.

Bertuccini, L., Alano, P., Silvestrini, F., Tibu, M., 2012. Differential Adhesive Properties of Sequestered Asexual and Sexual Stages of *Plasmodium falciparum* on Human Endothelial Cells Are Tissue Independent. *PloS one*, *7*(2), e31567. https://doi.org/10.1371/journal.pone.0031567.

Biruk, H., Sentayehu, B., Alebachew, Y., Tamiru, W., Ejigu, A., Assefa, S., 2020. In Vivo Antimalarial Activity of 80 % Methanol and Aqueous Bark Extracts of Terminalia brownii Fresen . (Combretaceae) against Plasmodium berghei in Mice. *Biochemistry research international*, *2020*, 9749410. https://doi.org/10.1155/2020/9749410.

Blasco, B., Leroy, D., Fidock, D.A., 2017. Antimalarial drug resistance : linking Plasmodium

falciparum parasite biology to the clinic. *Nature medicine*, *23*(8), 917–928. https://doi.org/10.1038/nm.4381

Brice, M., Tali, T., Derick, C., Mbouna, J., Rachel, L., Tchokouaha, Y., Valere, P., Fokou, T., Marius, J., Nangap, T., Keumoe, R., Mfopa, A.N., Bakarnga-via, I., Kamkumo, R.G., Boyom, F.F., 2020. In Vivo Antiplasmodial Activity of Terminalia mantaly Stem Bark Aqueous Extract in Mice Infected by *Plasmodium berghei*. *Journal of parasitology research*, *2020*, 4580526. https://doi.org/10.1155/2020/4580526.

Bzik, D. J., Fox, B. A., & Gonyer, K. (1993). Expression of *Plasmodium falciparum* lactate dehydrogenase in Escherichia coli. *Molecular and biochemical parasitology*, 59(1), 155–166. https://doi.org/10.1016/0166-6851(93)90016-q

Brown W.M., Yowell C.A., Hoard A., Vander Jagt T.A., Hunsaker L.A., Deck L.M., Royer R.E., Piper R.C., Dame J.B., Makler M.T., Vander Jagt D.L. Comparative structural analysis and kinetic properties of lactate dehydrogenases from the four species of human malarial parasites, Biochemistry (2004) 6219–6229, https://doi.org/10.1021/bi049892w

Brueckner, R.P., Lasseter, K.C., Lin, E.T., Schuster, B.G., 1998. First-time-in-humans safety and pharmacokinetics of WR 238605, a new antimalarial. *The American journal of tropical medicine and hygiene*, *58*(5), 645–649. https://doi.org/10.4269/ajtmh.1998.58.645.

Camara, A., Haddad, M., Reybier, K., Traoré, M.S., Baldé, M.A., Royo, J., Baldé, A.O., Batigne, P., Haidara, M., Baldé, E.S., Coste, A., 2019. Terminalia albida treatment improves survival in experimental cerebral malaria through reactive oxygen species scavenging and anti - inflammatory properties. *Malaria Journal*. 1–15. https://doi.org/10.1186/s12936-019-3071-9

Coates-Palgrave O.H, 1977. Trees of Central Africa. National publications trust Rhodesia and Nyasaland, Cape Town.

Coleman, B.I., Skillman, K.M., Jiang, R.H.Y., Childs, L.M., Altenhofen, L.M., Kafsack, F.C., Marti, M., Llina, M., Ganter, M., Leung, Y., Goldowitz, I., Buckee, C.O., Duraisingh, M.T., 2014. Article A Plasmodium falciparum Histone Deacetylase Regulates Antigenic Variation and Gametocyte Conversion. *Cell host & microbe*, *16*(2), 177–186. https://doi.org/10.1016/j.chom.2014.06.014.

Coleman, R.E., Polsa, N., Eikarat, N., Kollars, J., Sattabongkot, J., 2001. Prevention of sporogony of Plasmodium vivax in Anopheles dirus mosquitoes by transmission-blocking antimalarials. *American Journal of Tropical Medicine and Hygiene*. 65, 214–218. https://doi.org/10.4269/ajtmh.2001.65.214

Constantinou, A., Mehta, R., Runyan, C., Moon, R., Stoner, G.D., Rao, K., 1995. The Dietary Anticancer Agent Ellagic Acid is a Potent Inhibitor of DNA Topoisomerases in Vitro. *Nutrition and Cancer.* 23, 121–130. https://doi.org/10.1080/01635589509514368

Cowman, A.F., Crabb, B.S., 2006. Review Invasion of Red Blood Cells by Malaria Parasites. *Cell*, *124*(4), 755–766. https://doi.org/10.1016/j.cell.2006.02.006.

Cragg, G.M., Newman, D.J., 2013. Natural products: A continuing source of novel drug leads. *Biochimica et biophysica acta, 1830(6), 3670–3695. https://doi.org/10.1016/j.bbagen.2013.02.008*

Crockett, M., Kain, K.C., 2007. Tafenoquine : a promising new antimalarial agent. *Expert opinion on investigational drugs*, *16*(5), 705–715. https://doi.org/10.1517/13543784.16.5.705.

Czesny, B., Goshu, S., Cook, J.L., Williamson, K.C., 2009. The proteasome inhibitor epoxomicin has potent Plasmodium falciparum gametocytocidal activity. *Antimicrobial Agents and Chemotherapy,* 53, 4080–4085. https://doi.org/10.1128/AAC.00088-09.

Dalziel J.M, 1937. Useful Plants of West Tropical Africa. Crown Agents, London.

Deharo, E., Barkan, D., Krugliak, M., Golenser, J., Ginsburg, H., 2003. Potentiation of the antimalarial action of chloroquine in rodent malaria by drugs known to reduce cellular glutathione levels. *Biochemical pharmacology* 66, 809–817. https://doi.org/10.1016/s0006-2952(03)00396-4

Dell'Agli, M., Parapini, S., Basilico, N., Verotta, L., Taramelli, D., Berry, C.C., Bosisio, E., 2003. *In vitro* studies on the mechanism of action of two compounds with antiplasmodial activity: Ellagic acid and 3,4,5-trimethoxyphenyl (6′-O-galloyl)-β-D-glucopyranoside. *Planta Medica* 69, 162–164. https://doi.org/10.1055/s-2003-37706

Delves, M., Lafuente-monasterio, M.J., Upton, L., Ruecker, A., Leroy, D., Gamo, F., Sinden, R., 2019. Fueling Open Innovation for Malaria Transmission-Blocking Drugs : Hundreds of Molecules Targeting Early Parasite Mosquito Stages. *Frontiers in microbiology*, *10*, 2134. https://doi.org/10.3389/fmicb.2019.02134

Demain, A.L., Fang, A., 2000. The natural functions of secondary metabolites. *Advances in biochemical engineering/biotechnology,* 69, 1–39. https://doi.org/10.1007/3-540-44964-7_1

Dempsey, T.J.D.O., Infirmary, L.R., 1993. in the clinical features of pneumonia and malaria in African children. *Transactions of the Royal Society of Tropical Medicine and Hygiene*, *87*(6), 662–665. https://doi.org/10.1016/0035-9203(93)90279-y.

Derick, C., Mbouna, J., Mariscal, B., Tali, T., Valere, P., Fokou, T., Aimee, E., Kemgne, M.,

Keumoe, R., Marie, R., Kouipou, T., Rachel, L., Tchokouaha, Y., Aim, M., Kenou, D.K., Sahal, D., Fekam, F., 2022. Specific sub fractions from Terminalia mantaly (H . Perrier) extracts potently inhibit Plasmodium falciparum rings , merozoite egress and invasion *Journal of ethnopharmacology*, *285*, 114909. https://doi.org/10.1016/j.jep.2021.114909.

Dunn C.R., Banfield M.J., Barker J.J., Higham C.W., Moreton K.M., Turgut-Balik D., Brady R.L., Holbrook J.J. The structure of lactate dehydrogenase from *Plasmodium falciparum* reveals a new target for anti-malarial design, Nat. Struct. Biol. 3 (1996) 912–915, https://doi.org/10.1038/nsb1196-912.

Dunn, C. R., Wilks, H. M., Halsall, D. J., Atkinson, T., Clarke, A. R., Muirhead, H., & Holbrook, J. J. (1991). Design and synthesis of new enzymes based on the lactate dehydrogenase framework. Philosophical transactions of the Royal Society of London. *Series B, Biological sciences*, 332(1263), 177–184. https://doi.org/10.1098/rstb.1991.0047

Egan, T.J., 2008. Haemozoin formation. *Molecular and biochemical parasitology* 157, 127–136. https://doi.org/10.1016/j.molbiopara.2007.11.005

Egan, T.J., Combrinck, J.M., Egan, J., Hearne, G.R., Marques, H.M., Ntenteni, S., R, B.T.S., Smith, P.J., Taylor, D., Schalkwyk, D.A.V.A.N., Walden, J.C., 2002. Fate of haem iron in the malaria parasite *Plasmodium falciparum*. *The Biochemical journal*, *365*(Pt 2), 343–347. https://doi.org/10.1042/BJ20020793.

Eloff, J.N., Katerere, D.R., McGaw, L.J., 2008. The biological activity and chemistry of the southern African Combretaceae. *Journal of Ethnopharmacology* 119, 686–699. https://doi.org/10.1016/j.jep.2008.07.051

Erkan, D.Y., Saban, A.I., 2011. Writing performance relative to writing apprehension, self-efficacy in writing, and attitudes towards writing: A correlational study in Turkish tertiary-level EFL. *Asian EFL Journal* 13, 164–192.

Eventoff, W., Rossmann, M. G., Taylor, S. S., Torff, H. J., Meyer, H., Keil, W., & Kiltz, H. H. (1977). Structural adaptations of lactate dehydrogenase isozymes. *Proceedings of the National Academy of Sciences of the United States of America*, 74(7), 2677–2681. https://doi.org/10.1073/pnas.74.7.2677

Famin, O., Krugliak, M., Ginsburg, H., 1999. Kinetics of Inhibition of Glutathione-Mediated Degradation of Ferriprotoporphyrin IX by Antimalarial Drugs. *Biochemical pharmacology*, *58*(1), 59–68. https://doi.org/10.1016/s0006-2952(99)00059-3.

Fidock, D.A., Rosenthal, P.J., Croft, S.L., Brun, R., Nwaka, S., Einstein, A., 2004. Antimalarial drug discovery: efficacy models for compound screening. *Nature reviews. Drug discovery*, *3*(6), 509–520. https://doi.org/10.1038/nrd1416

Figueiredo, R.T., Fernandez, P.L., Mourao-sa, D.S., Porto, N., Dutra, F.F., Alves, S., Oliveira, M.F., Oliveira, P.L., Grac, V., Bozza, M.T., 2007. Characterization of Heme as Activator of Toll-like Receptor 4, *The Journal of biological chemistry*, *282*(28), 20221–20229. https://doi.org/10.1074/jbc.M610737200

Fivelman, Q.L., McRobert, L., Sharp, S., Taylor, C.J., Saeed, M., Swales, C.A., Sutherland, C.J., Baker, D.A., 2007. Improved synchronous production of Plasmodium falciparum gametocytes in vitro. *Molecular and Biochemical Parasitology* 154, 119–123. https://doi.org/10.1016/j.molbiopara.2007.04.008

Foli, E.G., 2009. Terminalia ivorensis A.Chev., in: Lemmens, R.H.M.J., Louppe, D. & Oteng-Amoako, A.A. (Editors). Prota 7(2): Timbers/Bois d'œuvre 2. [CD-Rom]. PROTA, Wageningen, Netherlands. pp. 1–5.

Fong, K.Y., Wright, D.W., 2013. Hemozoin and antimalarial drug discovery. *Future Medicinal Chemistry*. https://doi.org/10.4155/fmc.13.113

Fontaine, B.M., Nelson, K., Lyles, J.T., Jariwala, P.B., García-rodriguez, J.M., Quave, C.L., Weinert, E.E., 2017. Identification of Ellagic Acid Rhamnoside as a Bioactive Component of a Complex Botanical Extract with Anti-biofilm. Activity *Frontiers in microbiology*, *8*, 496. https://doi.org/10.3389/fmicb.2017.00496

Foster, R.C., 1981. Hemin Lyses Malaria Parasites. *Science (New York, N.Y.)*, *214*(4521), 667–669. https://doi.org/10.1126/science.7027441.

Gallup, J.L., Sachs, J.D., 2001. The Economic Burden of Malaria : Cross-Country Evidence. *The American journal of tropical medicine and hygiene*, *64*(1-2 Suppl), 85–96. https://doi.org/10.4269/ajtmh.2001.64.85.

Ganesh, D., Fuehrer, H.P., Starzengrüber, P., Swoboda, P., Khan, W.A., Reismann, J.A.B., Mueller, M.S.K., Chiba, P., Noedl, H., 2012. Antiplasmodial activity of flavonol quercetin and its analogues in *Plasmodium falciparum*: Evidence from clinical isolates in Bangladesh and standardized parasite clones. *Parasitology Research* 110, 2289–2295. https://doi.org/10.1007/s00436-011-2763-z

Geach, B.G.S., 2005. Indigenous forests and woodlands in South Africa: policy, people and practice. Choice Reviews Online 42, 42–5265. https://doi.org/10.5860/choice.42-5265

Ghasemzadeh, A., Ghasemzadeh, N., 2011. Flavonoids and phenolic acids : Role and biochemical activity in plants and human Figure 1 . Basic structure of flavonoids . *Journal of Medicinal Plants Research*, 5, 6697–6703. https://doi.org/10.5897/JMPR11.1404

Ginsburg, P.B. 2003. Payment and the future of primary care. *Annals of internal medicine*, *138*(3), 233–234. https://doi.org/10.7326/0003-4819-138-3-200302040-00020.

Gomez M.S., Piper R.C., Hunsaker L.A., Royer R.E., Deck L.M., Makler M.T., Vander D.L. Substrate and cofactor specificity and selective inhibition of lactate dehydrogenase from the malarial parasite *P. falciparum*, Mol. Biochem. Parasitol. 90 (1) (1997 Dec 1) 235–246, https://doi.org/10.1016/s0166-6851(97)00140-0.

Goldberg, D.E., Slater, A.F., Cerami, A., Henderson, G.B., 1990. Hemoglobin degradation in the malaria parasite *Plasmodium falciparum*: an ordered process in a unique organelle. *Proceedings of the National Academy of Sciences of the United States of America* 87, 2931–2935. https://doi.org/10.1073/pnas.87.8.2931

Goulart, H.R., Kimura, E.A., Peres, V.J., Couto, A.S., Duarte, F.A.A., Katzin, A.M., 2004. Terpenes Arrest Parasite Development and Inhibit Biosynthesis of Terpenes Arrest Parasite Development and Inhibit Biosynthesis of Isoprenoids in *Plasmodium falciparum. Antimicrobial agents and chemotherapy*, *48*(7), 2502–2509. https://doi.org/10.1128/AAC.48.7.2502-2509.2004

Grau, U. M., Trommer, W. E., & Rossmann, M. G. (1981). Structure of the active ternary complex of pig heart lactate dehydrogenase with S-lac-NAD at 2.7 A resolution. *Journal of molecular biology*, 151(2), 289–307. https://doi.org/10.1016/0022-2836(81)90516-7

Gwer, S., Newton, C.R.J.C., Berkley, J.A., 2007. Over-Diagnosis and Co-Morbidity of Severe Malaria in African Children : A Guide for Clinicians, *The American journal of tropical medicine and hygiene*, *77*(6 Suppl), 6–13.

Lebrun Jean-Pierre, Stork Adélaïde L. 1991. Enumération des plantes à fleurs d'Afrique tropicale - Volume 1 : Généralités et Annonaceae à Pandaceae. Genève : Conservatoire et Jardin botaniques de la Ville de Genève, 249 p. ISBN 2-8277-0108-1. https://agritrop.cirad.fr/317983/.

Hawking, F., Wilson, M., Kenneth, G., 1971. Evidence for cyclic development and short-lived maturity in the gametocytes of Plasmodium falciparum. *Transactions of the Royal Society of Tropical Medicine and Hygiene*, *65*(5), 549–559. https://doi.org/10.1016/0035-9203(71)90036-8.

Howland, S.W., Poh, C.M., Rénia, L., 2015. Activated Brain Endothelial Cells Cross- Present Malaria Antigen. *PLoS pathogens*, *11*(6), e1004963. https://doi.org/10.1371/journal.ppat.1004963

Hubs, R., Excellence, O.F., 2011. Report 2011.

Isah, M.B., Ibrahim, M.A., 2014. The role of antioxidants treatment on the pathogenesis of malarial infections : a review, *Parasitology research*, *113*(3), 801–809. https://doi.org/10.1007/s00436-014-3804-1

Iversen, P.W., Beck, B., Chen, Y., Dere, W., Devanarayan, V., Eastwood, B.J., Farmen, M.W., Iturria, S.J., Montrose, C., Moore, R.A., Weidner, J.R., Sittampalam, G.S., 2012. HTS Assay Validation 2 . Stability and Process Studies.

Irvine F.R, 1961. Woody plants of Ghana with a special reference to their uses. Oxford University Press, London.

Jana, S., Paliwal, J., 2007. Novel molecular targets for antimalarial chemotherapy. *International journal of antimicrobial agents*, *30*(1), 4–10. https://doi.org/10.1016/j.ijantimicag.2007.01.002.

Johnson, J.D., Dennull, R.A., Gerena, L., Lopez-sanchez, M., Roncal, N.E., Waters, N.C., 2007. Assessment and Continued Validation of the Malaria SYBR Green I-Based Fluorescence Assay for Use in Malaria Drug Screening. *Antimicrobial agents and chemotherapy*, *51*(6), 1926–1933. https://doi.org/10.1128/AAC.01607-06

Kafsack, B.F.C., Rovira-graells, N., Clark, T.G., Bancells, C., 2014. Europe PMC Funders Group Europe PMC Funders Author Manuscripts A transcriptional switch underlies commitment to sexual development in human malaria parasites. *Nature* 507, 248–252. https://doi.org/10.1038/nature12920.A

Källander, K., Nsungwa-Sabiiti, J., Peterson, S., 2004. Symptom overlap for malaria and pneumonia - Policy implications for home management strategies. *Acta Tropica* 90, 211–214. https://doi.org/10.1016/j.actatropica.2003.11.013

Kalra, B., Chawla, S., Gupta, P., Valecha, N., 2006. Screening of antimalarial drugs: An overview. *Indian Journal of Pharmacology* 38, 5–12.

Kamkumo, R.G., Ngoutane, A.M., Tchokouaha, L.R., Fokou, P.V., Madiesse, E.A., Legac, J., Kezetas, J.J., Lenta, B.N., Boyom, F.F., Dimo, T., Mbacham, W.F., Gut, J., Rosenthal, P.J., 2012. Compounds from Sorindeia juglandifolia (Anacardiaceae) exhibit potent anti-plasmodial activities in vitro and in vivo. *Malaria Journal* 11. https://doi.org/10.1186/1475-2875-11-382

Kavishe, R.A., Koenderink, J.B., Alifrangis, M., 2017. Oxidative stress in malaria and artemisinin combination therapy: Pros and Cons. *FEBS Journal* 284, 2579–2591. https://doi.org/10.1111/febs.14097

Kazi, Y.F., Parton, R., Memon, B.A., 1994. Haemolytic assay for the detection of adenylate cyclase toxin of Bordetella pertussis. *Pakistan journal of pharmaceutical sciences* 7, 55–559.

Klonis, N., Crespo-Ortiz, M.P., Bottova, I., Abu-Bakar, N., Kenny, S., Rosenthal, P.J., Tilley, L., 2011. Artemisinin activity against Plasmodium falciparum requires hemoglobin uptake

and digestion. *Proceedings of the National Academy of Sciences of the United States of America* 108, 11405–11410. https://doi.org/10.1073/pnas.1104063108

Knight, D.J., Peters, W., 1980. The antimalarial activity of N-benzyloxydihydrotriazines: I. The activity of clociguanil (BRL 50216) against rodent malaria, and studies on its mode of action. *Annals of Tropical Medicine and Parasitology* 74, 393–404. https://doi.org/10.1080/00034983.1980.11687360

Kuehn, A., Pradel, G., 2010. The Coming-Out of Malaria Gametocytes. *Journal of biomedicine & biotechnology*, *2010*, 976827. https://doi.org/10.1155/2010/976827

Kumar, M., Gupta, V., Kumari, P., Reddy, C.R.K., Jha, B., 2011. Assessment of nutrient composition and antioxidant potential of Caulerpaceae seaweeds. *Journal of Food Composition and Analysis* 24, 270–278. https://doi.org/10.1016/j.jfca.2010.07.007

Lambros, C., Vanderberg, J.P., 2012. Falciparum of Plasmodium Synch Stages in Culture. *The Journal of parasitology*, *65*(3), 418–420.

Landau, I., Chabaud, A.G., Mora-Silvera, E., Coquelin, F., Boulard, Y., Rénia, L., Snounou, G., 1999. Survival of rodent malaria merozoites in the lymphatic nerwork: Potential role in chronicity of the infection. *Parasite* 6, 311–322. https://doi.org/10.1051/parasite/1999064311

Landau, I., Chabaud, A.G., Vuong, P.N., Deharo, E., Gautret, P., 1995. Circulation in the lymphatic system and latency of *Plasmodium* merozoites. Preliminary note. *Parasite (Paris, France)*, *2*(2), 185–186. https://doi.org/10.1051/parasite/1995022185.

Lawes M.J, Eerley H.A.C, Shackleton C.M, Geach BGS, 2004. Indigenous forests and woodlands in South Africa. University of Kwazulu-Natal Press. Scottsville, Pietermaritzburg.

Lee W.S., Kang T., Kwak K.J., Park K., Yi S.Y., Lee U.J., Simple, rapid, and accurate malaria diagnostic platform using microfluidic - based immunoassay of *Plasmodium falciparum* lactate dehydrogenase, Nano Converg (2020), https://doi. org/10.1186/s40580-020-00223-w.

Liu, M., Katerere, D.R., Gray, A.I., Seidel, V., 2009. Fitoterapia Phytochemical and antifungal studies on *Terminalia mollis* and *Terminalia brachystemma*. *Fitoterapia* 80, 369–373. https://doi.org/10.1016/j.fitote.2009.05.006

Machumi, F., Midiwo, J.O., Jacob, M.R., Khan, S.I., Tekwani, B.L., Zhang, J., Walker, L.A., Muhammad, I., 2013. Phytochemical, antimicrobial and antiplasmodial investigations of Terminalia brownii. *Natural Product Communications* 8, 761–764. https://doi.org/10.1177/1934578x1300800619

Makler, M.T., Hinrichs, D.J., 1993. Measurement of the lactate dehydrogenase activity of Plasmodium falciparum as an assessment of parasitemia. *American Journal of Tropical Medicine and Hygiene,* 48, 205–210. https://doi.org/10.4269/ajtmh.1993.48.205

Makler, M.T., Palmer, C.J., Ager, A.L., 1998. A review of practical techniques for the diagnosis of malaria, in: *Annals of Tropical Medicine and Parasitology.* pp. 419–433. https://doi.org/10.1080/00034989859401

Makler, M.T., Ries, J.M., Williams, J.A., Bancroft, J.E., Piper, R.C., Gibbins, B.L., Hinrichs, D.J., 1993. Parasite lactate dehydrogenase as an assay for *Plasmodium falciparum* drug sensitivity. *American Journal of Tropical Medicine and Hygiene* 48, 739–741. https://doi.org/10.4269/ajtmh.1993.48.739

Malterud, K.E., 2017. Properties of Four Malian Medicinal Plants. *Plants (Basel, Switzerland)*, *6*(1), 11. https://doi.org/10.3390/plants6010011

Manach, C. Le, Scheurer, C., Sax, S., Schleiferböck, S., Cabrera, D.G., Younis, Y., Paquet, T., Street, L., Smith, P., Ding, X.C., Waterson, D., Witty, M.J., Leroy, D., Chibale, K., Wittlin, S., 2013. Fast in vitro methods to determine the speed of action and the stage-specificity of anti-malarials in *Plasmodium falciparum*, *Malaria journal*, *12*, 424. https://doi.org/10.1186/1475-2875-12-424.

Masevhe, N.A., Mabogo, D.E.N., 2007. An investigation on the biological activity of Acacia robusta subsp. robusta. *South African Journal of Botany* 73, 300. https://doi.org/10.1016/j.sajb.2007.02.082

Mbouna, C.D.J., Kouipou, R.M.T., Keumoe, R., Tchokouaha, L.R.Y., Fokou, P.V.T., Tali, B.M.T., Sahal, D., Boyom, F.F., 2018. Potent antiplasmodial extracts and fractions from Terminalia mantaly and Terminalia superba. *Malaria Journal* 1–9. https://doi.org/10.1186/s12936-018-2298-1

Mbwambo, Z.H., Moshi, M.J., Masimba, P.J., Kapingu, M.C., Nondo, R.S.O., 2007. BMC Complementary and Antimicrobial activity and brine shrimp toxicity of extracts of Terminalia brownii roots and stem. *BMC complementary and alternative medicine*, *7*, 9. https://doi.org/10.1186/1472-6882-7-9

Mccutchan, T.F., Piper, R.C., Makler, M.T., 2008. Use of Malaria Rapid Diagnostic Test to Identify Plasmodium knowlesi Infection, *Emerging infectious diseases*, *14*(11), 1750–1752. https://doi.org/10.3201/eid1411.080480.

McGaw L.J, Rabe T, Sparg SG, Jäger A.K, Eliff J.N, van Staden J, 2001. An investigation on the biological activity of Combretum spp. An investigation on the biological activity of Combretum species. *Journal of ethnopharmacology*, *75*(1), 45–50.

https://doi.org/10.1016/s0378-8741(00)00405-0.

Meibalan, E., Marti, M., 2017. Biology of Malaria Transmission. *Cold Spring Harbor perspectives in medicine*, *7*(3), a025452. https://doi.org/10.1101/cshperspect.a025452.

Menard, D., Dondorp, A., 2017. Antimalarial drug resistance: a threat to malaria elimination. *Cold Spring Harbor Perspectives in Medicine* 7, 1–24. https://doi.org/10.1101/cshperspect.a025619.

Miller, L.H., Baruch, D.I., Marsh, K., Doumbo, O.K., 2002. The pathogenic basis of malaria *Nature*, *415*(6872), 673–679. https://doi.org/10.1038/415673a.

Miret, S., Groene, E.L.S.M.D.E., Klaffke, W., 2006. Comparison of In Vitro Assays of Cellular Toxicity in the Human Hepatic Cell Line HepG2. *Journal of biomolecular screening*, *11*(2), 184–193. https://doi.org/10.1177/1087057105283787

Moody, A., 2002. Rapid Diagnostic Tests for Malaria Parasites. *Clinical microbiology reviews*, *15*(1), 66–78. https://doi.org/10.1128/CMR.15.1.66-78.2002

Moody, A., Hunt-cooke, A., Gabbett, E., Chiodini, P., 2000. Performance of the OptiMAL malaria antigen capture dipstick for malaria diagnosis and treatment monitoring at the Hospital for Tropical Diseases , London. *British journal of haematology*, *109*(4), 891–894. https://doi.org/10.1046/j.1365-2141.2000.01974.x

Moshi, M.J., Mbwambo, Z.H., 2005. Some pharmacological properties of extracts of *Terminalia sericea* roots. *Journal of ethnopharmacology*, *97*(1), 43–47. https://doi.org/10.1016/j.jep.2004.09.056.

Moyo, P., Botha, M.E., Nondaba, S., Niemand, J., Maharaj, V.J., Eloff, J.N., Louw, A.I., Birkholtz, L., 2016. In vitro inhibition of Plasmodium falciparum early and late stage gametocyte viability by extracts from eight traditionally used South African plant species. *Journal of Ethnopharmacology* 185, 235–242. https://doi.org/10.1016/j.jep.2016.03.036

Mueller, I., Zimmerman, P.A., Reeder, J.C., 2007. Plasmodium malariae and Plasmodium ovale - the "bashful" malaria parasites. *Trends in Parasitology* 23, 278–283. https://doi.org/10.1016/j.pt.2007.04.009

Muganza, D.M., Fruth, B., Nzunzu, J.L., Tuenter, E., Foubert, K., Cos, P., Maes, L., Kanyanga, R.C., Exarchou, V., Apers, S., Pieters, L., 2016. In vitro antiprotozoal activity and cytotoxicity of extracts and isolated constituents from Greenwayodendron suaveolens. *Journal of Ethnopharmacology* 193, 510–516. https://doi.org/10.1016/j.jep.2016.09.051

Muhia, D.K., Swales, C.A., Deng, W., Kelly, J.M., Baker, D.A., 2001. The gametocyte-activating factor xanthurenic acid stimulates an increase in membrane-associated guanylyl cyclase activity in the human malaria parasite *Plasmodium falciparum*. *Molecular*

microbiology, *42*(2), 553–560. https://doi.org/10.1046/j.1365-2958.2001.02665.x.

Murray, C.K., Bell, D., Gasser, R.A., Wongsrichanalai, C., 2003. Rapid diagnostic testing for malaria. *Tropical medicine & international health : TM & IH*, *8*(10), 876–883. https://doi.org/10.1046/j.1365-3156.2003.01115.x.

Murray, C.K., Bennett, J.W., 2009. Rapid Diagnosis of Malaria. *Interdisciplinary perspectives on infectious diseases*, *2009*, 415953. https://doi.org/10.1155/2009/415953

Murray, C.K., Gasser, R.A., Magill, A.J., Miller, R.S., 2008. Update on Rapid Diagnostic Testing for Malaria. *Clinical microbiology reviews*, *21*(1), 97–110. https://doi.org/10.1128/CMR.00035-07

Myint, H.Y., Tipmanee, P., Nosten, F., Day, N.P.J., Pukrittayakamee, S., Looareesuwan, S., White, N.J., 2004. A systematic overview of published antimalarial drug trials. *Transactions of the Royal Society of Tropical Medicine and Hygiene*. https://doi.org/10.1016/S0035-9203(03)00014-2

Veeresham. 2012. Natural products derived from plants as a source of drugs, 2012. *Journal of Advanced Pharmarceutical Technology and Research* 3, 200–202. https://doi.org/10.4103/2231-4040.104709

Ngasala, B., Mubi, M., Warsame, M., Petzold, M.G., Massele, A.Y., Gustafsson, L.L., Tomson, G., Premji, Z., Bjorkman, A., n.d. Impact of training in clinical and microscopy diagnosis of childhood malaria on antimalarial drug prescription and health outcome at primary health care level in Tanzania : A randomized controlled trial. *Malaria journal*, *7*, 199. https://doi.org/10.1186/1475-2875-7-199

Ngotho, P., Soares, A.B., Hentzschel, F., Achcar, F., Bertuccini, L., Marti, M., Marti, M., 2019. Revisiting gametocyte biology in malaria parasites. *FEMS microbiology reviews*, *43*(4), 401–414. https://doi.org/10.1093/femsre/fuz010

Ngum, N.H., Fakeh, N.B., Lem, A.E. et al. Prevalence of malaria and associated clinical manifestations and myeloperoxidase amongst populations living in different altitudes of Mezam division, North West Region, Cameroon. Malar J 22, 20 (2023). https://doi.org/10.1186/s12936-022-04438-6

Nilsson, S.K., Childs, L.M., Buckee, C., Marti, M., 2015. Targeting Human Transmission Biology for Malaria. Elimination *PLoS pathogens*, *11*(6), e1004871. https://doi.org/10.1371/journal.ppat.1004871

Ns, G., Maria, N.R.G., Schuck, D.C., Cruz, L.N., Moraes, M.S. De, Nakabashi, M., Graebin, C., Gosmann, G., Garcia, C.R.S., Gnoatto, S.C.B., 2013. Two series of new semisynthetic triterpene derivatives : differences in anti-malarial activity , cytotoxicity and mechanism

of action. *Malaria journal*, *12*, 89. https://doi.org/10.1186/1475-2875-12-89

Nwodo, U.U., Ngene, A.A., Iroegbu, C.U., Gc, O., 2010. Effects of fractionation on antibacterial activity of crude extracts of Tamarindus indica. *African Journal of Biotechnology*. 9, 7108–7113. https://doi.org/10.5897/AJB09.1662.

OECD, 2002. The Organization of Economic Co-operation and Development Guidelines Test No. 423: Acute Oral toxicity - Acute Toxic Class Method, OECD Guidelines for the Testing of Chemicals, Section 4. Oecd 1–14.

Okombo, J., Chibale, K., 2016. Antiplasmodial drug targets: A patent review (2000 - 2013). Expert Opinion on Therapeutic Patents. *Expert opinion on therapeutic patents*, *26*(1), 107–130. https://doi.org/10.1517/13543776.2016.1113258 26, 107–130. https://doi.org/10.1517/13543776.2016.1113258.

Organisation, W.H., 2009. World Malaria Report 2009. World 12, 66.

Organization, W.H., 2015. Global Malaria Programme. Eliminating malaria. Geneva: World Health Organization. World Health Organization 243. https://doi.org/ISBN 978 92 4 1564403

Organization, W.H., 2013. WHO. World malaria report 2013. Geneva: World Health Organization; 2014.

Ouattara, L.P., Sanon, S., Mahiou-Leddet, V., Gansané, A., Baghdikian, B., Traoré, A., Nébié, I., Traoré, A.S., Azas, N., Ollivier, E., Sirima, S.B., 2014. In vitro antiplasmodial activity of some medicinal plants of Burkina Faso. *Parasitology Research* 113, 405–416. https://doi.org/10.1007/s00436-013-3669-8

Pan, W., Xu, X., Shi, N., Tsang, S.W., Zhang, H., 2018. Antimalarial Activity of Plant Metabolites. *International journal of molecular sciences*, *19*(5), 1382. https://doi.org/10.3390/ijms19051382

Pandey, A. V, Tekwani, B.L., Singh, R.L., Chauhan, V.S., 1999. Artemisinin , an Endoperoxide Antimalarial , Disrupts the Hemoglobin Catabolism and Heme Detoxification Systems in Malarial Parasite. *The Journal of biological chemistry*, *274*(27), 19383–19388. https://doi.org/10.1074/jbc.274.27.19383.

Payne, D., 1988. Use and limitations of light microscopy for diagnosing malaria at the primary health care level. *Bulletin of the World Health Organization*, *66*(5), 621–626..

Peatey, C.L., Andrews, K.T., Eickel, N., Macdonald, T., Butterworth, A.S., Trenholme, K.R., Gardiner, D.L., Mccarthy, J.S., Skinner-adams, T.S., Mu, D.-, 2010. Antimalarial Asexual Stage-Specific and Gametocytocidal Activities of HIV Protease Inhibitors. *Antimicrobial agents and chemotherapy*, *54*(3), 1334–1337. https://doi.org/10.1128/AAC.01512-09

Peatey, C.L., Leroy, D., Gardiner, D.L., Trenholme, K.R., 2012. Anti-malarial drugs : how effective are they against *Plasmodium falciparum* gametocytes ? *Malaria journal*, *11*, 34. https://doi.org/10.1186/1475-2875-11-34.

Penna-coutinho J., Cortopassi W.A., Oliveira A.A., Costa T.C. Antimalarial activity of potential inhibitors of *Plasmodium falciparum* lactate dehydrogenase enzyme selected by docking studies, PLoS One 6 (2011), https://doi.org/10.1371/journal. pone.0021237.

Poindexter, H.A., 1976. Human malaria. *Journal of the National Medical Association* 68, 530–533. https://doi.org/10.32473/edis-mg103-2005

Rasoanaivo, P., Wright, C.W., Willcox, M.L., Gilbert, B., 2011. Whole plant extracts versus single compounds for the treatment of malaria : synergy and positive interactions. *Malaria journal*, *10 Suppl 1*(Suppl 1), S4. https://doi.org/10.1186/1475-2875-10-S1-S4.

Report, W.M., 2020. World malaria report 2020.

World Health Organization. World malaria report: 2010. World Health Organization. https://apps.who.int/iris/handle/10665/44451

Reyburn, H., Mbatia, R., Drakeley, C., Carneiro, I., Mwakasungula, E., Mwerinde, O., Saganda, K., Shao, J., Kitua, A., Olomi, R., Greenwood, B.M., Whitty, C.J.M., 2004. Tanzania : a prospective study. *BMJ (Clinical research ed.)*, *329*(7476), 1212. https://doi.org/10.1136/bmj.38251.658229.55.

Roberts, B.F., Zheng, Y., Cleaveleand, J., Lee, S., Lee, E., Ayong, L., Yuan, Y., Chakrabarti, D., 2017. International Journal for Parasitology : Drugs and Drug Resistance 4-Nitro styrylquinoline is an antimalarial inhibiting multiple stages of Plasmodium falciparum asexual life cycle. *International Journal for Parasitology*: Drugs and Drug Resistance 7, 120–129. https://doi.org/10.1016/j.ijpddr.2017.02.002

Rodrigues, Alyne, Araujo, D., Ramos-jesus, J., Maria, T., Oliveira, D., Maria, A., Carvalho, A. De, Humberto, P., Nunes, M., Caroline, T., Carvalho, A.P., Fátima, M., Peixoto, M., Almeida, D., Plácido, A., Rodrigues, Artur, Socodato, R., Relvas, J.B., Delerue-matos, C., Alves, D., Eaton, P., Roberto, J., Leite, D.S.D.A., 2019. Industrial Crops & Products Identi fi cation of Eschweilenol C in derivative of Terminalia fagifolia Mart . and green synthesis of bioactive and biocompatible silver nanoparticles. *Industrial Crops & Products* 137, 52–65. https://doi.org/10.1016/j.indcrop.2019.05.012.

Rogers C.B, Verotta L, 1996. Chemistry and biological properties of the African Combretaceae, in: Hostettman K, Chinyanganga F, Maillard M, Wolfender JL (Eds), Chemistry, Biological and Pharmacological Properties of African Medicinal Plants. University of Zimbabwe Publications, Harare. P. 136.

Rosenthal, P.J., 2003. Review Antimalarial drug discovery : old and new approaches. *The Journal of experimental biology*, *206*(Pt 21), 3735–3744. https://doi.org/10.1242/jeb.00589.

Rosenthal, P.J., 2021. Editorial Are Artemisinin-Based Combination Therapies For Malaria Beginning To Fail in Africa ? *The American journal of tropical medicine and hygiene*, *105*(4), 857–858. https://doi.org/10.4269/ajtmh.21-0797.

Tajuddeen, N., Heerden, F.R. Van, 2019. Antiplasmodial natural products : an update. Malaria Journal 1–62. https://doi.org/10.1186/s12936-019-3026-1.

Sanon, S., Gansane, A., Ouattara, L.P., Traore, A., Ouedraogo, I.N., Tiono, A., Taramelli, D., Basilico, N., Sirima, S.B., 2013. In vitro antiplasmodial and cytotoxic properties of some medicinal plants from western Burkina Faso. *African Journal of Laboratory Medicine* 2, 1–7. https://doi.org/10.4102/ajlm.v2i1.81.

Schmidt E, Lötter M, McCleland W, 2002. Trees and shrubs of the Mpumalanga & Kruger National Park. Jacana Publisher, Johannesburg.

Sherman B.I.W. Molecular heterogeneity of lactic dehydrogenase in avian malaria (*Plasmodium* lophurae), J. Exp. Med. 114 (6) (1961) 1049–1062, https://doi.org/ 10.1084/jem.114.6.1049, 1.

Sigala, P.A., Crowley, J.R., Hsieh, S., Henderson, J.P., Goldberg, D.E., 2012. Direct tests of enzymatic heme degradation by the malaria parasite Plasmodium falciparum. *The Journal of biological chemistry* 287, 37793–37807. https://doi.org/10.1074/jbc.M112.414078

Sinden, R.E., 2017. Developing transmission-blocking strategies for malaria control. *PLoS pathogens*, *13*(7), e1006336. https://doi.org/10.1371/journal.ppat.1006336.

Singh, B., Daneshvar, C., 2013. Human Infections and Detection of *Plasmodium knowlesi Clinical microbiology reviews*, *26*(2), 165–184. https://doi.org/10.1128/CMR.00079-12.

Sinha, A., Hughes, K.R., Modrzynska, K.K., Otto, T.D., Pfander, C., Dickens, N.J., Religa, A.A., Bushell, E., Graham, A.L., Cameron, R., Kafsack, B.F.C., Williams, A.E., Berriman, M., Billker, O., Waters, A.P., 2014. commitment and development in *Plasmodium. Nature*, *507*(7491), 253–257. https://doi.org/10.1038/nature12970

Sinha, S., Batovska, D.I., Medhi, B., Radotra, B.D., Bhalla, A., Markova, N., 2019. In vitro anti - malarial efficacy of chalcones : cytotoxicity profile , mechanism of action and their effect on erythrocytes. *Malaria Journal* 1–11. https://doi.org/10.1186/s12936-019-3060-z.

Sinha, S., Sarma, P., Sehgal, R., Medhi, B., 2017. Development in Assay Methods for in Vitro Antimalarial Drug Efficacy Testing : A Systematic Review. *Frontiers in pharmacology*,

8, 754. https://doi.org/10.3389/fphar.2017.00754.

Smilkstein, M., Sriwilaijaroen, N., Kelly, J.X., Wilairat, P., Riscoe, M., 2004. Simple and Inexpensive Fluorescence-Based Technique for High-Throughput Antimalarial Drug Screening. *Antimicrobial agents and chemotherapy*, *48*(5), 1803–1806. https://doi.org/10.1128/AAC.48.5.1803-1806.2004.

Smith N, Scott AM, Henderson A, Stevenson DWm, Scott VH, 2004. Flowering plants of the tropics. Princeton University Press. Princeton, New Jersey.

Soh, P.N., Witkowski, B., Gales, A., Huyghe, E., Berry, A., Pipy, B., 2012. Implication of Glutathione in the In Vitro Antiplasmodial Mechanism of Action of Ellagic Acid. *PloS one*, *7*(9), e45906. https://doi.org/10.1371/journal.pone.0045906

Soh, P.N., Witkowski, B., Olagnier, D., Nicolau, M., Berry, A., 2008. In Vitro and In Vivo Properties of Ellagic Acid in Malaria Treatment. *Antimicrobial agents and chemotherapy*, *53*(3), 1100–1106. https://doi.org/10.1128/AAC.01175-08.

Soré, H., Alessandro, S.D., Sanon, S., Parapini, S., Tiono, A., Valea, I., Sirima, S.B., Hilou, A., Taramelli, D., 2018. International Journal Of Current Medical And In Vitro Inhibitory Activity Against Plasmodium falciparum Sexual and Asexual. *International Journal of Current Medical and Pharmaceutical Research*. 4, 2976–2983. DOI: http://dx.doi.org/10.24327/23956429.ijcmpr20180380.

Spangenberg, T., Burrows, J.N., Kowalczyk, P., Mcdonald, S., Wells, T.N.C., Willis, P., 2013. The Open Access Malaria Box : A Drug Discovery Catalyst for Neglected Diseases. *PloS one*, *8*(6), e62906. https://doi.org/10.1371/journal.pone.0062906

Steenkamp, V., Mathivha, E., Gouws, M.C., Rensburg, C.E.J. Van, 2004. Studies on antibacterial , antioxidant and fibroblast growth stimulation of wound healing remedies from South Africa. *Journal of ethnopharmacology*, *95*(2-3), 353–357. https://doi.org/10.1016/j.jep.2004.08.020.

Sturm, N., Hu, Y., Zimmermann, H., Fritz-wolf, K., Wittlin, S., Rahlfs, S., Becker, K., 2009. Compounds Structurally Related to Ellagic Acid Show Improved Antiplasmodial Activity. *Antimicrobial agents and chemotherapy*, *53*(2), 622–630. https://doi.org/10.1128/AAC.00544-08.

Sullivan, D.J., Matile, H., Ridley, G., Goldberg, D.E., Sullivan, D.J., Matile, H., Ridley, R.G., Goldberg, D.E., 1998. Cell Biology and Metabolism : A Common Mechanism for Blockade of Heme Polymerization by Antimalarial Quinolines. *The Journal of biological chemistry*, *273*(47), 31103–31107. https://doi.org/10.1074/jbc.273.47.31103

Sutherland, C.J., Ord, R., Dunyo, S., Jawara, M., Drakeley, C.J., Alexander, N., Coleman, R.,

Pinder, M., Walraven, G., Targett, G.A.T., 2005. Reduction of malaria transmission to Anopheles mosquitoes with a six-dose regimen of co-artemether. *PLoS Medicine* 2, 338–346. https://doi.org/10.1371/journal.pmed.0020092

Tahita, M.C., Tinto, H., Menten, J., Ouedraogo, J., Guiguemde, R.T., Geertruyden, J.P. Van, Erhart, A., Alessandro, U.D., 2013. Clinical signs and symptoms cannot reliably predict Plasmodium falciparum malaria infection in pregnant women living in an area of high seasonal transmission. *Malaria journal*, *12*, 464. https://doi.org/10.1186/1475-2875-12-464

Tajuddeen, N., Heerden, F.R. Van, 2019. Antiplasmodial natural products : an update. *Malaria Journal* 1–62. https://doi.org/10.1186/s12936-019-3026-1

Teklehaimanot, A., Mejia, P., 2008. Malaria and poverty. *Annals of the New York Academy of Sciences* 1136, 32–37. https://doi.org/10.1196/annals.1425.037

Thiombiano, A., Schmidt, M., Kreft, H., Guinko, S., 2006. Influence du gradient climatique sur la distribution des espèces de Combretaceae au Burkina Faso (Afrique de l'Ouest). Candollea. *Journal international de botanique systématique* 61, 189–213.

Thu, A., Dvergsnes, C., Togola, A., Wangensteen, H., Diallo, D., Smestad, B., Egil, K., 2011. Terminalia macroptera , its current medicinal use and future perspectives. *Journal of Ethnopharmacology* 137, 1486–1491. https://doi.org/10.1016/j.jep.2011.08.029

Tilley, L., Straimer, J., Gnädig, N.F., Ralph, S.A., Fidock, D.A., 2016. Artemisinin Action and Resistance in *Plasmodium falciparum*. *Trends in Parasitology* 32, 682–696. https://doi.org/10.1016/j.pt.2016.05.010

Tlhapi, D.B., Ramaite, I.D.I., Ree, T. Van, Anokwuru, C.P., Orazio, T., Hoppe, H.C., 2018. from Rauvolfia caffra Sond. *Molecules (Basel, Switzerland)*, *24*(1), 39. https://doi.org/10.3390/molecules24010039

Tsabang, N., Valère, P., Fokou, T., Rachel, L., Tchokouaha, Y., Noguem, B., Bakarnga-via, I., Sylviane, M., Nguepi, D., Aloys, B., Fekam, F., 2012. Ethnopharmacological survey of Annonaceae medicinal plants used to treat malaria in four areas of Cameroon. *Journal of Ethnopharmacology* 139, 171–180. https://doi.org/10.1016/j.jep.2011.10.035

Tse, E.G., Korsik, M., Todd, M.H., 2019. The past, present and future of anti-malarial medicines. *Malaria Journal*. https://doi.org/10.1186/s12936-019-2724-z

Vander Jagt, D. L., Hunsaker, L. A., Campos, N. M., & Baack, B. R. (1990). D-lactate production in erythrocytes infected with *Plasmodium falciparum*. *Molecular and biochemical parasitology*, 42(2), 277–284. https://doi.org/10.1016/0166-6851(90)90171-h

Vander Jagt, D. L., Hunsaker, L. A., & Heidrich, J. E. (1981). Partial purification and characterization of lactate dehydrogenase from *Plasmodium falciparum*. *Molecular and biochemical parasitology*, 4(5-6), 255–264. https://doi.org/10.1016/0166-6851(81)90058-x

Wande, O.M., Babatunde, S.B., 2017. In vitro screening of ten Combretaceae plants for antimalarial activities applying the inhibition of beta-hematin formation. *International Journal of Biological and Chemical Sciences*. 11, 2971–2981. DOI : https://dx.doi.org/10.4314/ijbcs.v11i6.33.

Wang, J., Zhang, C., Chia, W.N., Loh, C.C.Y., Li, Z., Lee, Y.M., He, Y., Yuan, L., Lim, T.K., Liu, M., Liew, C.X., Lee, Y.Q., Zhang, J., Lu, N., Lim, C.T., Hua, Z., Liu, B., Shen, H., Tan, K.S.W., Lin, Q., 2015. Haem-activated promiscuous targeting of artemisinin in Plasmodium falciparum. *Nature Communications* 6, 1–11. https://doi.org/10.1038/ncomms10111

Wells, T.N.C., Alonso, P.L., Gutteridge, W.E., 2009. New medicines to improve control and contribute to the eradication of malaria. *8*(11), 879–891. *Nature Reviews Drug Discovery*. https://doi.org/10.1038/nrd2972

WHO, 2019. World Malaria Report 2019. Geneva. World Malaria Report 1–232.

WHO, 2011. World Malaria Report. Colombia, Google Scholar.

WHO, 2021a. World Malaria Report 2021, Word Malaria Report. World Health Organization, Geneva.

WHO, 2021b. https://www.who.int/news/item/06-10-2021-who-recommends-ground breaking-malaria-vaccine-for-children-at-risk?. (Accessed 22 March 2022).

World Health Organization, 2020. The E-2020 Eliminating 2019 progress report.

Wongsrichanalai, C., Barcus, M.J., Muth, S., Sutamihardja, A., Wernsdorfer, W.H., 2017. A Review of Malaria Diagnostic Tools : Microscopy and Rapid Diagnostic Test (RDT). *The American journal of tropical medicine and hygiene*, *77*(6 Suppl), 119–127.

Wongsrichanalai, C., Pickard, A.L., Wernsdorfer, W.H., Meshnick, S.R., 2002. Reviews Epidemiology of drug-resistant malaria. *The Lancet. Infectious diseases*, *2*(4), 209–218. https://doi.org/10.1016/s1473-3099(02)00239-6.

World Health Organization, 2010. World Malaria Report, World Health. https://doi.org/ISBN 978 92 4 1564403.

World Health Organization. (2023). World malaria report 2023. In *World malaria report 2023*.

Xie, K., Huang, K., Yang, L., Yu, P., Liu, H., 2011. Three-Liquid-Phase Extraction : A New Approach for Simultaneous Enrichment and Separation of Cr (III) and Cr (VI). *Industrial*
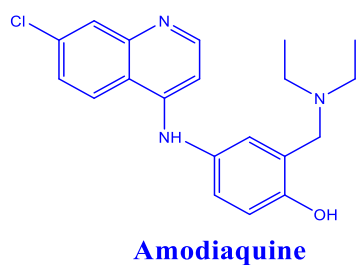
& Engineering Chemistry Research. 12767–12773. https://doi.org/10.1021/ie201816j.

Yamthe, L., Fokou, P., Mbouna, C., Keumoe, R., Ndjakou, B., Djouonzo, P., Mfopa, A., Legac, J., Tsabang, N., Gut, J., Rosenthal, P., Boyom, F., 2015. Extracts from Annona Muricata L. and Annona Reticulata L. (Annonaceae) Potently and Selectively Inhibit Plasmodium Falciparum. *Medicines* 2, 55–66. https://doi.org/10.3390/medicines2020055

Yang, S.-W., Zhou, B.-N., Wisse, J.H., Evans, R., van der Werff, H., Miller, J.S., Kingston, D.G.I., 1998. Three New Ellagic Acid Derivatives from the Bark of Eschweilera coriacea from the Suriname Rainforest. *Journal of Natural Products* 61, 901–906. https://doi.org/10.1021/np980046u.

Zhang, J., Krugliak, M., Ginsburg, H., 1999. The fate of ferriprotorphyrin IX in malaria infected erythrocytes in conjunction with the mode of action of antimalarial drugs. *Molecular and biochemical parasitology*, *99*(1), 129–141. https://doi.org/10.1016/s0166-6851(99)00008-0.

Zhang, J.H., Chung, T.D.Y., Oldenburg, K.R., 1999. A simple statistical parameter for use in evaluation and validation of high throughput screening assays. *Journal of Biomolecular Screening* 4, 67–73. https://doi.org/10.1177/108705719900400206.

Zofou, D., Tene, M., Tane, P., Titanji, V.P.K., 2012. Antimalarial drug interactions of compounds isolated from Kigelia africana (Bignoniaceae) and their synergism with artemether , against the multidrug-resistant W2mef Plasmodium falciparum strain. *Parasitology research*, *110*(2), 539–544. https://doi.org/10.1007/s00436-011-2519-9.
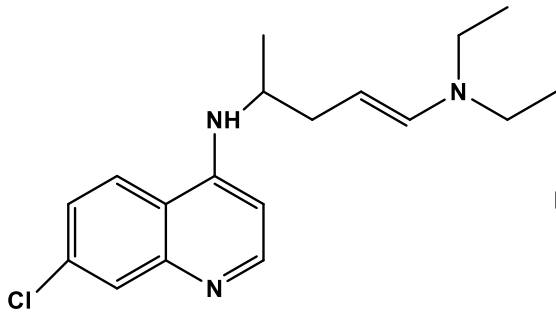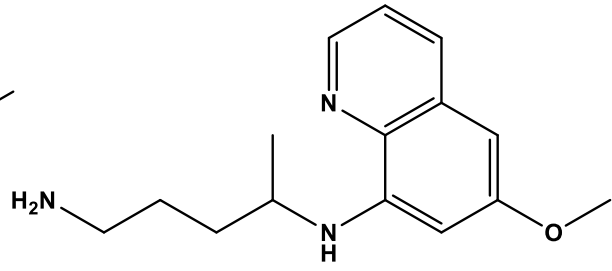
APPENDIX

APPENDIX

Appendix 1: Name and Structure of MMV Compounds used for *Pf*LDH-based antiplasmodial assay implementation and validation.
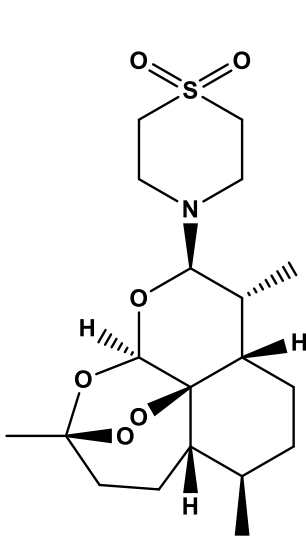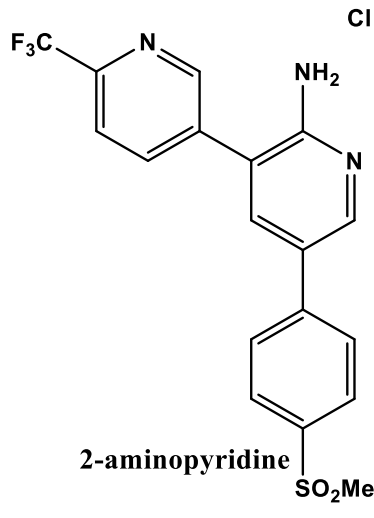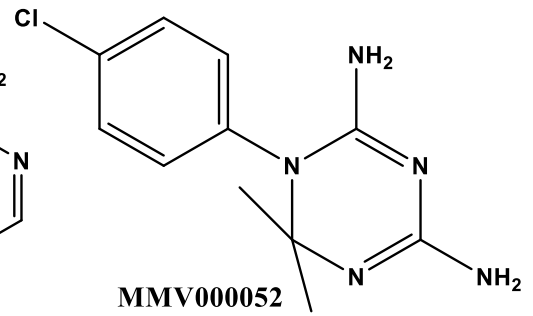

Artesunate

Artemether

Dihydroartemisinin

Amodiaquine

Mefloquine

Lumefantrine

Piperaquine

Proguanil

Atovaquone

Sulfadoxine

Pyrimethamine

Pyronaridine

Tafenoquine
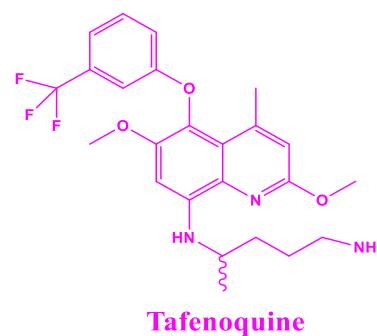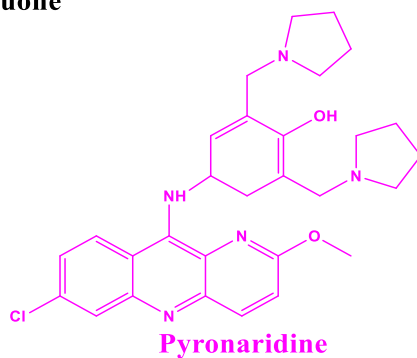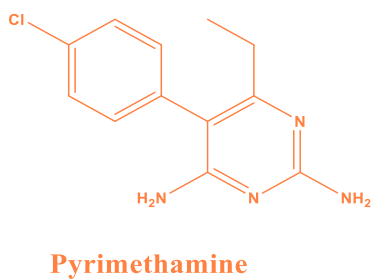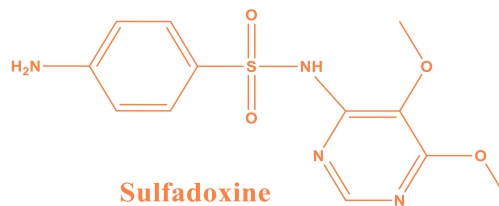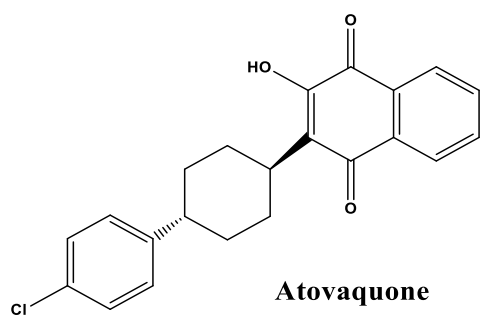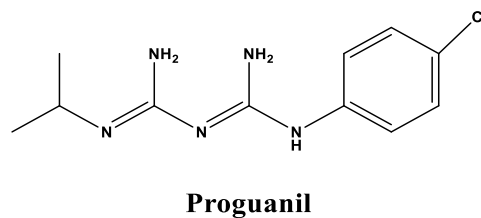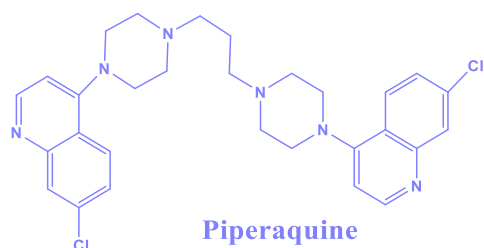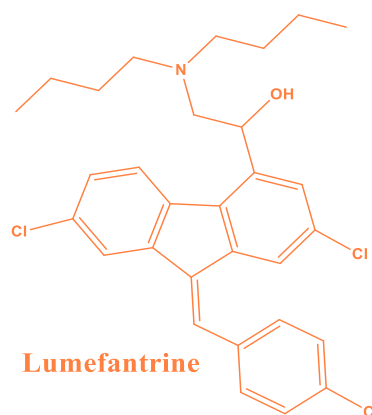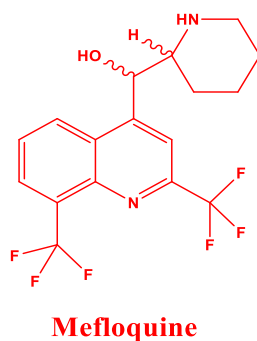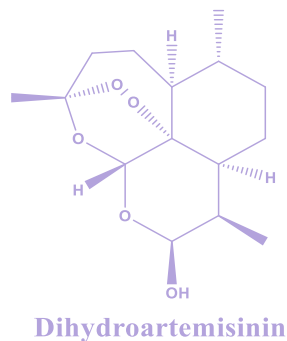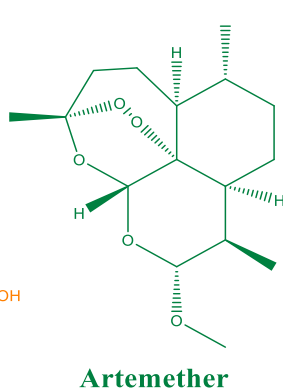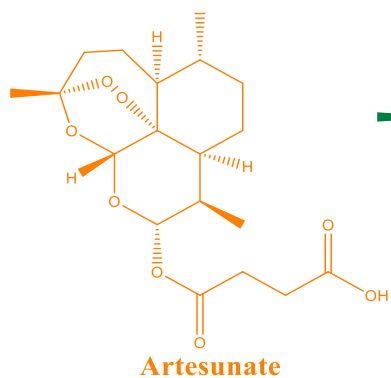
Chloroquine

Primaquine

Artemisone

2-aminopyridine

MMV000052

Methylene blue

Quinine sulfate dihydrate

b
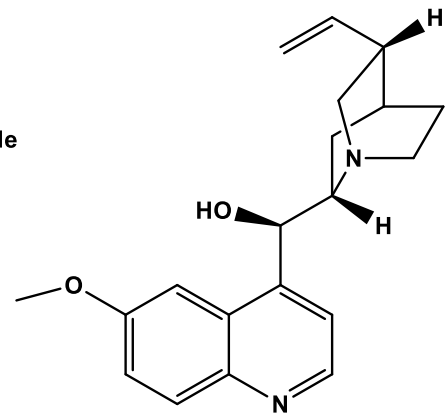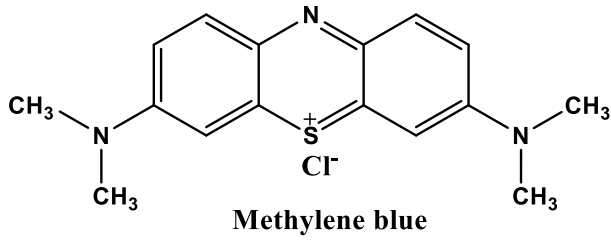
Appendix 2: Preparation of reagents and malaria culture medium.

1. Thawing solution A – 12% NaCl solution.

In 1 mL of sterile water, 120 mg of NaCl (Sigma-Aldrich, Germany) was solubilized and filter sterilized in a 0.22 µm filter and stored at 4°C.

2. Thawing solution B – 1.6% NaCl solution.

In 5 mL of sterile water, 80 mg of NaCl (Sigma-Aldrich, Germany) was solubilized and filter sterilized in a 0.22 µm filter and stored at 4°C.

3. Fresh red blood cells

Blood was extracted from volunteers in 5 mL EDTA collection vials after consent forms were signed by the volunteer using compliance forms approved by the Antimicrobial and Biocontrol Agents Units (University of Yaoundé I). Immediately after collection, the blood was transferred to a 50 mL falcon tube and placed at 4°C until two layers were visible – the serum layer containing plasma and white blood cells and the lower layer containing the fresh RBCs. The serum layer was aspirated leaving behind the RBC pellet. The pellet was washed in CM (culture medium) and centrifuged at 3000 rpm for 5 min to further isolate and remove any residual serum. A 5 mL layer of CM was left above the fresh RBC pellet and the tube was placed at 4°C for use for up to two weeks.

4. Preparation of Malaria Culture Medium (MCM) for *P. falciparum* asexual blood stages.

In a sterile 1 L bottle, a bottle of RPMI 1640 medium containing 25 mM HEPES and 2 mM L-glutamine (Sigma - Aldrich, Germany) corresponding to 10.4 g was introduced and gently mixed with 700 mL of sterile distilled water. After that, 26.7 mL of 7.5% sodium bicarbonate was added and the volume was brought to 1 L. The medium was filtered sterilized through a 0.22 µM filter and supplemented with 10 mM of sodium hypoxanthine and 1.6 mM thymidine; 10% Albumax II (Sigma - Aldrich, Germany) and gentamicin at 50 mg/mL. After solubilization, the complete malaria culture medium was aliquoted into a 50 mL tube. The samples were stored at 4°C.

5. Giemsa stain

A 10% working solution of Giemsa was prepared from 5 mL Giemsa solution (Sigma - Aldrich, Germany) in 45 mL of 1X phosphate-buffered saline in a 50 mL falcon tube and wrapped in tin foil to minimize light exposure.

6. Sorbitol solution (5%)

In a 50 mL falcon tube, 2.5 g of D-sorbitol (Sigma - Aldrich, Germany) was solubilized in 50 mL of distilled water and filter sterilized through a 0.22 µM filter before being stored at 4°C.

7. Drug stock solutions

A panel of standard antimalarial drug compounds was purchased from Sigma - Aldrich, Germany and solubilized to a concentration of 10 mM as per the following profile – chloroquine in sterile water and artemisinin in DMSO. These stock solutions were stored at -20°C. Intermediate solutions were prepared on the day of use as per the IC_{50} profile of each drug.

8. Malstat solution

In 80 mL of sterile distilled water, 4 g of L-lactate (Sigma - Aldrich, Germany), 1.32 g of Trizma base (Sigma - Aldrich, Germany), and 22 mg of 3-acetylpyridine nicotinamide adenine dinucleotide (APAD; Sigma - Aldrich, Germany) were solubilized. The pH of the solution was adjusted to 9 and 400 µL of Triton-X 100 was added. The volume was adjusted to 200 mL and stored at 4°C.
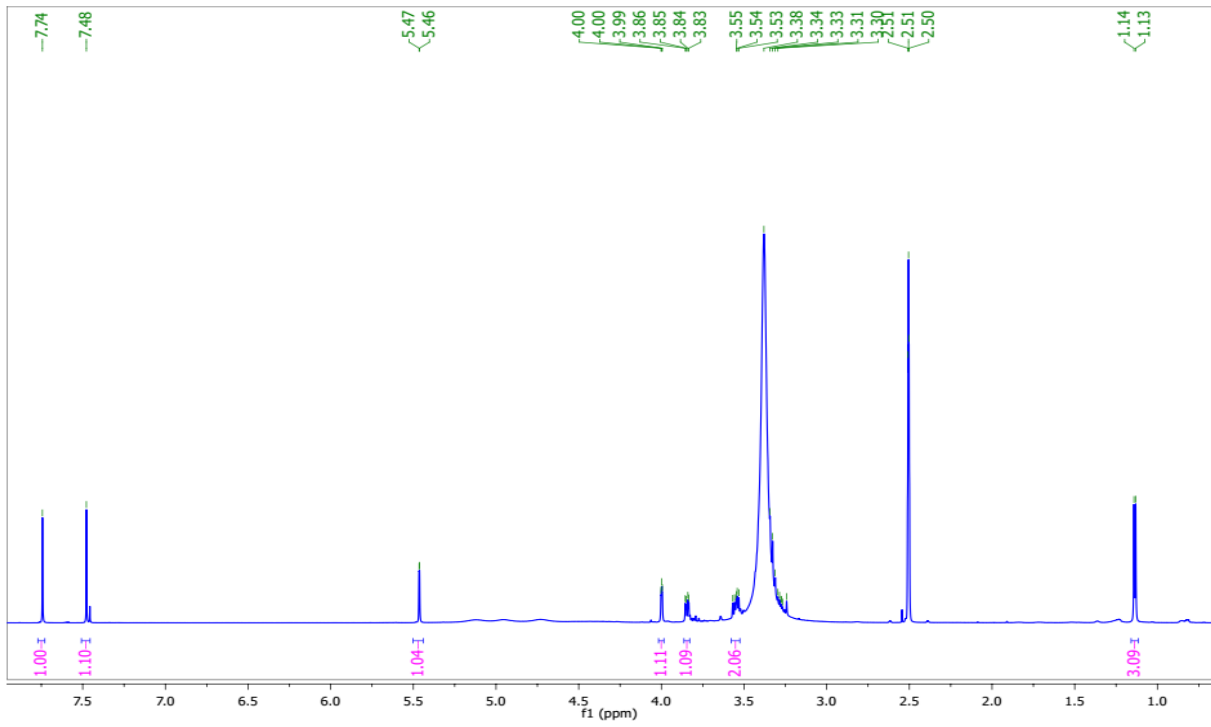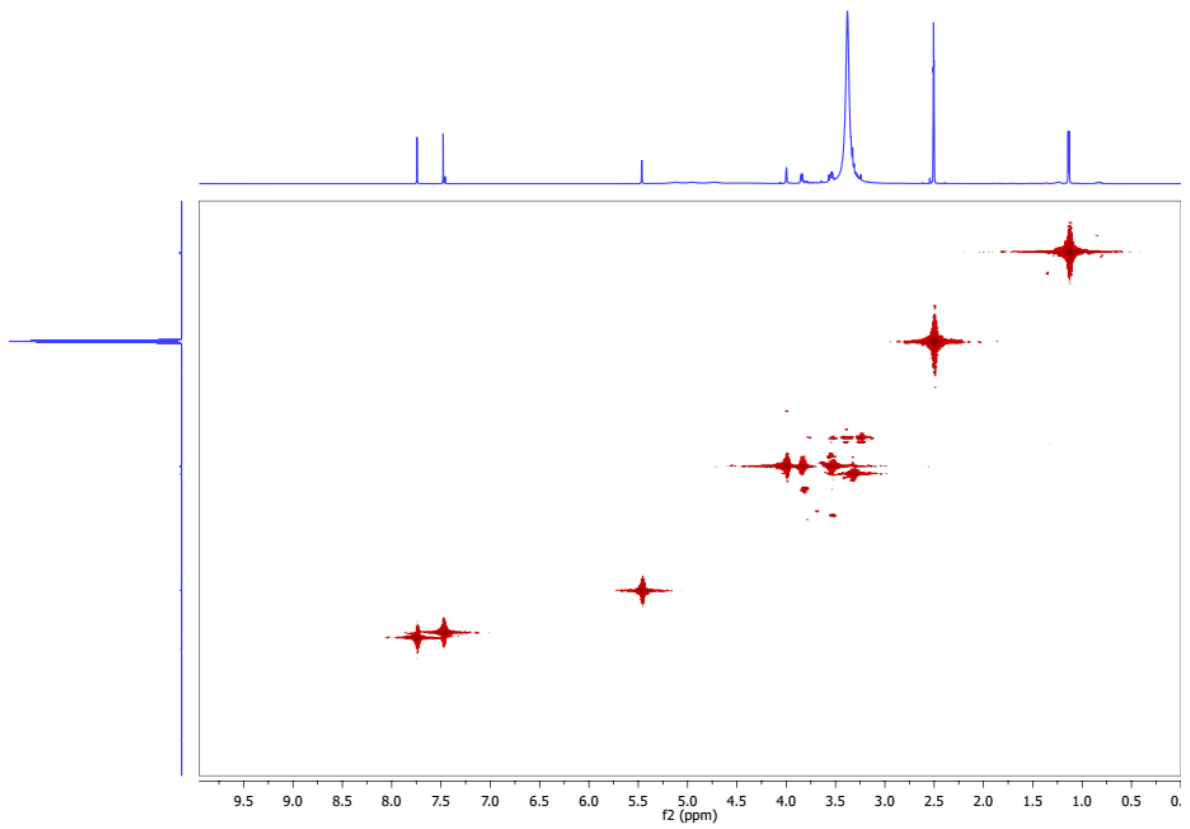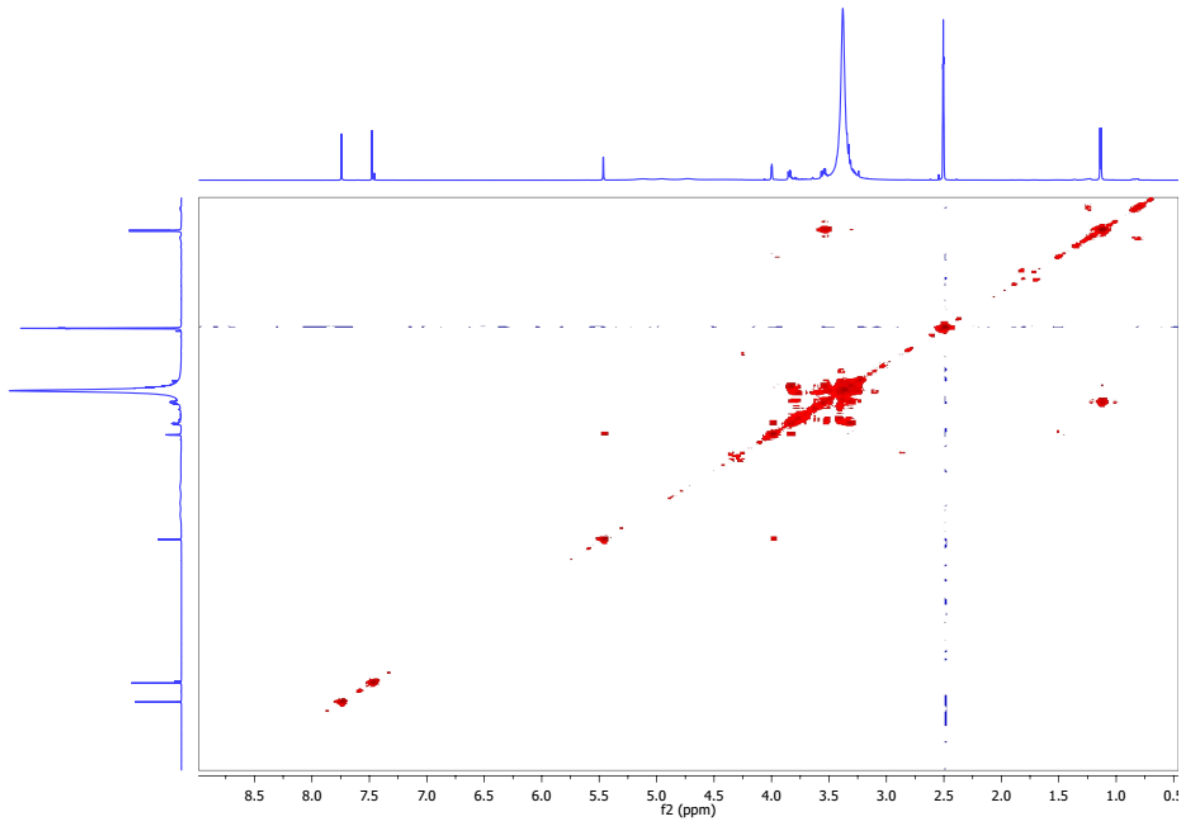
9. NBT/PES solution

In 100 mL of sterile distilled water, 160 mg of nitro blue tetrazolium (NBT; Sigma - Aldrich, Germany) and 8 mg of phenazine ethosulfate (PES; Sigma - Aldrich, Germany) were solubilized and stored at 4°C in a Schott bottle wrapped in tin foil to minimize light exposure.
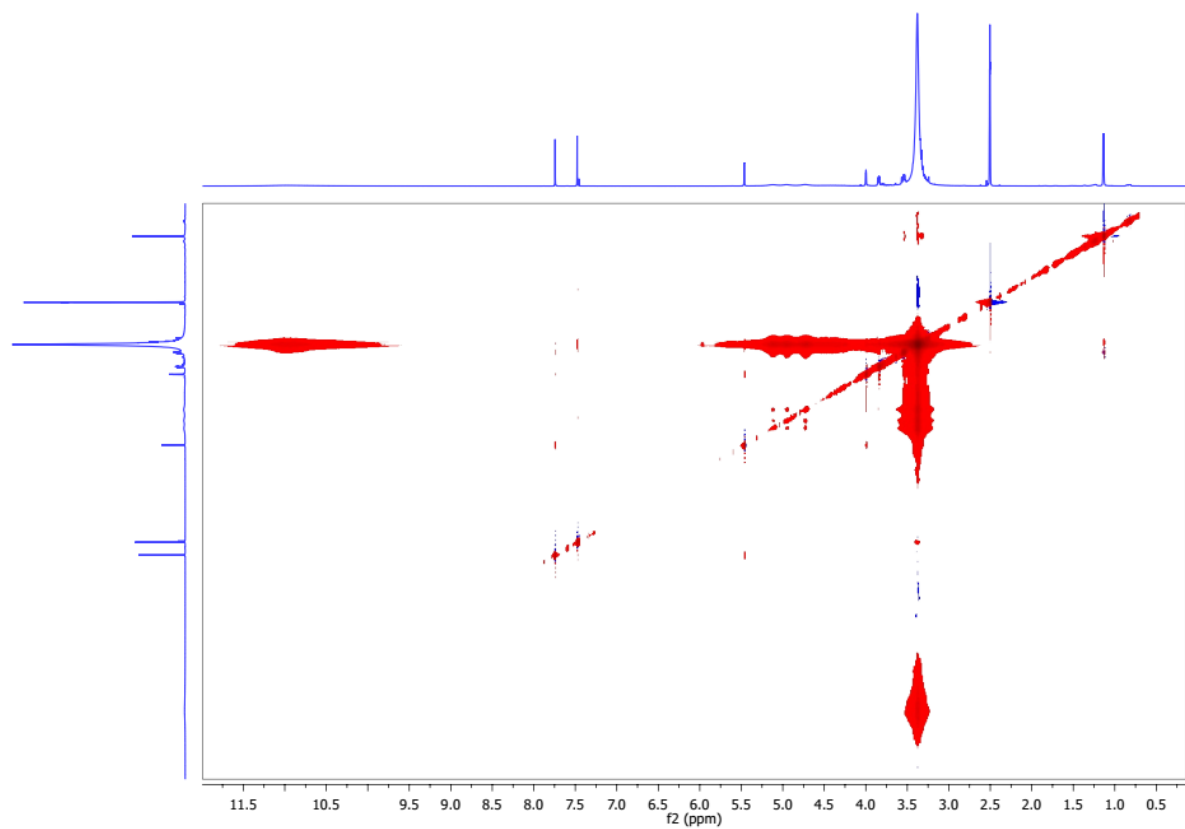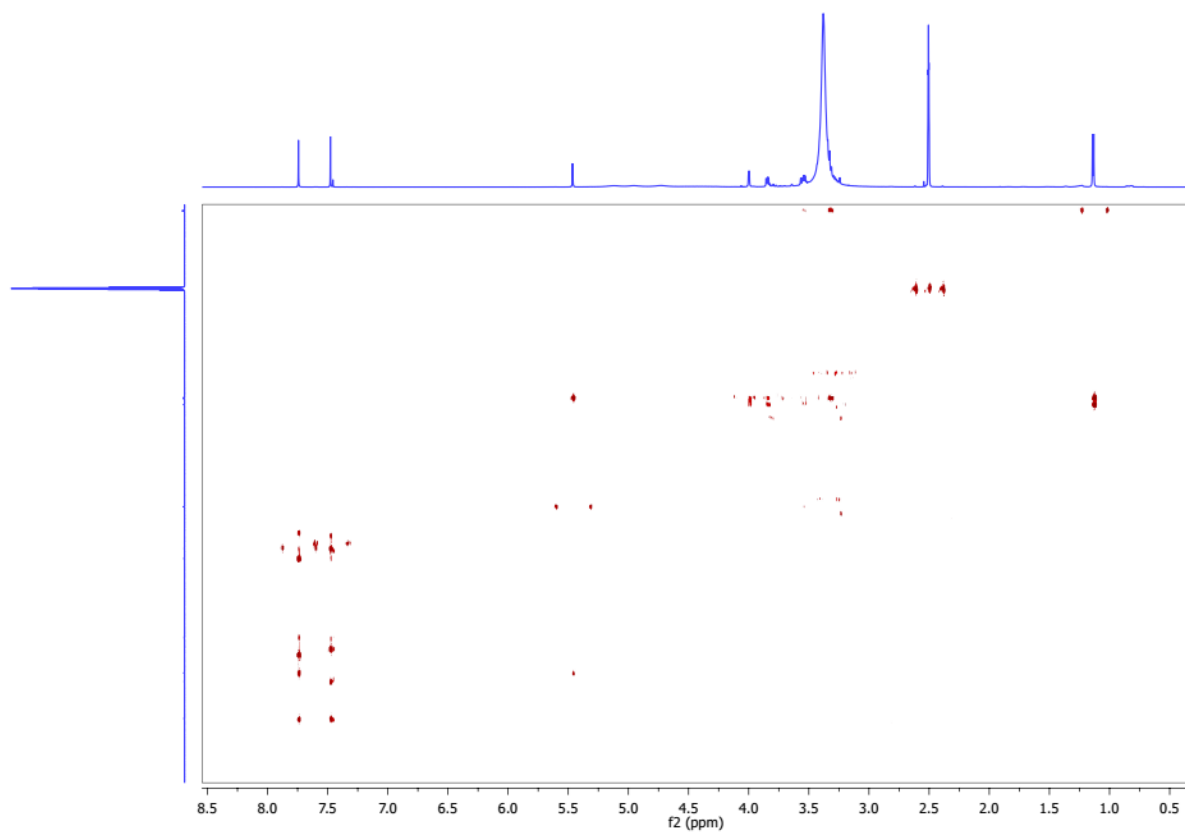
10-SyBr Green solution

SYBR Green I buffer [6 µL of 10,000 × SYBR Green I (Invitrogen) + 600 µL of Red Blood Cells lysis buffer {Tris (25 mM; pH 7.5)} + 360 µL of EDTA (7.5 mM) + 19,2 µL of parasite lysis solution {saponin (0.012%; wt/vol)} and 28,8 µL of Triton X-100 (0.08%; vol/vol)}]

Appendix 3: NMR Spectra of the characterized compounds.

e

f

g
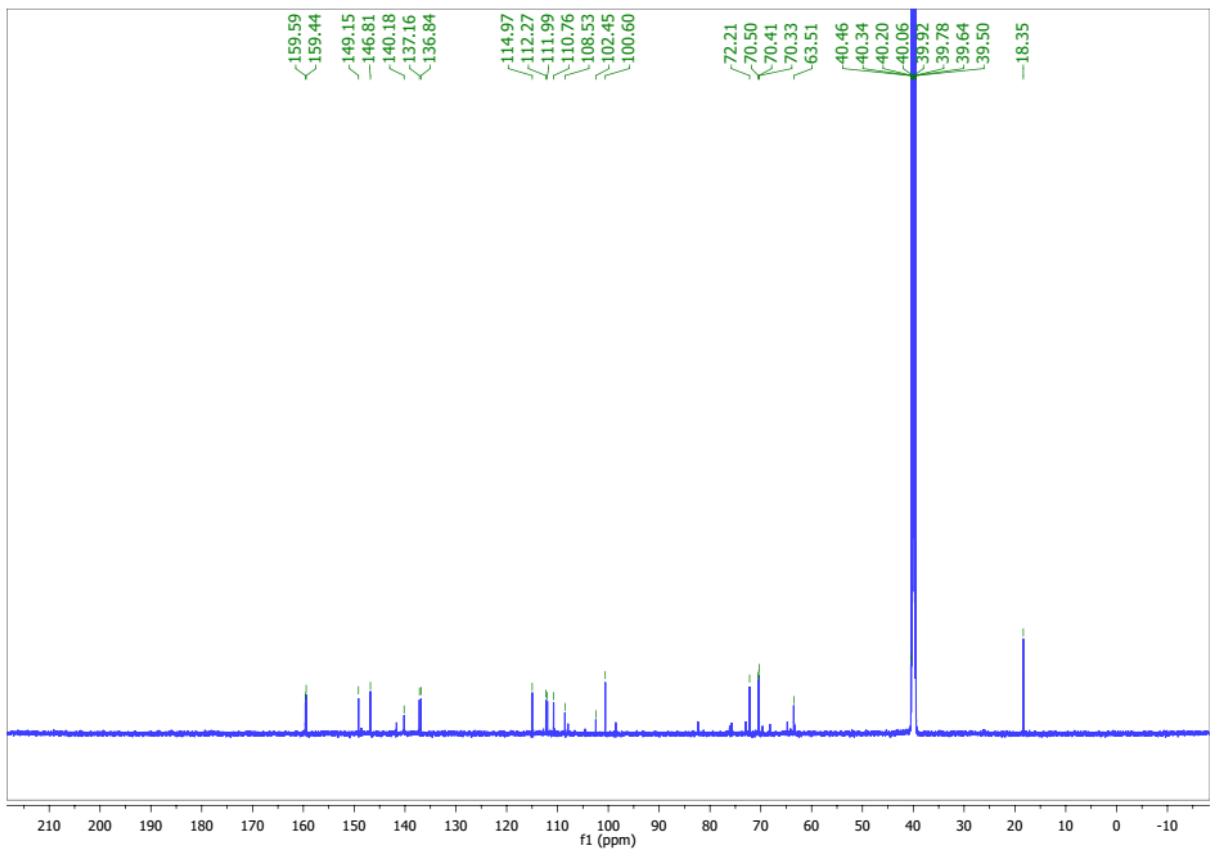
PUBLICATION

PUBLICATIONS